1975

Development of helicopter flight path models utilizing modern control techniques

Alfred Fermelia

DEVELOPMENT OF HELICOPTER FLIGHT PATH MODELS UTILIZING MODERN CONTROL TECHNIQUES

by

ALFRED FERMELIA, 1942 -

A DISSERTATION

Presented to the Faculty of the Graduate School of the

UNIVERSITY OF MISSOURI - ROLLA

In Partial Fulfillment of the Requirements for the Degree

DOCTOR OF PHILOSOPHY

in

MECHANICAL ENGINEERING

1975

Advisor

PUBLICATION THESIS OPTION

The papers presented within the body of this thesis have been prepared in the style utilized by the American Society of Mechanical Engineers. Pages 1-18 and pages 71-117 will be submitted to the A.S.M.E. Journal of Dynamic Systems, Measurement and Control for publication.

Because of journal requirements, matrices and vectors have been denoted by placing a solid line below their corresponding symbols. Symbols designated in this manner will appear in bold-face type within the journal copy.

ACKNOWLEDGMENTS

I would like to thank many people for the roles which they have played in my pursuit of graduate work.

Initially I would like to thank Dr. J. Earl Foster for encouraging my return to school; Dr. Richard D. Rocke for his unfailing interest in my personal endeavor; Dr. Donald A. Gyorog for his many ideas and suggestions. Particular thanks go to Dr. Virgil J. Flanigan for the guidance and encouragement he provided during the course of this investigation. I would also like to thank Dr. Donald L. Cronin, Dr. Thomas L. Noack and Professor Sylvestor J. Pagano for serving on my doctoral committee. Additional appreciation is expressed to Mrs. Toby Cohen for typing the manuscript.

I am further indebted to the Department of Mechanical and Aerospace Engineering of the University of Missouri-Rolla, the National Science Foundation, and the U.S. Army Weapons Command for partial support of this work.

Grateful appreciation is also expressed to my father and mother, Mr. and Mrs. Rudolph Fermelia, whose encouragement to pursue a higher education has always served as an inspiration to me. Thanks are also due to Eileen, Jeanne, and Mary Kate who many times had to sacrifice our family days during the course of this work.

No acknowledgment would be complete without my expressed appreciation to my wife, Kathleen, for her prayers, understanding and many sacrifices she endured in order to make the completion of graduate work possible. It is to her that I owe the greatest debt of gratitude.

ABSTRACT

The nonlinear set of equations which represents helicopter motion are linearized about a prescribed nominal state. Once the linearized system is obtained it is validated by comparing the output of the nonlinear system to that of its linearized counterpart. Having obtained a linear model, linear system theory may then be applied in order to investigate the stability and control characteristics of the aricraft.

General techniques for simulating helicopter pilot response for inclusion in a flight path simulation program have been devised. To provide the desired flight goal, a nominal flight trajectory is obtained from an existing nonlinear model. With this basis a deterministic pilot model which attempts to minimize flight deviations from the nominal can be developed for generating descriptions of the desired flight path.

TABLE OF CONTENTS

	Page
PUBLICATION THESIS OPTION	ii
ACKNOWLEDGEMENTS	iii
ABSTRACT	v
LIST OF TABLES	viii
LIST OF ILLUSTRATIONS	x
I. LINEARIZATION OF EQUATIONS WHICH GOVERN THE MOTION OF A HELICOPTER	1
INTRODUCTION	4
PROBLEM STATEMENT	6
SOLUTION	7
VALIDATION	9
CONCLUSIONS AND RECOMMENDATIONS	12
REFERENCES	15
APPENDIX A - EQUATIONS OF MOTION	19
APPENDIX B - LIFT AND DRAG CURVES	36
APPENDIX C - STATIC TESTS	42
APPENDIX D - HOMOGENEOUS TEST	61
APPENDIX E - OBJECTIVE FUNCTION TEST	65
II. APPLICATION OF MODERN CONTROL TECHNIQUES TO DEVELOP HELICOPTER FLIGHT PATHS	71
INTRODUCTION	74
DETERMINISTIC PILOT MODEL	76
RESULTS AND CONCLUSIONS	84
FUTURE CONSIDERATIONS AND EXTENSIONS	87

Page

REFERENCES 90

APPENDIX A - WEIGHTING MATRICES 118

APPENDIX B - SOLUTION OF THE MATRIX RICCATI EQUATION 119

III. VITA 122

LIST OF TABLES

Table | Page

Al-1. Elements of A_1 24

Al-2. Elements of A_2 25

Al-3. Elements of A_3 26

Al-4. Elements of A_4 27

CT-1. Effect of State Perturbations on Forces (Speed Equals 50 Knots) 43

CT-2. Effect of State Perturbations on Moments (Speed Equals 50 Knots) 44

CT-3. Effect of State Perturbations on Forces (Speed Equals 50 Knots) 45

CT-4. Effect of State Perturbations on Moments (Speed Equals 50 Knots) 46

CT-5. Effect of State Perturbations on Forces (Speed Equals 50 Knots) 47

CT-6. Effect of State Perturbations on Moments (Speed Equals 50 Knots) 48

CT-7. Effect of Control Perturbations on Forces (Speed Equals 50 Knots) 49

CT-8. Effect of Control Perturbations on Moments (Speed Equals 50 Knots) 49

CT-9. Effect of Control Perturbations on Forces (Speed Equals 50 Knots) 50

CT-10. Effect of Control Perturbations on Moments (Speed Equals 50 Knots) 50

CT-11. Effect of Control Perturbations on Forces (Speed Equals 50 Knots) 51

CT-12. Effect of Control Perturbations on Moments (Speed Equals 50 Knots) 51

CT-13. Effect of State Perturbations on Forces (Speed Equals 110 Knots) 52

Table		Page
CT-14.	Effect of State Perturbations on Moments (Speed Equals 110 Knots)	53
CT-15.	Effect of State Perturbations on Forces (Speed Equals 110 Knots)	54
CT-16.	Effect of State Perturbations on Moments (Speed Equals 110 Knots)	55
CT-17.	Effect of State Perturbations on Forces (Speed Equals 110 Knots)	56
CT-18.	Effect of State Perturbations on Moments (Speed Equals 110 Knots)	57
CT-19.	Effect of Control Perturbations on Forces (Speed Equals 110 Knots)	58
CT-20.	Effect of Control Perturbations on Moments (Speed Equals 110 Knots)	58
CT-21.	Effect of Control Perturbations on Forces (Speed Equals 110 Knots)	59
CT-22.	Effect of Control Perturbation on Moments (Speed Equals 110 Knots)	59
CT-23.	Effect of Control Perturbations on Forces (Speed Equals 110 Knots)	60
CT-24.	Effect of Control Perturbations on Moments (Speed Equals 110 Knots)	60
DT-1.	Helicopter Position	62
DT-2.	Helicopter Velocity	63
DT-3.	Angular Orientation	64
ET-1.	Helicopter Position	67
ET-2.	Helicopter Velocity	68
ET-3.	Angular Orientation	69
ET-4.	Linear Velocity	70

LIST OF ILLUSTRATIONS

Figure/Part I--Linearization Page

1. Control Position Trim Curves 17
2. Transient Response Due to Longitudinal Cyclic Pitch 18

BF-1. Coefficient of Drag Vs. Angle of Attack 37

BF-2. Coefficient of Drag Vs. Angle of Attack 37

BF-3. Partitioned Drag Curve 39

Figure/Part II--Application

1. Helicopter Flight Path Model 94
2. Pilot Model Function 95
3. Control Problem 95
4. Inertial Position for Level Flight 96
5. Inertial Position for Climb Configuration 97
6. Inertial Position for Climb Configuration 97
7. Inertial Position for Dive Configuration 98
8. Inertial Position for Dive Configuration 98
9. Inertial Position for Turn Configuration 99
10. Turn Configuration Altitude Vs. Time 100
11. Level Flight Roll Vs. Time 101
12. Climb Configuration Roll Vs. Time 101

Figure Page

13. Dive Configuration Roll Vs. Time 102

14. Turn Configuration Roll Vs. Time 102

15. Level Flight Pitch Vs. Time 103

16. Climb Configuration Pitch Vs. Time 103

17. Dive Configuration Pitch Vs. Time 104

18. Turn Configuration Pitch Vs. Time 104

19. Level Flight YAW Vs. Time 105

20. Climb Configuration YAW Vs. Time 105

21. Dive Configuration YAW Vs. Time 106

22. Turn Configuration YAW Vs. Time 106

23. Level Flight Collective Pitch 107

24. Level Flight Lateral Cyclic 107

25. Level Flight Longitudinal Cyclic 108

26. Level Flight Tail Rotor Pitch 108

27. Climb Configuration Collective Pitch 109

28. Climb Configuration Lateral Cyclic 109

29. Climb Configuration Longitudinal Cyclic 110

30. Climb Configuration Tail Rotor Pitch 110

31. Dive Configuration Collective Pitch 111

32. Dive Configuration Lateral Cyclic 111

33. Dive Configuration Longitudinal Cyclic 112

34. Dive Configuration Tail Rotor Pitch 112

Figure | Page

35. Turn Configuration Collective Pitch 113

36. Turn Configuration Lateral Cyclic 114

37. Turn Configuration Longitudinal Cyclic 115

38. Turn Configuration Tail Rotor Pitch 116

39. Pilot Action Response 117

LINEARIZATION OF EQUATIONS WHICH GOVERN THE MOTION OF A HELICOPTER

by

Alfred Fermelia

and

Virgil J. Flanigan*

ABSTRACT

The nonlinear set of equations which represents helicopter motion are linearized about a prescribed nominal state. Once the linearized system is obtained it is validated by comparing the output of the nonlinear system to that of its linearized counterpart. Having obtained a linear model, linear system theory may then be applied in order to investigate the stability and control characteristics of the aircraft.

---

*The authors are associated with the Department of Mechanical and Aerospace Engineering, University of Missouri-Rolla, Rolla, Missouri, where Mr. Fermelia is a Graduate Student and Dr. Flanigan (member ASME) is an Associate Professor.

TABLE OF CONTENTS

	Page
ABSTRACT	1
NOTATION	3
INTRODUCTION	4
PROBLEM STATEMENT	6
SOLUTION	7
VALIDATION	9
CONCLUSIONS AND RECOMMENDATIONS	12
ACKNOWLEDGMENTS	14
REFERENCES	15
LIST OF ILLUSTRATIONS	16

NOTATION

In the paper all bold-face capital letters denote matrices. Vectors are defined in column format and are denoted by lower case letters in bold face type. All scalars will be denoted by plain upper or lower case letters. Occasionally it may be necessary to illustrate a vector in the following format:

$$\underline{x} = \begin{bmatrix} x_1 \\ x_2 \\ \cdot \\ \cdot \\ \cdot \\ x_n \end{bmatrix}$$

These general rules will hold unless otherwise specified in the text.

Numbers in brackets designate references at the end of the paper.

INTRODUCTION

In order to investigate the stability and control characteristics of a helicopter, a suitable mathematical model which represents the dynamics of the vehicle must be selected. Several mathematical models describing helicopter dynamics are available. Two of these, the Bell C-81 program [1] and the U.S. Army ECOM hybrid simulator [2] are especially notable in that the necessary aerodynamic coefficients and various simulation constants have been established for a particular helicopter. The major limitations for the present C-81 program are its large size and lengthy computation time for simulated maneuvers. The C-81 program developed by Bell requires approximately 200 seconds of computer time to yield 1 second of helicopter flight simulation, whereas the ECOM model takes approximately 32 computer seconds to yield 1 second of flight simulation. This reduction in time is attributed to the simplified analysis of the transient aerodynamics and rotor force in the latter model. Since the ECOM model represents a considerable savings in computer costs, has been validated by the Bell Helicopter Corporation [3], contains a simplified analysis of the transient aerodynamics and rotor forces, and is a general purpose simulation designed for simulation of ten or more helicopters, it was selected to provide the basic structure for the helicopter dynamics.

Validation of the nonlinear model was achieved by (1) a comparison check with actual flight test data under trim conditions and (2) evaluation of the transient response due to control inputs. Figure 1 shows the comparison between actual flight test and the ECOM model. Transient responses of pitch, roll and yaw and their rates due to a longitudinal cyclic input are illustrated in Figure 2. The responses are typical of actual flight data.

In actual flight the pilot manipulates the controls, cyclic, collective, and pedal, either to trim the helicopter for steady flight by balancing the external forces and moments or to produce a desired maneuver by controlling the unbalance of these forces and moments. These external actions on the aircraft are expressed as nonlinear functions of the independent variables which are used to describe the state of the helicopter. Even though the control system being considered is nonlinear, the equations governing its motion may be characterized as linear over certain regions of the state space.

Computational techniques for the analysis of nonlinear control systems are not well understood and are in their infancy, even with the present state of the art. Nevertheless, there are some useful mathematical tools which may be applied to nonlinear systems. One such tool, linearization, is a very powerful and useful technique. In implementing linearization, it is usually assumed that the nonlinear control problem has been completely solved for one set of parameters, initial conditions and system inputs, and then seeks the solution for different parameters, initial conditions or inputs which are "sufficiently close" to those of the exact solution. The exact solution, often called the nominal solution or nominal trajectory is assumed known for one set of conditions.

The purpose of this paper is to describe the linearization procedure as applied to the equations of motion which represents helicopter motion. Once the linearized system is obtained it is discretized and then validated by comparing the output of the nonlinear system to that of its linearized counterpart.

A listing of the nonlinear equations of motion and the linearization technique is described in the appendix.

Problem Statement

The helicopter airframe simulation provided by ECOM presents the equations of motion in the form

$$\dot{\underline{x}} = \underline{\phi}[\underline{f},\underline{m},\underline{x}] \qquad (1)$$

where $\underline{\phi}$ (a 10 x 1 vector) is a nonlinear function of the vector forces, moments, and state variables. The external vector forces and moments active on the airframe may be expressed as

$$\underline{f} = \underline{g}[\underline{x},\underline{u}] \qquad (2)$$

$$\underline{m} = \underline{h}[\underline{x},\underline{u}] \qquad (3)$$

where $\underline{g}$ (a 3 x 1 vector) and $\underline{h}$ (a 3 x 1 vector) are nonlinear functions of state vector, $\underline{x}$, and the control vector $\underline{u}$. Hence equation (1) may be written as

$$\dot{\underline{x}} = \underline{\phi}(\underline{x},\underline{u}). \tag{4}$$

Hence it is desirable to obtain a linear system which approximates the system described by equation (4).

Solution

Allow the state vector and the control vector to be perturbed from some nominal condition, i.e.,

$$\underline{x} = \underline{x}^* + \delta\underline{x} \tag{5}$$

$$\underline{u} = \underline{u}^* + \delta\underline{u} \tag{6}$$

where $\underline{x}^*$ and $\underline{u}^*$ are defined as nominal state and control vectors respectively. Similarly $\delta\underline{u}$ is the perturbed control and $\delta\underline{x}$ is the change in $\underline{x}$ due to the new control and also possibly to perturbed boundary conditions. Expanding $\underline{\phi}(\underline{x},\underline{u})$ about the point $(\underline{x}^*,\underline{u}^*)$ and retaining only first order terms in powers of $(\underline{x}-\underline{x}^*)$ and $(\underline{u}-\underline{u}^*)$ yields

$$\underline{\Phi}(\underline{x},\underline{u}) \approx \underline{\Phi}(\underline{x}^*,\underline{u}^*) + \left.\frac{\partial \Phi}{\partial \underline{x}}\right|_{\substack{\underline{x}^* \\ \underline{u}^*}} \delta\underline{x} + \left.\frac{\partial \Phi}{\partial \underline{u}}\right|_{\substack{\underline{x}^* \\ \underline{u}^*}} \delta\underline{u} \tag{7}$$

where, by definition

$$\frac{\partial \underline{\phi}}{\partial \underline{x}} = \begin{bmatrix} \frac{\partial \phi_1}{\partial \underline{x}_1} & \cdots & \frac{\partial \phi_1}{\partial \underline{x}_{10}} \\ \vdots & & \\ \frac{\partial \phi_{10}}{\partial \underline{x}_1} & \cdots & \frac{\partial \phi_{10}}{\partial \underline{x}_{10}} \end{bmatrix} \tag{8}$$

$$\frac{\partial \Phi}{\partial \underline{u}} = \begin{bmatrix} \frac{\partial \phi_1}{\partial \underline{u}_1} & \cdots & \frac{\partial \phi_1}{\partial \underline{u}_4} \\ \cdot & & \\ \cdot & & \\ \cdot & & \\ \frac{\partial \phi_{10}}{\partial \underline{u}_1} & \cdots & \frac{\partial \phi_{10}}{\partial \phi_4} \end{bmatrix} \tag{9}$$

Denoting the 10 x 10 Jacobian matrix, $\frac{\partial \Phi}{\partial \underline{x}}$, by $A(\underline{x},\underline{u})$ and the 10 x 4 Jacobian matrix, $\frac{\partial \Phi}{\partial \underline{u}}$ by $B(\underline{x},\underline{u})$, equation (7) can be written as

$$\underline{\phi}(\underline{x},\underline{u}) \approx \underline{\phi}(\underline{x}^*, \underline{u}^*) + A(\underline{x}^*,\underline{u}^*)\delta\underline{x} + B(\underline{x}^*,\underline{u}^*)\delta\underline{u}. \tag{10}$$

Substituting this expression into the right hand side of equation (4) and using (5) yields

$$\dot{\underline{x}}^* + \delta\dot{\underline{x}} = \phi(\underline{x}^*,\underline{u}^*) + A(\underline{x}^*,\underline{u}^*)\delta\underline{x} + B(\underline{x}^*,\underline{u}^*)\delta\underline{u}. \tag{11}$$

But since

$$\dot{\underline{x}}^* = \phi(\underline{x}^*,\underline{u}^*),$$

equation (11) simplifies to

$$\delta\dot{\underline{x}} = A(\underline{x}^*,\underline{u}^*)\delta\underline{x} + B(\underline{x}^*,\underline{u}^*)\delta\underline{u}. \tag{12}$$

The boundary conditions for the linearized equation are obtained in a straightforward fashion. Assume, for example, that only the initial condition is prescribed and for the nominal solution is $\underline{x}^*(t_o) = \underline{x}_o^*$. If the initial condition for the perturbed problem is changed to $\underline{x}(t_o) = \underline{x}_o$, then the initial condition for the solution to the linearized equation is

$$\delta\underline{x}(t_o) = \underline{x}_o - \underline{x}_o^*.$$

Having obtained a solution to the linear perturbation equation (12), the approximate state of the vehicle is obtained by using equation (5).

Since the system being considered is essentially discrete in form, i.e., the pilot manipulates the controls at a sampling rate compatible with his reactive time, it is convenient to discretize equation (12).

Consider the derivative $\delta \underline{x}(t)$ to be approximated as

$$\delta \dot{\underline{x}}(t) = \frac{\delta \underline{x}(t + \Delta t) - \delta \underline{x}(t)}{\Delta t} . \qquad (13)$$

Substituting equation (13) into (12) yields

$$\frac{\delta \underline{x}(t + \Delta t) - \delta \underline{x}(t)}{\Delta t} = A(\underline{x}^*,\underline{u}^*)\delta \underline{x}(t) + B(\underline{x}^*,\underline{u}^*)\delta \underline{u}(t)$$

or

$$\delta \underline{x}(t + \Delta t) = (I + A\Delta t)\delta \underline{x}(t) + B\Delta t\delta \underline{u}(t) \qquad (14)$$

where the arguments of A and B have been suppressed in order to simplify the notation. Note that I represents the 10 x 10 identity matrix.

Note also that equation (14) can also be written as

$$\delta \underline{x}(t) = (I + A\Delta t)\delta \underline{x}(t - \Delta t) + B\Delta t\delta \underline{u}(t - \Delta t). \qquad (15)$$

Using equation (15) and the discrete version of (5), i.e.,

$$\underline{x}(t + \Delta t) = \underline{x}(t) + \delta \underline{x}(t), \qquad (16)$$

will yield a set of discrete equations which represent the motion of a helicopter.

Validation

Once the linearized system is obtained it is validated by 1) a static check, 2) a homogeneous test case, and 3) by implementing an objecting function test. All three methods of validating the linear model compare the output of the nonlinear system to its linearized counterpart. This section will describe the above comparison tests.

Static Check: In order to linearize the equations of motion all variables describing the internal dynamics of the vehicle had to be expressed in terms of the state and control parameters. An examination of the equations in Appendix A illustrates the complexity of this objective. In order to insure that all auxiliary variables were properly expressed the static test was contrived.

To illustrate the static test, consider the partial

$$\frac{\partial \phi_1}{\partial \underline{x}_1} = \frac{\partial \phi_1'}{\partial f_1} \frac{\partial f_1}{\partial \underline{x}_1} + \frac{\partial \phi_1'}{\partial \underline{x}_1} \tag{17}$$

where the right hand side of equation (17) is obtained from (1). Note the force, f_1, is the sum of forces acting on the aircraft c.g. along the longitudinal axis--see Appendix A. It can be shown that

$$\frac{\partial \phi_1'}{\partial f_1} = \frac{1}{m}$$

where m is the mass of the aircraft. Also examination of Appendix A illustrates that the last term of (17) is easily verified. Hence the only term to substantiate is the partial

$$\frac{\partial f_1}{\partial \underline{x}_1}$$

Assuming that $\underline{x}_1$ is the only variable allowed to change, the total variation in the force, f_1, can be approximated as

$$\delta f_1 = \frac{\partial f_1}{\partial \underline{x}_1} \delta \underline{x}_1, \tag{18}$$

where

$$\delta \underline{x}_1 \triangleq \underline{x}_1 - \underline{x}_1^*, \tag{19}$$

$$\delta f_1 \triangleq f_1 - f_1^*. \tag{20}$$

The true variation, δf_1, due to the perturbation, $\delta \underline{x}_1$, is obtained from the nonlinear system as indicated by equation (20). Hence the partial of f_1 with respect to $\underline{x}_1$ can be substantiated by comparing the output of the linear system (18) with that of its nonlinear counterpart (20). The remaining elements in the matrices A, and B can be verified in a similar manner. Appendix C contains tables of data recorded from the static tests.

Homogeneous Test: In this test the aircraft obtains a trim configuration after which the nonlinear equations are integrated. The solution of (4) is given by

$$\underline{x}(k+1) = \underline{x}(k) + \dot{\underline{x}}(k) \cdot \Delta t. \tag{21}$$

Its linearized counterpart is obtained by solving (14) with the control perturbation set equal to zero, i.e.,

$$\delta \underline{x}(k) = (I + A\Delta t) \delta \underline{x}(k-1). \tag{22}$$

Substituting (22) into (5) yields

$$\underline{x}(k+1) = \underline{x}^*(k) + \delta \underline{x}(k). \tag{23}$$

Results of the homogeneous test are given in Appendix D.

Objective Function Test: A pseudo flight path is chosen and compared with the state generated by the linear system. This error is fed into an objective function which in turn is minimized. That is, a control goal is calculated which minimizes the objective function. The control goal is fed into both linear and non-linear systems and the corresponding outputs are then compared. Appendix E contains the results of the objective function tests.

Conclusions and Recommendations

With a few exceptions, the results obtained in the state check indicates that the linear model gives a good approximation to the nonlinear system. Examination of Table CT-2 shows a larger error in the change of the yawing moment, δN_A, due to approximately a 2% change in the w velocity. However, for larger percentage changes in w and at higher flight speeds this error decreases. The large error at 50 knots can be attributed to the change in engine torque. In the derivations of the linearized equations it was assumed that the engine torque, Q_E, was not a function of the w velocity. However, this torque does indeed change as a function of w and hence introduces an error when ignored. For larger changes in w, the effect of the change in engine torque is negated by changes in the other parameters. This is also true at higher speeds.

At higher speeds the linearization deteriorates for larger percentage changes in the state variable--see

Tables CT-5, CT-6, CT-17, and CT-18. However, the linearization with respect to the control variables is valid for changes up to 10%.

The inability to match the rate of climb is inherent to both the homogeneous test and the objective function means of validation. To explain this error, consider equation (24),

$$\dot{H} = u \cdot \sin\theta - (v \cdot \sin\phi + w \cdot \cos\phi)\cos\theta. \qquad (24)$$

As illustrated by the preceding equation, the change in the rate of climb depends on the variation in the linear velocities and the euler angles, θ and ϕ. Now consider the fourth entry of $\dot{H}$ in Table ET-2. Note that a reversal of sign exists between the two models. However, comparison of the other independent variables which comprise $\dot{H}$ shows good agreement--see Table ET-4. For this particular entry, calculation indicates the error is due to incorrect matching of the w velocity. Note that this velocity, when obtained via the linear model, is less than 0.3% of the actual. Obviously prediction of the w velocity is within reason, and therefore either a new linear model must be implemented or this error must be tolerated. While it appears that there is another linear representation that could be used, further tests have been conducted that indicate the simulation can endure this error without serious degradation of overall performance.

Acknowledgements

The authors wish to express their gratitude to Dr. D. A. Gyorog for his assistance in preparation of this work.

REFERENCES

1. Blankenship, B. L. and Bird, B. J., "Program C81-11 Rotorcraft Flight Simulation," Three Volumes, Bell Helicopter Company Report No. 599-068-900.

2. Baker, E., Hay, I., and Mitchell, E., "Development of Hybrid Computer Programs for Simulation of Cobra," Two Volumes, ECOM TR 0387-F2a, U.S. Army Electronics Command, January 1969.

3. Sonnebord and Tiller, "AH-1G Data for Hybrid Computer Simulation," Bell Helicopter Company, Report No. 209-099-112, September 1966.

LIST OF ILLUSTRATIONS

Figure Page

1. Control Position Trim Curves 17

2. Transient Response Due to Longitudinal Cyclic Pitch 18

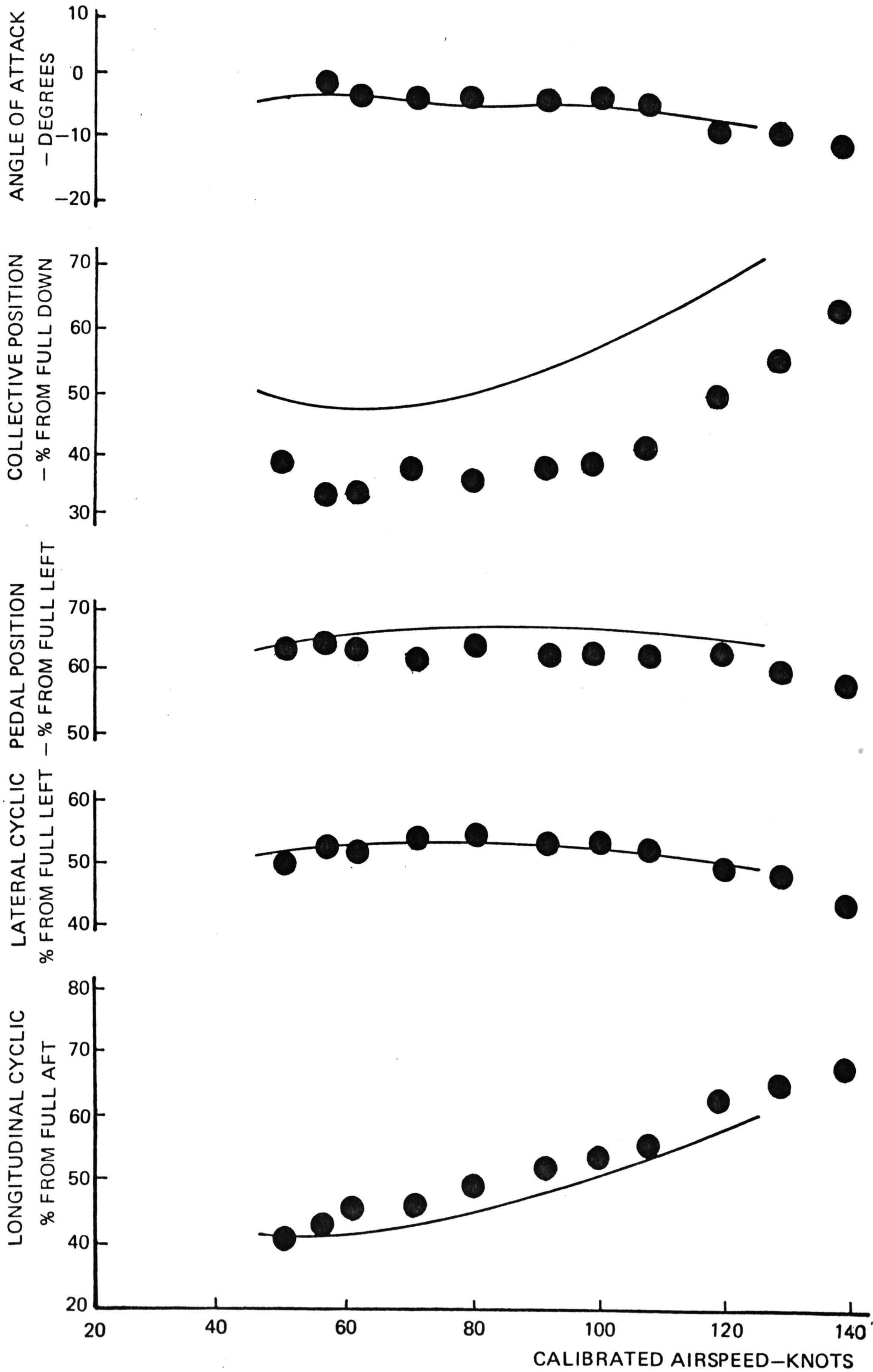
ANGLE OF ATTACK
— DEGREES
10
0
−10
−20
COLLECTIVE POSITION
— % FROM FULL DOWN
70
60
50
40
30
PEDAL POSITION
— % FROM FULL LEFT
70
60
50
LATERAL CYCLIC
% FROM FULL LEFT
60
50
40
LONGITUDINAL CYCLIC
% FROM FULL AFT
80
70
60
50
40
20
20
40
60
80
100
120
140
CALIBRATED AIRSPEED—KNOTS

Figure 1

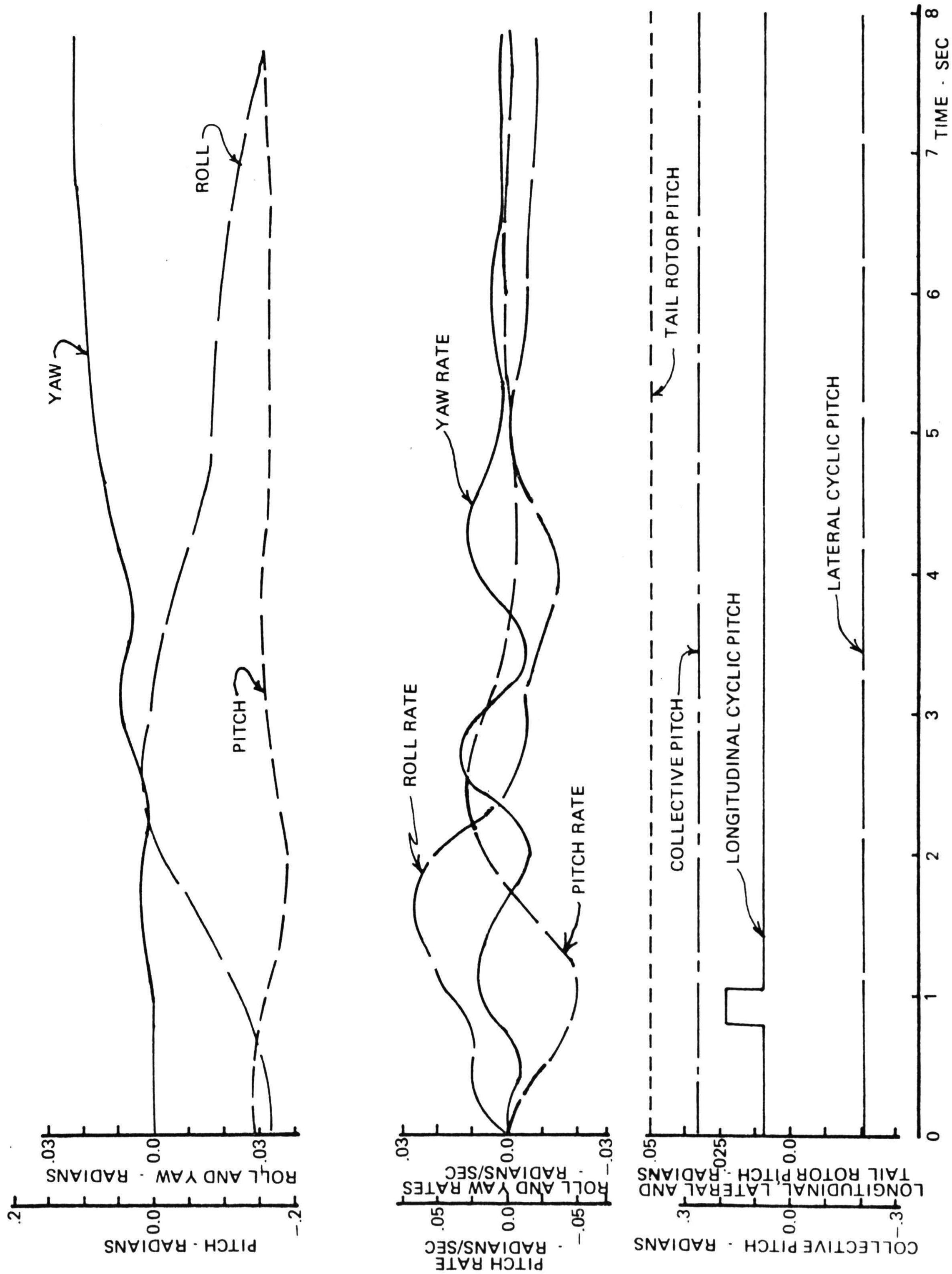
YAW
ROLL
PITCH
ROLL AND YAW - RADIANS
.03
0.0
.03
PITCH - RADIANS
.2
0.0
-.2
ROLL RATE
YAW RATE
PITCH RATE
ROLL AND YAW RATES - RADIANS/SEC
PITCH RATE - RADIANS/SEC
.05
-.05
TAIL ROTOR PITCH
COLLECTIVE PITCH
LONGITUDINAL CYCLIC PITCH
LATERAL CYCLIC PITCH
LONGITUDINAL, LATERAL AND TAIL ROTOR PITCH - RADIANS
.025
COLLECTIVE PITCH - RADIANS
.3
-.3
TIME - SEC
0
1
2
3
4
5
6
7
8

Figure 2

APPENDIX A

EQUATIONS OF MOTION

The U.S. ECOM simulation is designed to compute the forces and moments acting on the helicopter rotor and airframe. These forces and moments are resolved in a body axis coordinate frame. Body axes are defined with the origin at the aircraft center of gravity and axes oriented as:

$X \triangleq$ Forward through the nose, perpendicular to the rotor shaft;

$Y \triangleq$ Out to the right, perpendicular to the plane containing the rotor shaft and X;

$Z \triangleq$ Down and parallel to the shaft.

The state variables are defined as follows:

1. $u \triangleq$ Forward velocity, positive directed along X.
2. $v \triangleq$ Side velocity, positive directed along Y.
3. $w \triangleq$ Down velocity, positive directed along Z.
4. $p \triangleq$ Roll rate, directed along X.
5. $q \triangleq$ Pitch rate, directed along Y.
6. $r \triangleq$ Yaw rate, directed along Z.
7. $\phi \triangleq$ Roll angle.
8. $\theta \triangleq$ Pitch angle.
9. $\psi \triangleq$ Yaw angle.
10. $\Omega \triangleq$ Rotor rpm.

Parameters 7-9 are the Euler angles which relate the actual position of the aircraft to an inertial reference frame.

The pilot input control variables are defined as follows:

1. $u_1 \triangleq$ collective pitch
2. $u_2 \triangleq$ lateral cyclic
3. $u_3 \triangleq$ longitudinal cyclic
4. $u_4 \triangleq$ tail rotor pitch

Having defined the coordinate frame and the independent variables, linear perturbation theory can be applied to obtain a linear model. However, before linearization is performed the nonlinear equations of motion will be summarized below:

Forces

$$\dot{u} = \frac{X_A}{m} + rv - qw - g \sin \theta$$

$$\dot{v} = \frac{Y_A}{m} + pw - ru + g \cos \theta \sin \phi$$

$$\dot{w} = \frac{Z_A}{m} + qu = pv + g \cos \theta \cos \Phi$$

Moments

$$\dot{p} = [L_A - (I_{yy}-I_{zz})qr]/I_{xx}$$

$$\dot{q} = [M_A - (I_{zz}-I_{xx})rp]/I_{yy}$$

$$\dot{r} = [N_A - (I_{xx}-I_{yy})pq]/I_{zz}$$

Euler Angles

$$\dot{\phi} = p + \dot{\psi} \sin \theta$$

$$\dot{\theta} = r \sin \phi + q \cos \phi$$

$$\dot{\psi} = (r \cos \phi + q \sin \phi)/\cos \theta$$

Rotor speed

$$\dot{\Omega} = (QMR)/IROT$$

To illustrate the method of linearization, consider the equation representing the sum of forces acting on the aircraft c.g. along the longitudinal axis, i.e.,

$$\dot{u} = \frac{X_A}{m} + rv - qw - g \sin \theta \tag{1}$$

where

$$X_A = f(u,v,w,p,q,r,\Omega,\underline{u})$$

and the control vector, $\underline{u}$,is defined as

$$u \triangleq \begin{bmatrix} u_1 \\ u_2 \\ u_3 \\ u_4 \end{bmatrix}$$

Now by letting all variables be perturbed from some nominal value, i.e., let

$$\begin{aligned} u &= u^* + \delta u \\ v &= v^* + \delta v \\ &\vdots \\ &\text{etc.} \end{aligned} \tag{2}$$

and since X_A may be expanded as

$$\delta X_A = \frac{\partial f}{\partial \underline{x}}\bigg|_{\underline{x}^*,\underline{u}^*} \delta\underline{x} + \frac{\partial f}{\partial \underline{u}}\bigg|_{\underline{x}^*,\underline{u}^*} \delta\underline{u} \tag{3}$$

Equation (1) can be expressed as

$$\delta \dot{u} = \frac{1}{m}\left.\frac{\partial f}{\partial \underline{x}}\right|_{\underline{x}^*,\underline{u}^*} \delta \underline{x} + \left.\frac{\partial f}{\partial \underline{u}}\right|_{\underline{x}^*,\underline{u}^*} \delta \underline{u}$$

$$+ r^*\delta v + q^*\delta w - w^*\delta q + v^*\delta r - g \cos \theta^* \; \delta\theta \quad (4)$$

Note that the vector $\delta\underline{x}$ represents the perturbed state; i.e.,

$$\delta\underline{x}^T = (\delta u \; \delta v \; \delta w \; \delta p \; \delta q \; \delta r \; \delta\phi \quad \delta\theta \quad \delta\psi \quad \delta\Omega),$$

and that $\delta\underline{u}$ is the perturbed control vector

$$\delta\underline{u}^T = (\delta u_1 \; \delta u_2 \; \delta u_3 \; \delta u_4).$$

Also it should be pointed out that the partials in equation (3), are evaluated along a prespecified nominal state, $\underline{x}^*$, and a nominal control, $\underline{u}^*$.

By inspection (4) may now be expressed in the form

$$\delta\dot{u} = \underline{a} \; \delta\underline{x} + \underline{b} \; \delta\underline{u},$$

where $\underline{a}$ and $\underline{b}$ are (1x10) and (1x4) row vectors respectively.

Implementing the perturbation technique on the remaining equations yields a set of linear differential equations of the form

$$\delta\dot{\underline{x}} = A\delta\underline{x} + B\delta\underline{u},$$

where A is a (10x10) stability matrix and B is a (10x4) control matrix.

Matrix A

In order to examine the elements which comprise the A matrix, consider the partitioned form of A, i.e.,

$$A = \left[\begin{array}{c|c} A_1 & A_2 \\ \hline A_3 & A_4 \end{array}\right]$$

where

$A_1 = A_{ij}$ $\quad$ $i = 1\text{-}6$ $\quad$ $j = 1\text{-}6$

$A_2 = A_{ij}$ $\quad$ $i = 1\text{-}6$ $\quad$ $j = 7\text{-}10$

$A_3 = A_{ij}$ $\quad$ $i = 7\text{-}10$ $\quad$ $j = 1\text{-}6$

$A_4 = A_{ij}$ $\quad$ $i = 7\text{-}10$ $\quad$ $k = 7\text{-}10$

The elements of A_1, A_2, A_3, and A_4 are given in Tables A1-1, A1-2, A1-3, and A1-4, respectively.

TABLE A1-1

ELEMENTS OF A_1

	1	2	3	4	5	6
1	$\frac{f_{1,1}}{m}$	$\frac{f_{1,2}}{m} + r$	$\frac{f_{1,3}}{m} - q$	$\frac{f_{1,4}}{m}$	$\frac{f_{1,5}}{m} - w$	$\frac{f_{1,6}}{m} + v$
2	$\frac{f_{2,1}}{m} - r$	$\frac{f_{2,2}}{m}$	$\frac{f_{2,3}}{m} + p$	$\frac{f_{2,4}}{m} + w$	$\frac{f_{2,5}}{m}$	$\frac{f_{2,6}}{m} - u$
3	$\frac{f_{3,1}}{m} + q$	$\frac{f_{3,2}}{m} - q$	$\frac{f_{3,3}}{m}$	$\frac{f_{3,4}}{m} - v$	$\frac{f_{3,5}}{m} + u$	$\frac{f_{3,6}}{m}$
4	$\frac{f_{4,1}}{I_{xx}}$	$\frac{f_{4,2}}{I_{xx}}$	$\frac{f_{4,3}}{I_{xx}}$	$\frac{f_{4,4}}{I_{xx}}$	$\frac{[f_{4,5}+(I_{yy}-I_{zz})]r}{I_{xx}}$	$\frac{[f_{4,6}+(I_{yy}-I_{zz})]q}{I_{xx}}$
5	$\frac{f_{5,1}}{I_{yy}}$	$\frac{f_{5,2}}{I_{yy}}$	$\frac{f_{5,3}}{I_{yy}}$	$\frac{f_{5,4}}{I_{yy}} + \frac{(I_{zz}-I_{xx})r}{I_{yy}}$	$\frac{f_{5,5}}{I_{yy}}$	$\frac{(I_{zz}-I_{yy})}{I_{yy}} + \frac{f_{5,6}}{I_{yy}}$
6	$\frac{f_{6,1}}{I_{zz}}$	$\frac{f_{6,2}}{I_{zz}}$	$\frac{f_{6,3}}{I_{zz}}$	$\frac{(I_{xx}-I_{yy})}{I_{zz}} + \frac{f_{6,4}}{I_{zz}}$	$\frac{(I_{xx}-I_{yy})}{I_{zz}} + \frac{f_{6,5}}{I_{zz}}$	$\frac{f_{6,6}}{I_{zz}}$

TABLE A1-2

ELEMENTS OF A_2

	7	8	9	10
1	0	$-g \cos \theta$	0	$\frac{f_{1,10}}{m}$
2	$g \cos \phi \cos \theta$	$-g \sin \phi \sin \theta$	0	$\frac{f_{2,10}}{m}$
3	$-g \sin \phi \cos \theta$	$-g \cos \phi \sin \theta$	0	$\frac{f_{3,10}}{m}$
4	0	0	0	$\frac{f_{4,10}}{m}$
5	0	0	0	$\frac{f_{5,10}}{m}$
6	0	0	0	$\frac{f_{6,10}}{m}$

TABLE A1-3

ELEMENTS OF A_3

	1	2	3	4	5	6
7	0	0	0	1	$-\tan\theta \sin\phi$	$-\tan\theta \cos\phi$
8	0	0	0	0	$\cos\phi$	$-\sin\phi$
9	0	0	0	0	$\frac{\sin\phi}{\cos\theta}$	$\frac{\cos\phi}{\cos\theta}$
10	$\frac{f_{10,1}}{I_{ROT}}$	$\frac{f_{10,2}}{I_{ROT}}$	$\frac{f_{10,3}}{I_{ROT}}$	$\frac{f_{10,4}}{I_{ROT}}$	$\frac{f_{10,5}}{I_{ROT}}$	$\frac{f_{10,6}}{I_{ROT}}$

TABLE A1-4

ELEMENTS OF A_4

	7	8	9	10
7	$-\tan\theta(q\cos\phi - r\sin\phi)$	$-\dot{\psi}(\cos\theta + \tan\theta\sin\theta)$	0	0
8	$-(r\cos\phi + q\sin\phi)$	0	0	0
9	$\frac{q\cos\phi}{\cos\theta} - \frac{r\sin\phi}{\cos\theta}$	$\dot{\psi}\tan\theta$	0	0
10	0	0	0	0

Note the $f_{i,j}$ components of the A_1 matrix represents partial derivatives with respect to specific states evaluated at some nominal state, x_2^*, and a nominal control, u*. They are as follows:

$$f_{1,j} = \left.\frac{\partial X_A}{\partial x_j}\right|_{\underline{x}^*,\underline{u}^*} \qquad j = 1\text{-}6$$

$$f_{2,j} = \left.\frac{\partial Y_A}{\partial x_j}\right|_{\underline{x}^*,\underline{u}^*} \qquad j = 1\text{-}6$$

$$f_{3,j} = \left.\frac{\partial Z_A}{\partial x_j}\right|_{\underline{x}^*,\underline{u}^*} \qquad j = 1\text{-}6$$

$$f_{4,j} = \left.\frac{\partial L_A}{\partial x_j}\right|_{\underline{x}^*,\underline{u}^*} \qquad j = 1\text{-}6$$

$$f_{5,j} = \left.\frac{\partial M_A}{\partial x_j}\right|_{\underline{x}^*,\underline{u}^*} \qquad j = 106$$

$$f_{6,j} = \left.\frac{\partial N_A}{\partial x_j}\right|_{\underline{x}^*,\underline{u}^*} \qquad j = 1\text{-}6$$

The forces acting on the aircraft are given by the equations

$$X_A = X_F + X_W + F_{XR},$$

$$Y_A = Y_F + Y_{TR} + V_{VS} + F_{YR},$$

$$Z_A = Z_F + Z_W + Z_{HS} - L_{MR},$$

and the external moments acting along the X, Y, and Z axes of the aircraft are

$$L_A = DZ \cdot F_{YR} + DZTR \cdot Y_{TR} + DZVS \cdot Y_{VS} + L_F,$$

$$M_A = -DZ \cdot F_{XR} + DZ \cdot L_{MR} + (DXW-DX) \cdot Z_N - DZW \cdot X$$
$$+ DXHS \cdot Z_{HS} + M_F,$$

$$N_A = -DX \cdot F_{YR} - DXTR \cdot Y_{TR} - DXVS \cdot Y_{VS} + Q_E + N_F,$$

respectively.

At this point the components of the A_1 matrix may be expanded as follows:

$$\frac{\partial X_A}{\partial \underline{y}} = \frac{\partial X_F}{\partial \underline{y}} + \frac{\partial X_W}{\partial \underline{y}} + \frac{\partial F_{XR}}{\partial \underline{y}}$$

$$\frac{\partial Y_A}{\partial \underline{y}} = \frac{\partial Y_F}{\partial \underline{y}} + \frac{\partial Y_{TR}}{\partial \underline{y}} + \frac{\partial Y_{VS}}{\partial \underline{y}} + \frac{\partial F_{YR}}{\partial \underline{y}}$$

$$\frac{\partial Z_A}{\partial \underline{y}} = \frac{\partial Z_F}{\partial \underline{y}} + \frac{\partial Z_W}{\partial \underline{y}} + \frac{\partial Z_{HS}}{\partial \underline{y}} - \frac{\partial L_{MR}}{\partial \underline{y}}$$

$$\frac{\partial L_A}{\partial \underline{y}} = DZ \cdot \frac{\partial F_{YR}}{\partial \underline{y}} + DZTR \cdot \frac{\partial Y_{TR}}{\partial \underline{y}} + DZVS \cdot \frac{\partial Y_{VS}}{\partial \underline{y}} + \frac{\partial L_F}{\partial \underline{y}}$$

$$\frac{\partial M_A}{\partial \underline{y}} = -DZ \cdot \frac{\partial F_{XR}}{\partial \underline{y}} + DZ \cdot \frac{\partial L_{MR}}{\partial \underline{y}} + (DXW - DX) \cdot \frac{\partial Z_W}{\partial \underline{y}}$$
$$-DZW \cdot \frac{\partial X_W}{\partial \underline{y}} + DXHS \cdot \frac{\partial Z_{HS}}{\partial \underline{y}} + \frac{\partial M_F}{\partial \underline{y}}$$

$$\frac{\partial N_A}{\partial \underline{y}} = -DX \cdot \frac{\partial F_{YR}}{\partial \underline{y}} - DXTR \cdot \frac{\partial Y_{TR}}{\partial \underline{y}} - DXVS \cdot \frac{\partial Y_{VS}}{\partial \underline{y}}$$
$$+ \frac{\partial Q_E}{\partial \underline{y}} + \frac{\partial N_F}{\partial \underline{y}}$$

where the state vector, y, is defined as

$$\underline{y}^T = (u \quad v \quad w \quad p \quad q \quad r \ ).$$

The fuselage, wing, main rotor, and tail rotor forces along the X, Y, and Z axes of the aircraft are

X Axis

$$X_F = q_L \cdot SYF \cdot CYF1$$

$$X_W = q_V \cdot SXW \cdot CSW1 + i_w \cdot Z_W$$

$$F_{XR} = \sum_{\psi_i} \left\{ \left(\sum_{y_j} \Delta L_{\psi_i} \right) \beta_{\psi_i} \sin \psi_i + \left(\sum_{y_j} \Delta D_{\psi_i, y_j} \right) \cos \psi_i \right\}$$

Y Axis

$$Y_F = q_L \cdot SYF \cdot CYFI$$

$$Y_{VS} = q_L \cdot SYVS \cdot CYVS$$

$$F_{YR} = -\left[\sum_{\psi_i} \left\{ \left(\sum_{y_j} \Delta L_{\psi_i, y_j} \right) \beta_{\psi_i} \sin\psi_i + \left(\sum_{y_j} \Delta D_{\psi_i, y_j} \right) \cos \psi_i \right\} \right]$$

$$Y_{TR} = FKTR1 \cdot \theta_{TR} \cdot (V_T^{\,2} + FKTR2)$$

$$- FKTR3\ (V_{TR} + V_{IM})$$

Z Axis

$$Z_F = q_V \cdot SZF \cdot CZFI$$

$$Z_W = q_V \cdot SZM \cdot CZW1$$

$$L_{MR} = \sum_{\psi_i} \sum_{y_j} \Delta L_{\psi_i, y_j}$$

$$Z_{HS} = q_V \cdot SZHS \cdot CZHS$$

Therefore the partials of forces and moments with respect to the state variable, y, are given as

Forces:

$$\frac{\partial X_A}{\partial \underline{y}} = \frac{\partial q_L}{\partial \underline{y}} \cdot SXF1 \cdot CXF1 + q_L \cdot SXF1 \cdot \frac{\partial CSF1}{\partial \underline{y}}$$

$$+ \frac{\partial qv}{\partial \underline{y}}\ SXF2 \cdot CXF2 + SXW \cdot CXW1 + i_w \cdot SZW \cdot CZW1$$

$$+ q_v\ SXFZ \cdot \frac{\partial CXFZ}{\partial \underline{y}} + SXW \cdot \frac{\partial CXW1}{\partial \underline{y}} + i_w \cdot SXW \cdot \frac{\partial CZW1}{\partial \underline{y}}$$

$$+ \sum_{\psi_i} \Bigg\{ \Bigg(\sum_{y_j} \frac{\partial \Delta L_{\psi_i, y_j}}{\partial \underline{y}} \beta_{\psi_i} \sin\psi_i \cdot S\psi_i$$

$$+ \sum_{y_j} \Delta L_{\psi_i, y_j} \sin \psi_i \frac{\partial \beta_{\psi_i}}{\partial \underline{y}} \Bigg) - \Bigg(\sum_{y_j} \frac{\partial \Delta D_{\psi_i, y_j}}{\partial \underline{y}} \Bigg) \cos\psi_i \Bigg\}$$

$$\frac{\partial Y_A}{\partial \underline{y}} = \frac{\partial q_L}{\partial \underline{y}} \left\{ SYF \cdot CYF1 + SYVS \cdot CYVS \right\}$$

$$+ q_L \left\{ SYF \cdot \frac{\partial CYF1}{\partial \underline{y}} + SYVS \cdot \frac{\partial CYVS}{\partial \underline{y}} \right\}$$

$$- \sum_{\psi_i} \left\{ \left(\sum_{y_j} \frac{\partial \Delta L\psi_i, y_j}{\partial \underline{y}} \right) \beta_{\psi_i} \sin\psi_i + \sum_{y_j} \left(\frac{\partial \Delta D\psi_i, y_j}{\partial \underline{y}} \right) \cos\psi_i \right\}$$

$$- \sum_{\psi_i} \left\{ \left(\sum_{y_j} \Delta L_{\psi_i, y_j} \right) \sin\psi_i \frac{\partial \beta_{\psi_i}}{\partial \underline{y}} \right\}$$

$$+ \frac{\partial Y_{TR}}{\partial V_T^{\,2}} \frac{\partial V_T^{\,2}}{\partial \underline{y}} + \frac{\partial Y_{TR}}{\partial V_{TR}} \frac{\partial V_{TR}}{\partial \underline{y}} + \frac{\partial Y_{TR}}{\partial V_{IV}} \frac{\partial V_{IM}}{\partial \underline{y}}$$

$$\frac{\partial Z_A}{\partial \underline{y}} = \frac{\partial q_v}{\partial \underline{y}} \left(SZF \cdot CZF1 + SZW \cdot CZW1 + SZHS \cdot CZHS \right)$$

$$+ q_v \left(SZF \cdot \frac{\partial CZF1}{\partial \underline{y}} + SZW \cdot \frac{\partial CZW1}{\partial \underline{y}} + SZHS \cdot \frac{\partial CZHS}{\partial \underline{y}} \right)$$

$$- \sum_{\psi_i} \sum_{y_j} \frac{\partial \Delta L_{\psi_i, y_j}}{\partial \underline{y}}$$

Moment

$$\frac{\partial L_A}{\partial \underline{y}} = DZ \cdot \frac{\partial F_{YR}}{\partial \underline{y}} + DZTR \cdot \frac{\partial Y_{TR}}{\partial \underline{y}} + DZVS \cdot \frac{\partial Y_{VS}}{\partial \underline{y}} + \frac{\partial L_F}{\partial \underline{y}}$$

$$\frac{\partial M_A}{\partial \underline{y}} = -DZ \cdot \frac{\partial F_{XR}}{\partial \underline{y}} + DX \cdot \frac{\partial L_{MR}}{\partial \underline{y}} + (DXW-DX) \frac{\partial Z_W}{\partial \underline{y}}$$

$$- DZW \cdot \frac{\partial X_W}{\partial \underline{y}} + DXHS \cdot \frac{\partial Z_{HS}}{\partial \underline{y}} + \frac{\partial M_F}{\partial \underline{y}}$$

$$\frac{\partial N_A}{\partial \underline{Y}} = -DX \quad \frac{\partial F_{YR}}{\partial \underline{Y}} - DXTR \cdot \frac{\partial Y_{TR}}{\partial \underline{Y}} - DXVS \cdot \frac{\partial Y_{VS}}{\partial \underline{Y}}$$

$$+ \frac{\partial Q_E}{\partial \underline{Y}} + \frac{\partial N_F}{\partial \underline{Y}}$$

At this point the elements of matrix A_1 are fully described. Considering the matrix A_2, the only elements to be clarified are those in the fourth row. These elements are given as

$$f_{1,10} = \frac{\partial X_A}{\partial \Omega} = \frac{\partial X_F}{\partial \Omega} + \frac{\partial X_W}{\partial \Omega} + \frac{\partial F_{XR}}{\partial \Omega}$$

$$f_{2,10} = \frac{\partial Y_A}{\partial \Omega} = \frac{\partial Y_F}{\partial \Omega} + \frac{\partial Y_{TR}}{\partial \Omega} + \frac{\partial Y_{YS}}{\partial \Omega} + \frac{\partial F_{YR}}{\partial \Omega}$$

$$f_{3,10} = \frac{\partial Z_A}{\partial \Omega} = \frac{\partial Z_F}{\partial \Omega} + \frac{\partial Z_W}{\partial \Omega} + \frac{\partial Z_{HS}}{\partial \Omega} - \frac{\partial L_{MR}}{\partial \Omega}$$

$$f_{4,10} = \frac{\partial L_A}{\partial \Omega} = DZ \cdot \frac{\partial F_{YR}}{\partial \Omega} + DZTR \cdot \frac{\partial Y_{TR}}{\partial \Omega} + DZVS \cdot \frac{\partial Y_{YS}}{\partial \Omega}$$

$$+ \frac{\partial L_F}{\partial \Omega}$$

$$f_{5,10} = \frac{\partial M_A}{\partial \Omega} = -DZ \cdot \frac{\partial F_{XR}}{\partial \Omega} + DX \cdot \frac{\partial L_{MR}}{\partial \Omega}$$

$$+ (DXW-DX) \cdot \frac{\partial Z_W}{\partial \Omega} - DZW \cdot \frac{\partial X_W}{\partial \Omega} + DXHJ \cdot \frac{\partial Z_{HS}}{\partial \Omega} + \frac{\partial M_F}{\partial \Omega}$$

$$f_{6,10} = \frac{\partial N_A}{\partial \Omega} = -DX \cdot \frac{\partial F_{YR}}{\partial \Omega} - DXTR \cdot \frac{\partial Y_{TR}}{\partial \Omega}$$

$$- DXVS \cdot \frac{\partial Y_{VS}}{\partial \Omega} + \frac{\partial Q_E}{} + \frac{\partial N_F}{\partial \Omega}$$

Utilizing the definition of the fuselage, wing, main rotor, and tail rotor forces and movements, the above equations can be expanded in the same manner as were the elements of Matrix A_1.

Matrix B

In order to facilitate the description of the control matrix, B, consider the partitioned form, i.e.,

$$B = \left[\begin{array}{c} B_1 \\ \hline B_2 \end{array}\right]$$

where

$$B_1 = B_{ij} \qquad i = 1\text{-}6 \qquad j = 1\text{-}4$$

$$B_2 = B_{ij} \qquad i = 6\text{-}10 \qquad j = 1\text{-}4.$$

Matrix B_1 can be expanded as follows

$$B_1 = \begin{bmatrix} b_{1,1} & \cdots & b_{1,4} \\ \vdots & & \\ b_{6,1} & \cdots & b_{6,4} \end{bmatrix}$$

where

$$b_{1,j} = \frac{1}{m}\frac{\partial X_A}{\partial u_j}, \qquad b_{5,j} = \frac{1}{m}\frac{\partial M_A}{\partial u_j},$$

$$b_{2,j} = \frac{1}{m}\frac{\partial Y_A}{\partial u_j}, \qquad b_{6,j} = \frac{1}{m}\frac{\partial N_A}{\partial u_j},$$

$$b_{3,j} = \frac{1}{m}\frac{\partial Z_A}{\partial u_j}, \qquad j = 1,4.$$

$$b_{4,j} = \frac{1}{m}\frac{\partial L_A}{\partial u_j},$$

Similarly the matrix B_2 is given as

$$B_2 = \begin{bmatrix} b_{7,1} & \cdots & b_{7,4} \\ \vdots & & \\ b_{10,1} & \cdots & b_{10,4} \end{bmatrix}$$

where

$$b_{i,j} = 0.0 \qquad i = 7\text{-}9 \qquad j = 1\text{-}4$$

and

$$b_{10,j} = \frac{1}{IROT}\frac{\partial\Omega}{\partial u_j} \qquad j = 1\text{-}4.$$

Utilizing the equations representing the forces and moments and performing the differentiation required of them, the control matrix B is totally defined. Therefore the objective of this appendix has been completed.

APPENDIX B
LIFT AND DRAG CURVES

Investigation of the ECOM model reveals that the changes of the incremental lift and drag parameters generated by the main rotor are both of the order of 6000 pounds. Therefore it is mandatory that the approximation of the lift and drag coefficient be as accurate as possible. The purpose of this appendix is to illustrate the technique developed to linearize these coefficients.

Before discussing the linearization technique, the method by which these coefficients are obtained will be explained. Since both lift and drag coefficients are generated in the same manner, this presentation will only consider the latter parameter.

The inputs required to obtain the drag coefficient, CD, are the rotor blade angle of attack, α, and that component of velocity, U_T, which is tangent to the cord of the rotor blade. Since the data available exists only for particular values of the velocity, U_T, an interpolation technique must be employed to give values of CD for any velocity and any angle of attack (Figure BF-1).

A simple example best illustrates the interpolation technique employed. Consider Figure BF-2 and suppose that the rotor blade at a particular station is operating with a tangential velocity between 250 and 500 feet per second. Knowing the angle of attack, α, the drag coefficient for the velocities of 500 and 250 feet per second are obtained. Therefore since

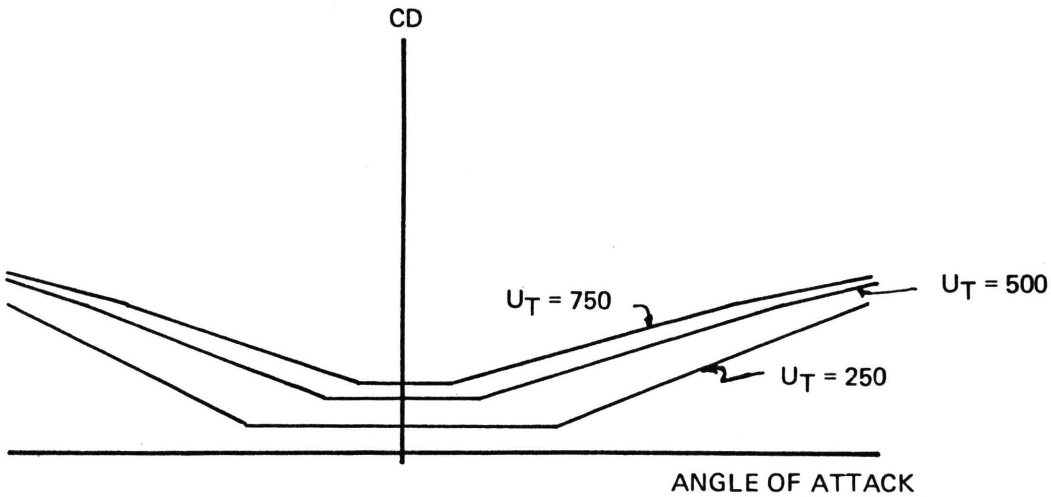

Figure BF-1 Coefficient of Drag Vs. Angle of Attack

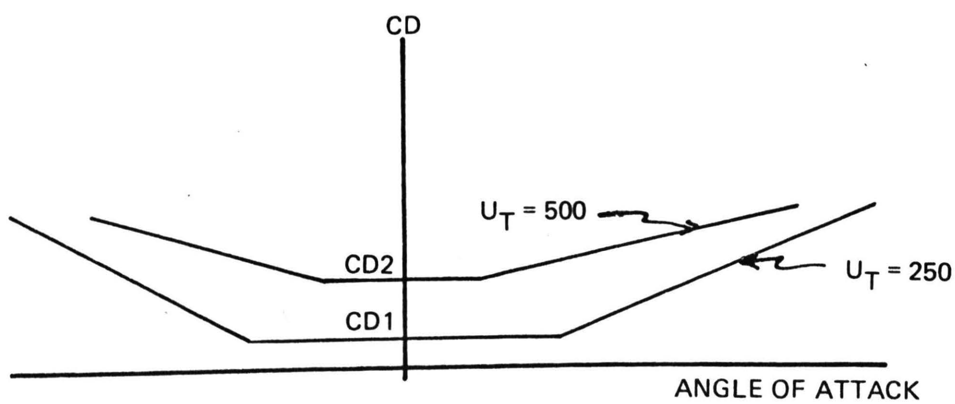

Figure BF-2

$$U_T = 250 \rightarrow CD1$$

$$U_T = 500 \rightarrow CD2$$

Simple interpolation allows the drag coefficient at a velocity between 500 and 250 to be calculated as

$$CD = \frac{U_T - 250}{500 - 250} (CD2 - CD1) + CD1.$$

Using this form, the total variation of CD is given by

$$\delta CD = \frac{\partial CD}{\partial U_T} \delta U_T + \frac{\partial CD}{\partial \alpha} \delta\alpha.$$

At this point it should be noted that the coefficient of $\delta\alpha$ represents the slope of the curves presented in Figure BF-2. Note that for small perturbations in the angle of attack, the slope $\partial CD/\partial\alpha$ will be constant. But if the change, $\delta\alpha$, is large enough to cross the break point of the curve, the slope $\partial CD/\partial\alpha$ will also change values. Hence a sensing device must be implemented to determine these break points.

It can be verified that the variation in the angle of attack can be obtained very accurately. If this is the case, then it is possible to partition $\delta\alpha$ into m parts--see Figure BF-3. At a particular station, the only parameters known are the angle of attack, α, the corresponding drag coefficient, CD, the slope of the drag curve, $\partial CD/\partial\alpha$, and the total variation of the angle of attack, $\delta\alpha$. Assume that the angle of attack is increasing

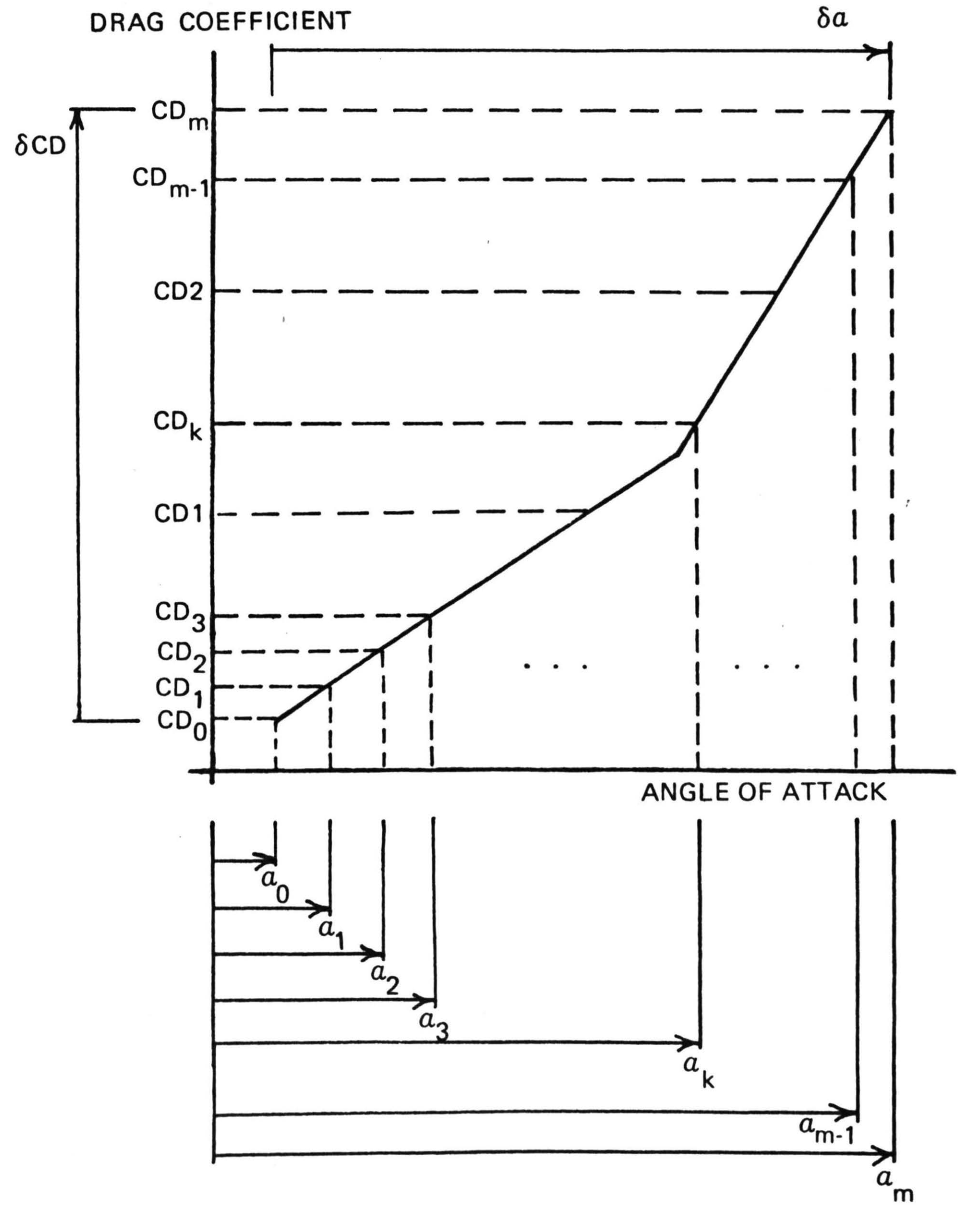
DRAG COEFFICIENT
δa
δCD
CDm
CDm-1
CD2
CDk
CD1
CD3
CD2
CD1
CD0
. . .
. . .
ANGLE OF ATTACK
a0
a1
a2
a3
ak
am-1
am

Figure BF-3

and that we partition its total change into m parts. Since α is increasing, a new angle of attack, α_1, can be obtained as follows:

$$\alpha_1 = \alpha_o + \frac{\delta\alpha}{m}$$

Introducing α_1 into the drag routine yields a corresponding drag coefficient, CD_1 and the slope, $\partial CD/\partial\alpha$. By repeating this procedure over the entire interval,

$$\alpha_o \leq \alpha \leq \alpha_m,$$

the drag coefficient and the slope, $\partial CD/\partial\alpha$, will be known at all partitioned points.

The total change of the drag coefficient can now be expressed as

$$\delta CD = \frac{\partial CD}{\partial U_T}\,\delta U_T + (CD_1 - CD_0)$$

$$+ (CD_2 - CD_1) + \ldots + (CD_m - CD_{m-1}),$$

or

$$\delta CD = \frac{\partial CD}{\partial U_T}\,\partial U_T + \frac{\partial CD}{\partial\alpha}\left(\frac{\delta\alpha}{m}\right)$$

$$+ \frac{\partial CD}{\partial\alpha}\left(\frac{\delta\alpha}{m}\right) + \ldots + \frac{\partial CD1}{\partial\alpha}\left(\frac{\delta\alpha}{m}\right)$$

$$+ \ldots + \frac{\partial CD1}{\partial\alpha}\left(\frac{\delta\alpha}{m}\right)$$

where

$\frac{\partial CD}{\partial\alpha} \triangleq$ slope before the break point

$\frac{\partial CD1}{\partial\alpha} \triangleq$ slope after the break point.

Assuming there are n values of $\partial CD/\partial\alpha$, the above equation becomes

$$\delta CD = \frac{\partial CD}{\partial U_T}\ \delta U_T + \frac{n}{m}\ \frac{\partial CD}{\partial \alpha}\ \delta\alpha + \frac{(m-n)}{m}\ \frac{\partial CD1}{\partial \alpha}\ \delta\alpha.$$

Utilizing this equation yields a very accurate linearization of the incremental drag force. Note that the choice of the value m is arbitrary. However, a choice of m equal to 20 gave excellent results for both the lift and drag forces.

APPENDIX C

STATIC TESTS

This appendix contains data obtained from static tests conducted at airspeeds of 50 and 110 knots. Tables CT-1 through CT-12 contain data pertaining to an airspeed of 50 knots. Data corresponding to the airspeed of 110 knots are presented in Tables CT-13 through CT-24.

TABLE CT-1

EFFECT OF STATE PERTURBATIONS ON FORCES
(SPEED EQUALS 50 KNOTS)

% Change in State Variable	Model*	Perturbed Forces		
		δX_A	δY_A	δZ_A
$\delta u \approx 2\%$	NM	-1.092	-0.042	-3.207
	LM	-1.091	-0.042	-3.210
$\delta v \approx 2\%$	NM	0.022	-0.843	-0.281
	LM	0.022	-0.843	-0.287
$\delta w \approx 2\%$	NM	-0.170	-0.070	-3.700
	LM	-0.169	-0.077	-3.649
$\delta p \approx 2\%$	NM	1.048	-1.529	-7.781
	LM	1.043	-1.530	-7.781
$\delta q \approx 2\%$	NM	1.406	0.914	-1.805
	LM	1.406	0.914	-1.806
$\delta r \approx 2\%$	NM	0.002	13.762	-0.129
	LM	0.002	13.762	-0.129

*NM indicates Nonlinear Model
LM indicates Linear Model

TABLE CT-2

EFFECT OF STATE PERTURBATIONS ON MOMENTS
(SPEED EQUALS 50 KNOTS)

% Change in State Variable	Model*	Perturbed Moments		
		δL_A	δM_A	δN_A
$\delta u \approx 2\%$	NM	-1.968	5.938	-6.469
	LM	-1.968	5.936	-6.491
$\delta v \approx 2\%$	NM	-2.775	-0.308	15.678
	LM	-2.779	-0.310	15.462
$\delta w \approx 2\%$	NM	-0.600	-0.690	0.004
	LM	-0.602	-0.690	-0.217
$\delta p \approx 2\%$	NM	-54.122	-11.938	-0.769
	LM	-54.124	-11.893	-0.987
$\delta q \approx 2\%$	NM	6.910	-38.491	0.484
	LM	6.907	-38.472	0.265
$\delta r \approx 2\%$	NM	46.444	-0.078	-425.121
	LM	46.443	-0.078	-425.343

*NM indicates Nonlinear Model
LM indicates Linear Model

TABLE CT-3

EFFECT OF STATE PERTURBATIONS ON FORCES
(SPEED EQUALS 50 KNOTS)

% Change in State Variable	Model*	Perturbed Forces δX_A	δY_A	δZ_A
$\delta u \approx 5\%$	NM	-23.233	-.884	-65.285
	LM	-23.049	-.987	-65.059
$\delta v \approx 5\%$	NM	.042	-1.693	-.438
	LM	.042	-1.694	-.444
$\delta w \approx 5\%$	NM	-2.952	-1.449	-61.12
	LM	-2.955	-1.450	-61.13
$\delta p \approx 5\%$	NM	2.135	-3.067	-15.434
	LM	2.127	-3.067	-15.432
$\delta q \approx 5\%$	NM	2.810	1.820	-3.484
	LM	2.809	1.820	-3.481
$\delta r \approx 5\%$	NM	0.002	27.517	-0.129
	LM	0.002	27.517	-0.130

*NM indicates Nonlinear Model
LM indicates Linear Model

TABLE CT-4

EFFECT OF STATE PERTURBATIONS ON MOMENTS
(SPEED EQUALS 50 KNOTS)

% Change in State Variable	Model*	Perturbed Moments		
		δL_A	δM_A	δN_A
$\delta u \approx 5\%$	NM	-41.872	128.161	-140.067
	LM	-41.750	126.859	-135.978
$\delta v \approx 5\%$	NM	-5.587	-0.544	31.345
	LM	-5.590	-0.542	31.123
$\delta w \approx 5\%$	NM	-10.970	-10.680	-0.293
	LM	-10.972	-10.691	-0.512
$\delta p \approx 5\%$	NM	-108.279	-24.103	-1.555
	LM	-108.280	-24.037	-1.775
$\delta q \approx 5\%$	NM	13.784	-76.939	0.949
	LM	13.782	-76.867	0.730
$\delta r \approx 5\%$	NM	92.855	-0.078	-850.246
	LM	92.854	-0.078	-850.487

*NM indicates Nonlinear Model
LM indicates Linear Model

TABLE CT-5

EFFECT OF STATE PERTURBATIONS ON FORCES
(SPEED EQUALS 50 KNOTS)

% Change in State Variable	Model*	Perturbed Forces		
		δX_A	δY_A	δZ_A
$\delta u \approx 10\%$	NM	-45.060	-1.469	-125.644
	LM	-44.335	-1.346	-124.914
$\delta v \approx 10\%$	NM	0.081	-3.394	-0.754
	LM	0.082	-3.395	-0.757
$\delta w \approx 10\%$	NM	-6.919	-3.359	-143.199
	LM	-6.935	-3.361	-143.237
$\delta p \approx 10\%$	NM	4.314	-6.141	-30.734
	LM	4.231	-6.141	-30.734
$\delta q \approx 10\%$	NM	5.618	3.633	-6.848
	LM	5.618	3.633	-6.834
$\delta r \approx 10\%$	NM	0.002	55.022	-0.129
	LM	0.002	55.027	-0.130

*NM indicates Nonlinear Model
LM indicates Linear Model

TABLE CT-6

EFFECT OF STATE PERTURBATIONS ON MOMENTS
(SPEED EQUALS 50 KNOTS)

% Change in State Variable	Model*	Perturbed Moments δL_A	δM_A	δN_A
$\delta u \approx 10\%$	NM	-80.245	249.386	-275.211
	LM	-79.817	244.166	-262.768
$\delta v \approx 10\%$	NM	-11.210	-1.006	62.663
	LM	-11.213	-1.006	62.445
$\delta w \approx 10\%$	NM	-25.394	-24.905	-0.699
	LM	-25.403	-24.978	-0.907
$\delta p \approx 10\%$	NM	-216.593	-48.472	-3.133
	LM	-216.594	-48.217	-3.350
$\delta q \approx 10\%$	NM	27.533	-153.932	1.879
	LM	27.531	-153.657	1.659
$\delta r \approx 10\%$	NM	185.676	-0.078	-1700.425
	LM	185.674	-0.078	-1700.775

*NM indicates Nonlinear Model
LM indicates Linear Model

TABLE CT-7

EFFECT OF CONTROL PERTURBATION ON FORCES
(SPEED EQUALS 50 KNOTS)

% Change in Control Variable	Model*	Perturbed Forces		
		δX_A	δY_A	δZ_A
$\delta u_1 \approx 2\%$	NM	-27.630	-14.040	-493.700
	LM	-27.632	-14.062	-493.681
$\delta u_2 \approx 2\%$	NM	-1.120	1.99	0.200
	LM	-1.118	2.010	0.253
$\delta u_3 \approx 2\%$	NM	1.387	0.940	7.900
	LM	1.387	0.927	7.938
$\delta u_4 \approx 2\%$	NM	0.024	11.497	0.253
	LM	0.020	11.500	0.200

*NM indicates Nonlinear Model
LM indicates Linear Model

TABLE CT-8

EFFECT OF CONTROL PERTURBATIONS ON MOMENTS
(SPEED EQUALS 50 KNOTS)

% Change in Control Variable	Model*	Perturbed Moments		
		δL_A	δM_A	δN_A
$\delta u_1 \approx 2\%$	NM	-106.570	-43.460	-7.230
	LM	-106.652	-43.454	-7.243
$\delta u_2 \approx 2\%$	NM	15.042	8.614	.957
	LM	15.241	8.611	.994
$\delta u_3 \approx 2\%$	NM	7.068	6.449	0.390
	LM	7.028	6.450	0.439
$\delta u_4 \approx 2\%$	NM	54.306	-0.049	-305.892
	LM	54.306	-0.051	-307.253

*NM indicates Nonlinear Model
LM indicates Linear Model

TABLE CT-9

EFFECT OF CONTROL PERTURBATION ON FORCES
(SPEED EQUALS 50 KNOTS)

% Change in Control Variable	Model*	Perturbed Forces		
		δX_A	δY_A	δZ_A
$\delta u_1 \approx 5\%$	NM	-68.460	-35.410	-1227.700
	LM	-68.540	-35.378	-1228.484
$\delta u_2 \approx 5\%$	NM	-2.830	4.970	0.200
	LM	-2.832	5.039	0.215
$\delta u_3 \approx 5\%$	NM	3.430	2.310	19.400
	LM	3.488	2.288	20.073
$\delta u_4 \approx 5\%$	NM	0.020	5.760	0.200
	LM	0.024	5.758	0.251

*NM indicates Nonlinear Model
LM indicates Linear Model

TABLE CT-10

EFFECT OF CONTROL PERTURBATIONS ON MOMENTS
(SPEED EQUALS 50 KNOTS)

% Change in Control Variable	Model*	Perturbed Moments		
		δL_A	δM_A	δN_A
$\delta u_1 \approx 5\%$	NM	-268.640	-109.968	-18.179
	LM	-268.313	-109.791	-18.168
$\delta u_2 \approx 5\%$	NM	37.643	21.609	2.485
	LM	38.213	21.606	2.546
$\delta u_3 \approx 5\%$	NM	17.483	-16.048	1.094
	LM	17.349	-16.169	1.136
$\delta u_4 \approx 5\%$	NM	27.214	-0.049	-153.603
	LM	27.214	-0.052	-153.746

*NM indicates Nonlinear Model
LM indicates Linear Model

TABLE CT-11

EFFECT OF CONTROL PERTURBATION ON FORCES
(SPEED EQUALS 50 KNOTS)

% Change in Control Variable	Model*	Perturbed Forces		
		δX_A	δY_A	δZ_A
$\delta u_1 \approx 10\%$	NM	-161.460	-74.701	-2551.300
	LM	-161.197	-74.694	-2551.327
$\delta u_2 \approx 10\%$	NM	-5.690	9.990	0.200
	LM	-5.687	10.227	0.249
$\delta u_3 \approx 10\%$	NM	6.84	4.600	38.600
	LM	8.973	4.546	40.798
$\delta u_4 \approx 10\%$	NM	0.020	50.240	0.200
	LM	0.023	50.232	0.249

*NM indicates Nonlinear Model
LM indicates Linear Model

TABLE CT-12

EFFECT OF CONTROL PERTURBATION ON MOMENTS
(SPEED EQUALS 50 KNOTS)

% Change in Control Variable	Model*	Perturbed Moments		
		δL_A	δM_A	δN_A
$\delta u_1 \approx 10\%$	NM	-566.589	-82.804	-38.316
	LM	-566.481	-85.039	-38.317
$\delta u_2 \approx 10\%$	NM	75.731	43.268	5.059
	LM	77.560	43.256	5.205
$\delta u_3 \approx 10\%$	NM	34.843	-32.042	2.269
	LM	34.472	-47.147	2.269
$\delta u_4 \approx 10\%$	NM	237.180	-0.049	-1343.273
	LM	237.177	-0.051	-1343.880

*NM indicates Nonlinear Model
LM indicates Linear Model

TABLE CT-13

EFFECT OF STATE PERTURBATIONS ON FORCES
(SPEED EQUALS 110 KNOTS)

% Change in State Variable	Model*	Perturbed Forces δX_A	δY_A	δZ_A
$\delta u \approx 2\%$	NM	-34.767	5.538	15.793
	LM	-34.555	5.407	14.635
$\delta v \approx 2\%$	NM	0.027	-1.332	-0.602
	LM	0.027	-1.332	-0.600
$\delta w \approx 2\%$	NM	0.520	-1.021	-69.176
	LM	0.520	-1.021	-69.178
$\delta p \approx 2\%$	NM	0.528	-1.441	-15.570
	LM	0.527	-1.441	-15.567
$\delta q \approx 2\%$	NM	1.416	1.018	-3.840
	LM	1.416	1.018	-3.836
$\delta r \approx 2\%$	NM	0.001	18.034	-0.488
	LM	0.001	18.034	0.486

*NM indicates Nonlinear Model
LM indicates Linear Model

TABLE CT-14

EFFECT OF STATE PERTURBATIONS ON MOMENTS
(SPEED EQUALS 110 KNOTS)

% Change in State Variable	Model*	Perturbed Moments		
		δL_A	δM_A	δN_A
$\delta u \approx 2\%$	NM	-26.800	233.662	-250.062
	LM	-26.945	232.757	-246.995
$\delta v \approx 2\%$	NM	-3.653	-0.511	21.993
	LM	-3.655	-0.507	21.941
$\delta w \approx 2\%$	NM	-7.730	-32.921	-0.355
	LM	-7.733	-32.923	-0.406
$\delta p \approx 2\%$	NM	-99.752	-11.985	-0.781
	LM	-99.754	-11.968	-0.835
$\delta q \approx 2\%$	NM	7.709	-66.452	0.480
	LM	7.707	-66.429	0.425
$\delta r \approx 2\%$	NM	46.414	-0.254	-601.914
	LM	46.414	-0.250	-601.972

*NM indicates Nonlinear Model
LM indicates Linear Model

TABLE CT-15

EFFECT OF STATE PERTURBATIONS ON FORCES
(SPEED EQUALS 110 KNOTS)

% Change in State Variable	Model*	Perturbed Forces		
		δX_A	δY_A	δZ_A
$\delta u \approx 5\%$	NM	-70.210	11.322	-33.089
	LM	-69.141	10.812	-28.796
$\delta v \approx 5\%$	NM	0.053	-2.665	-0.711
	LM	0.053	-2.665	-0.713
$\delta w \approx 5\%$	NM	-0.150	-2.967	-198.062
	LM	-0.149	-2.968	-198.101
$\delta p \approx 5\%$	NM	1.058	-2.884	-30.648
	LM	1.053	-2.884	-30.646
$\delta q \approx 5\%$	NM	2.830	2.034	-7.191
	LM	2.830	2.033	-7.186
$\delta r \approx 5\%$	NM	0.000	36.070	-0.500
	LM	-0.001	35.066	-0.487

*NM indicates Nonlinear Model
LM indicates Linear Model

TABLE CT-16

EFFECT OF STATE PERTURBATIONS ON MOMENTS
(SPEED EQUALS 110 KNOTS)

% Change in State Variable	Model*	Perturbed Moments δL_A	δM_A	δN_A
$\delta u \approx 5\%$	NM	-53.413	471.468	-506.180
	LM	-53.896	465.996	-493.830
$\delta v \approx 5\%$	NM	-7.311	-0.765	44.030
	LM	-7.313	-0.764	43.978
$\delta w \approx 5\%$	NM	-7.730	-32.921	-0.355
	LM	-7.733	-32.923	-0.406
$\delta p \approx 5\%$	NM	-199.509	-23.729	-1.519
	LM	-199.512	-23.687	-1.575
$\delta q \approx 5\%$	NM	15.414	-132.686	1.000
	LM	15.411	-132.604	.945
$\delta r \approx 5\%$	NM	92.824	-0.254	-1203.799
	LM	92.825	-0.250	-1203.850

*NM indicates Nonlinear Model
LM indicates Linear Model

TABLE CT-17

EFFECT OF STATE PERTURBATIONS ON FORCES
(SPEED EQUALS 110 KNOTS)

% Change in State Variable	Model*	Perturbed Forces		
		δX_A	δY_A	δZ_A
$\delta u \approx 10\%$	NM	145.651	24.071	-75.238
	LM	140.760	21.988	-58.122
$\delta v \approx 10\%$	NM	0.100	-5.230	-0.900
	LM	0.106	-5.333	-0.940
$\delta w \approx 10\%$	NM	-1.269	-5.568	-368.707
	LM	-2.639	-5.562	-368.815
$\delta p \approx 10\%$	NM	2.125	-5.769	-60.809
	LM	2.105	-5.770	-60.806
$\delta q \approx 10\%$	NM	5.659	4.066	-13.906
	LM	5.656	4.065	-13.885
$\delta r \approx 10\%$	NM	0.001	72.127	-0.488
	LM	0.001	72.129	-0.487

*NM indicates Nonlinear Model
LM indicates Linear Model

TABLE CT-18

EFFECT OF STATE PERTURBATIONS ON MOMENTS
(SPEED EQUALS 110 KNOTS)

% Change in State Variable	Model*	Perturbed Moments		
		δL_A	δM_A	δN_A
$\delta u \approx 10\%$	NM	-107.838	975.564	-1055.101
	LM	-109.632	949.021	-1004.724
$\delta v \approx 10\%$	NM	-14.630	-1.280	88.098
	LM	-14.630	-1.277	88.051
$\delta w \approx 10\%$	NM	-42.122	-186.288	-1.785
	LM	-42.075	-176.784	-1.792
$\delta p \approx 10\%$	NM	-399.020	-47.274	-3.000
	LM	-399.027	-47.123	-3.054
$\delta q \approx 10\%$	NM	30.824	-265.270	2.043
	LM	30.819	-264.967	1.987
$\delta r \approx 10\%$	NM	185.645	-0.254	-2407.487
	LM	185.645	-0.250	-2407.604

*NM indicates Nonlinear Model
LM indicates Linear Model

TABLE CT-19

EFFECT OF CONTROL PERTURBATION ON FORCES
(SPEED EQUALS 110 KNOTS)

% Change in Control Variable	Model*	Perturbed Forces		
		δX_A	δY_A	δZ_A
$\delta u_1 \approx 2\%$	NM	-9.610	-12.810	-563.200
	LM	-10.684	-12.800	-563.277
$\delta u_2 \approx 2\%$	NM	-0.770	1.530	.900
	LM	-0.770	1.526	.926
$\delta u_3 \approx 2\%$	NM	3.920	2.720	47.700
	LM	3.976	2.701	48.186
$\delta u_4 \approx 2\%$	NM	0.000	4.630	0.900
	LM	-0.005	4.625	0.926

*NM indicates Nonlinear Model
LM indicates Linear Model

TABLE CT-20

EFFECT OF CONTROL PERTURBATION ON MOMENTS
(SPEED EQUALS 110 KNOTS)

% Change in Control Variable	Model*	Perturbed Moments		
		δL_A	δM_A	δN_A
$\delta u_1 \approx 2\%$	NM	-97.210	-215.751	-6.629
	LM	-97.083	-207.651	-6.622
$\delta u_2 \approx 2\%$	NM	11.554	6.327	0.710
	LM	11.567	6.314	0.720
$\delta u_3 \approx 2\%$	NM	20.609	-5.292	1.320
	LM	20.479	-5.459	1.322
$\delta u_4 \approx 2\%$	NM	21.887	0.507	-123.255
	LM	21.883	0.510	-123.257

*NM indicates Nonlinear Model
LM indicates Linear Model

TABLE CT-21

EFFECT OF CONTROL PERTURBATIONS ON FORCES
(SPEED EQUALS 110 KNOTS)

% Change in Control Variable	Model*	Perturbed Forces		
		δX_A	δY_A	δZ_A
δu_1 ∿ 5%	NM	-33.680	-32.530	-1408.400
	LM	-34.609	-32.498	-1408.674
δu_2 ∿ 5%	NM	-1.920	3.780	0.900
	LM	-1.914	3.840	0.926
δu_3 ∿ 5%	NM	11.180	6.740	118.800
	LM	12.096	6.717	119.293
δu_4 ∿ 5%	NM	0.000	15.370	0.926
	LM	0.002	15.370	0.900

*NM indicates Nonlinear Model
LM indicates Linear Model

TABLE CT-22

EFFECT OF CONTROL PERTURBATION ON MOMENTS
(SPEED EQUALS 110 KNOTS)

% Change in Control Variable	Model*	Perturbed Moment		
		δL_A	δM_A	δN_A
δu_1 ∿ 5%	NM	-246.745	-466.361	-16.734
	LM	-246.474	-459.472	-16.714
δu_2 ∿ 5%	NM	28.664	15.055	1.867
	LM	29.118	14.992	1.905
δu_3 ∿ 5%	NM	47.036	-23.940	3.379
	LM	50.934	-30.603	3.380
δu_4 ∿ 5%	NM	72.614	0.507	-410.685
	LM	72.612	0.457	-410.684

*NM indicates Nonlinear Model
LM indicates Linear Model

TABLE CT-23

EFFECT OF CONTROL PERTURBATIONS ON FORCES
(SPEED EQUALS 110 KNOTS)

% Change in Control Variable	Model*	Perturbed Forces		
		δX_A	δY_A	δZ_A
$\delta u_1 \approx 10\%$	NM	-46.870	-51.670	-2239.700
	LM	-55.990	-51.532	-2240.362
$\delta u_2 \approx 10\%$	NM	-3.840	7.540	0.900
	LM	-3.832	8.017	0.923
$\delta u_3 \approx 10\%$	NM	21.180	13.430	237.300
	LM	26.340	13.160	244.789
$\delta u_4 \approx 10\%$	NM	0.000	30.720	0.900
	LM	0.003	30.720	0.921

*NM indicates Nonlinear Model
LM indicates Linear Model

TABLE CT-24

EFFECT OF CONTROL PERTURBATIONS ON MOMENTS
(SPEED EQUALS 110 KNOTS)

% Change in Control Variable	Model*	Perturbed Moments		
		L_A	M_A	N_A
u_1 10%	NM	-391.895	-792.191	-26.543
	LM	-390.825	-723.561	-26.472
u_2 10%	NM	57.181	29.634	3.793
	LM	60.797	29.530	4.047
u_3 10%	NM	101.849	-39.007	6.809
	LM	99.803	-74.315	6.682
u_4 10%	NM	145.084	0.507	-821.295
	LM	145.080	0.445	-821.293

*NM indicates Nonlinear Model
LM indicates Linear Model

APPENDIX D

HOMOGENEOUS TEST

Results of the homogeneous test used for substantiating the linear model are tabulated in this appendix. Table DT-1 compares nonlinear and linear position of the aircraft with respect to an inertial reference frame. Respective components of the velocity are compared in Table DT-2, and the angular orientation of the aircraft body axis with respect to the inertial frame is tabulated in Table DT-3.

TABLE DT-1

HELICOPTER POSITION

Model*	North (feet)	East (feet)	Altitude (feet)
NM	8.908	-0.020	1000.00
LM	8.908	-0.020	999.989
NM	17.816	-0.041	1000.000
LM	17.816	-0.041	999.999
NM	26.724	-0.061	999.999
LM	26.724	-0.061	999.999
NM	35.632	-0.081	999.999
LM	35.632	-0.081	999.997
NM	44.539	-0.101	999.998
LM	44.540	-0.100	999.994
NM	53.448	-0.121	999.996
LM	53.448	-0.120	999.989
NM	62.356	-0.141	999.993
LM	62.357	-0.139	999.982
NM	71.264	-0.161	999.987
LM	71.265	-0.157	999.973
NM	80.171	-0.180	999.986
LM	80.174	-0.175	999.964
NM	89.079	-0.199	999.981
LM	89.083	-0.191	999.953

*NM indicates Nonlinear Model
LM indicates Linear Model

TABLE DT-2

HELICOPTER VELOCITY

Model*	$\dot{N}$ (ft/sec)	$\dot{E}$ (ft/sec)	$\dot{H}$ (ft/sec)
NM	178.160	-0.406	-0.001
LM	178.160	-0.406	-0.001
NM	178.160	-0.406	-0.004
LM	178.160	-0.405	-0.005
NM	178.160	-0.405	-0.012
LM	178.160	-0.403	-0.013
NM	178.160	-0.404	-0.023
LM	178.161	-0.400	-0.034
NM	178.160	-0.402	-0.036
LM	178.163	-0.395	-0.068
NM	178.160	-0.399	-0.050
LM	178.166	-0.388	-0.102
NM	178.160	-0.393	-0.064
LM	178.168	-0.379	-0.135
NM	178.160	-0.384	-0.078
LM	178.170	-0.367	-0.166
NM	178.160	-0.372	-0.089
LM	178.173	-0.352	-0.195
NM	178.160	-0.356	-0.099
LM	178.176	-0.330	-0.216

*NM indicates Nonlinear Model
LM indicates Linear Model

TABLE DT-3

ANGULAR ORIENTATION

Model*	ϕ (RAD)	θ (RAD)	ψ (RAD)
NM	-0.030	-0.077	0.000
LM	-0.030	-0.077	0.000
NM	-0.030	-0.077	0.000
LM	-0.030	-0.077	0.000
NM	-0.030	-0.077	0.000
LM	-0.030	-0.077	0.000
NM	-0.030	-0.077	0.000
LM	-0.030	-0.077	0.000
NM	-0.030	-0.077	0.000
LM	-0.030	-0.077	0.000
NM	-0.029	-0.077	0.001
LM	-0.030	-0.077	0.001
NM	-0.029	-0.077	0.002
LM	-0.029	-0.077	0.001
NM	-0.029	-0.077	0.003
LM	-0.028	-0.077	0.002
NM	-0.029	-0.077	0.004
LM	-0.027	-0.077	0.003
NM	-0.028	-0.077	0.006
LM	-0.027	-0.076	0.005

*NM indicates Nonlinear Model
LM indicates Linear Model

APPENDIX E

OBJECTIVE FUNCTION TEST

The control goal which is fed into both linear and nonlinear systems is chosen to minimize the quadratic form

$$J = [\underline{x}_d\,(k+1) - \underline{x}_1\,(k+1)]^T\, W_E\, [\underline{x}_d\,(k+1) - \underline{x}_1\,(k+1)]$$
$$+ \underline{u}\,(k)^T\, W_{\underline{u}}\underline{u}\,(k)$$

where W_E and $W_{\underline{u}}$ are arbitrary weighting matrices for the predicted state error and the control efforts, respectively. Specification of the desired flight path is characterized by the state vector, $\underline{x}_d\,(k+1)$.

By substituting (15) and (16) into the objective function and utilizing the fact that

$$\underline{u}_g\,(k) \overset{\Delta}{=} \underline{u}_g\,(k-1) + \delta\underline{u}\,(k-1),$$

the objective function may be minimized with respect to $\delta\underline{u}\,(k-1)$. The result of this minimization is the control goal, $\underline{u}_g\,(k)$, required to drive the aircraft to the desired state. This is obtained by adding the perturbed control given by

$$\delta\underline{u}^T\,(k-1) = \left\{ \left[\underline{x}_d^T\,(k+1) - \underline{x}_1^T(k) + \phi^T(k-1)\ \delta\underline{x}^T(k-1)\right] \left[W_E\ \theta(k-1)\right] - \underline{u}^T\,(k-1)\ W_{\underline{u}} \right\} \left[\theta^T(k-1)\ W_E\ \theta(k-1) + W_{\underline{u}}\right]$$

to the nominal control $\underline{u}(k-1)$.

Results of the objective function test are contained in the appendix. Table ET-1 compares nonlinear and linear position of the aircraft with respect to an inertial reference frame. Respective components of the velocity are compared in Table ET-2, angular orientation of the aircraft body axes with respect to the inertial frame is tabulated in Table ET-3, and the linear velocities of the aircraft with respect to the body axes are given in Table ET-4.

TABLE ET-1

HELICOPTER POSITION

Model*	North (feet)	East (feet)	Altitude (feet)
NM	8.908	-0.020	1000.000
LM	8.908	-0.020	999.999
NM	17.816	-0.041	1000.000
LM	17.816	-0.041	999.999
NM	26.724	-0.061	999.999
LM	26.723	-0.061	999.998
NM	35.632	-0.081	999.999
LM	35.632	-0.081	999.997
NM	44.541	-0.102	999.999
LM	44.541	-0.101	999.994
NM	53.449	-0.122	1000.00
LM	53.450	-0.120	999.990
NM	62.356	-0.143	1000.001
LM	62.359	-0.140	999.985
NM	71.264	-0.163	1000.002
LM	71.268	-0.159	999.979
NM	80.171	-0.183	1000.003
LM	80.177	-0.177	999.972
NM	89.077	-0.202	1000.005
LM	89.086	-0.195	999.965

*NM indicates Nonlinear Model
LM indicates Linear Model

TABLE ET-2

HELICOPTER VELOCITY

Model*	$\dot{N}$ (ft/sec)	$\dot{E}$ (ft/sec)	$\dot{H}$ (ft/sec)
NM	178.160	-0.406	-0.001
LM	178.160	-0.406	-0.001
NM	178.160	-0.406	-.004
LM	178.159	-0.405	-.005
NM	178.170	-0.406	-.009
LM	178.165	-0.404	-.010
NM	178.170	-0.409	0.009
LM	178.168	-0.402	-0.032
NM	178.160	-0.410	0.012
LM	178.171	-0.399	-0.054
NM	178.160	-0.408	0.020
LM	178.174	-0.394	-0.076
NM	178.160	-0.405	0.024
LM	178.170	-0.388	-0.098
NM	178.140	-0.398	0.032
LM	178.179	-0.379	-0.118
NM	178.130	-0.390	0.045
LM	178.180	-0.368	-0.134
NM	178.120	-0.376	0.058
LM	178.182	-0.352	-0.143

*NM indicates Nonlinear Model
LM indicates Linear Model

TABLE ET-3

ANGULAR ORIENTATION

Model*	ϕ (RAD)	θ (RAD)	ψ (RAD)
NM	-0.030	-0.077	0.000
LM	-0.030	-0.077	0.000
NM	-0.030	-0.077	0.000
LM	-0.030	-0.077	0.000
NM	-0.030	-0.077	0.000
LM	-0.030	-0.077	0.000
NM	-0.030	-0.077	0.000
LM	-0.030	-0.077	0.000
NM	-0.030	-0.077	0.000
LM	-0.030	-0.077	0.000
NM	-0.030	-0.077	0.001
LM	-0.029	-0.077	0.001
NM	-0.030	-0.077	0.001
LM	-0.029	-0.077	0.002
NM	-0.030	-0.007	0.002
LM	-0.029	-0.007	0.003
NM	-0.030	-0.077	0.004
LM	-0.029	-0.077	0.004
NM	-0.030	-0.077	0.006
LM	-0.028	-0.077	0.000

*NM indicates Nonlinear Model
LM indicates Linear Model

TABLE ET-4

LINEAR VELOCITY

Model*	U (ft/sec)	V (ft/sec)	W (ft/sec)
NM	177.630	0.001	-13.736
LM	177.630	0.001	-13.736
NM	177.630	0.001	-13.736
LM	177.629	0.001	-13.736
NM	177.636	-0.005	-13.733
LM	177.634	-0.003	-13.731
NM	177.634	-0.017	-13.760
LM	177.640	-0.018	-13.720
NM	177.629	-0.049	-13.773
LM	177.643	-0.057	-13.708
NM	177.623	-0.116	-13.784
LM	177.647	-0.134	-13.693
NM	177.615	-0.232	-13.784
LM	177.651	-0.259	-13.678
NM	177.607	-0.411	-13.776
LM	177.655	-0.439	-13.663
NM	177.596	-0.665	-13.756
LM	177.657	-0.681	-13.648
NM	177.536	-1.008	-13.729
LM	177.658	-0.984	-13.634

*NM indicates Nonlinear Model
LM indicates Linear Model

APPLICATION OF MODERN CONTROL TECHNIQUES TO DEVELOP HELICOPTER FLIGHT PATHS

by

Alfred Fermelia

and

Virgil J. Flanigan*

ABSTRACT

General techniques for simulating helicopter pilot response for inclusion in a flight path simulation program have been devised. To provide the desired flight goal, a nominal flight trajectory is obtained from an existing nonlinear model. With this basis a deterministic pilot model which attempts to minimize flight deviations from the nominal can be developed for generating descriptions of the desired flight path.

---

*The authors are associated with the Department of Mechanical and Aerospace Engineering, University of Missouri-Rolla, Rolla, Missouri, where Mr. Fermelia is a graduate student and Dr. Flanigan (member ASME) is an Associate Professor.

TABLE OF CONTENTS

	Page
ABSTRACT	71
NOTATION	73
INTRODUCTION	74
DETERMINISTIC PILOT MODEL	76
RESULTS AND CONCLUSIONS	84
FUTURE CONSIDERATIONS AND EXTENSIONS	87
ACKNOWLEDGMENTS	89
REFERENCES	90
LIST OF ILLUSTRATIONS	92

NOTATION

In the paper all bold-face capital letters denote matrices. Vectors are defined in column format and are denoted by lower case letters in bold face type. All scalars will be denoted by plain upper or lower case letters. Occasionally it may be necessary to illustrate a vector in the following format:

$$\underline{x} = \begin{bmatrix} x_1 \\ x_2 \\ \cdot \\ \cdot \\ \cdot \\ x_n \end{bmatrix}$$

These general rules will hold unless otherwise specified in the text.

Numbers in brackets designate references at the end of the paper.

INTRODUCTION

The objective of this paper is to present general techniques for simulating helicopter pilot response. During flight the pilot manipulates the controls either to trim the helicopter for steady flight by balancing the external forces and moments or to produce a desired maneuver by controlling the unbalance of these forces and moments. Discussions of the physical phenomena involved with the aerodynamics of the rotors and fuselage are given in several references [1, 2, 3].

The cyclic stick, collective stick, and foot pedal comprise the controls of the vehicle. Cyclic stick control (forward-aft and lateral displacements) causes a cyclic variation in the main rotor blade pitch which results in the reorientation of the rotor thrust vector. This tilt of the rotor thrust provides the moment for pitch and roll motions. A change in blade pitch is also obtained by the collective stick control. However, the variation in pitch is the same for all blade azimuth positions which effects the magnitude of the rotor thrust primarily for vertical and forward speed control of the aircraft. Since the required engine power is related to the rotor thrust, the engine fuel control is usually synchronized with collective pitch. In addition, the pilot may vary the fuel setting by slight adjustments of the fuel control. During flight the pilot maintains a constant awareness of turbine speed and power. To reduce the complexity of the simulation model, the usual approximation of constant rotor RPM is assumed, and pilot manipulation of the fuel control is avoided. Through the foot pedals the pilot can control the tail rotor pitch, hence thrust and thereby the yawing moment. Thus, the simulated pilot's control will be composed of forward-aft cyclic, lateral cyclic, pedal and collective. The control will be represented by the vector

$$\underline{u} = \begin{bmatrix} u_1 \\ u_2 \\ u_3 \\ u_4 \end{bmatrix} \begin{array}{l} \triangleq \text{ collective} \\ \triangleq \text{ lateral cyclic} \\ \triangleq \text{ longitudinal cyclic} \\ = \text{ pedal} \end{array} \tag{1}$$

The purpose of the pilot control input is to create necessary aerodynamic forces and moments to control helicopter motion and attitude which is measured by the c.g. velocity and the angular orientation (yaw, pitch, and roll) and velocity of the fuselage. This output state will be denoted by the vector

$$\underline{x} = \begin{bmatrix} u \\ v \\ w \\ p \\ q \\ r \\ \psi \\ \theta \\ \phi \\ \Omega \end{bmatrix} \begin{array}{l} \\ \text{velocity of the c.g.} \\ \\ \text{angular velocity of} \\ \text{the fuselage} \\ \\ \text{angular orientation} \\ \text{of the fuselage} \\ \\ \text{rotor speed} \end{array} \tag{2}$$

To provide closed-loop action for the simulation, the pilot model must interpret the necessary control $\underline{u}$ as a result of any deviation in $\underline{x}$ from the desired state. A block diagram illustrating the overall concept of the flight path simulation is shown in Figure 1. The blocks numbered 1 through 6 are included in the helicopter dynamics model (reference 4). In the present study only block 8 will be considered. Hence the pilot control action, block 9 of Figure 1, will be assumed to be a unit gain. This assumption implies that the control goal is instantaneously predicted, i.e., a perfect pilot.

DETERMINISTIC PILOT MODEL

There are two basic approaches to developing a mathematical representation of the human operator's data sampling, error quantization and control goal decision roles. These two approaches are significantly different in their characterization of the operator. One method involves the qualitative and psychological aspects of the pilot. Functions such as sensing of the aircraft state and various instruments, the categorizing of these measurements as acceptable or non-acceptable, the human prediction and memory capability, and the human ability to adapt his response to the given situation would be included in this type of model. Probably one of the better illustrations of this approach is given by

Benjamin [6]. His study was for the relatively uncomplicated case of single input-output tracking whereas the helicopter pilot has four control inputs at his disposal with the desirability of controlling at least ten output variables. Adding to this complexity to a model such as Benjamin's which is already elaborate from the standpoint of the logic structure is not feasible due to computer limitations.

The second approach can be entitled a quasi-pilot engineering model which describes the overall performance of the pilot without close regard to psychological functions of the human operator. Some authors [7] have referred to these two approaches in a descriptive way as microscopic and macroscopic modeling of the pilot, respectively. From the results of the many previous investigations concerned with the modeling of a human operator in various tasks, it is apparent that the engineering model approach is the most feasible based on the current simulation state-of-the art.

The essential functions of the pilot model are to evaluate the system error, predict the necessary control input goal, and perform the control input manipulation. These functions are illustrated in Figure 2. Thus the pilot model provides the feedback (see Figure 1) required for the closed-loop simulation of the helicopter flight path in conjunction with the helicopter dynamics model [4]. Since the development of the pilot logic for a general maneuver is impractical, the desired trajectory for the helicopter state is prescribed [5]. Comparison of this nominal with the actual state produces the error from which the control goal can be resolved. Once the goal is established the pilot response and dynamics in performing the control manipulation can be modeled as a multi-variable tracking task.

The first consideration will be the general features of the discrete time deterministic control goal model. From the desired trajectory the state $\underline{x}_d$ (t) is known at discrete time intervals o, T, ..., kT, ..., etc., as depicted in Figure 3. In addition, from the trimmed flight conditions, the initial state $\underline{x}(0)$ and the control vector $\underline{u}(0)$ are known. It is presumed that the starting point of the trajectory will be a steady or trimmed flight condition. With these quantities given as initial data the helicopter dynamics portion of the simulation will yield the new state at t=T, i.e., $\underline{x}(T)$. At the time T a new selection of control is necessary for the next interval T to 2T. The control vector is constant for the length of the discrete sampling time and is only changed by some amount $\delta u(kT)$ at the next sampling instant. With the new control the dynamics model again yields the subsequent state of the helicopter. This repetitive process continues for the desired time of the prescribed nominal path. The question to be answered is, what control goal or change of control is required at each of the sampling times?

For small perturbations the nonlinear helicopter dynamics can be approximated by the linear state equation [5].

$$\delta\dot{\underline{x}}(t) = A\delta\underline{x}(t) + B\delta u(t) \tag{3}$$

where the system and control time-invariant matrices, A and B, are evaluated at the particular state from which the control change is to be calculated. The solution of equation 3 for the time interval kT to (k+1)T is known to be [8, 9, 10]

$$\delta x_1[(k+1)T] = \phi(T)\delta\underline{x}(kT) + \theta(T)\delta\underline{u}\ (kT) \tag{4}$$

where ϕ is a (10x10) stability matrix and θ is a (10x4) control matrix [5].

Since the desired state vector is given at the discrete time increments $\underline{x}_d(kT)$, it is proposed that the necessary control goal $u_g(kT)$ to follow the desired path be calculated with the simplified linear model. The selected goal should minimize the deviation between the nominal and linear helicopter states. Hence, a cost function, J, which provides the basis for selecting the best control vector should include these considerations. For convenience, a quadratic form is defined

$$J = E^T[(k+1)T]W_e[(k+1)T]E[(k+1)T] \tag{5}$$

the function J is to be minimized by the proper selection of $\underline{u}(kT)$ where W_e^* is a time varying matrix for the predicted state error at time, $(k+1)T$. Note that the predicted error at the time, $(k+1)T$, is

$$E[(k+1)T] = \underline{x}_d[(k+1)T] - \underline{x}_1[(k+1)T] \tag{6}$$

but from equation (4) with $\underline{x}_1(kT)$ set equal to the actual state $\underline{x}(kT)$, the cost functional is

$$\begin{aligned} J = {} & \underline{x}_d^T[(k+1)T]W_e[(k+1)T]\underline{x}_d[(k+1)T] \\ & -2\,\underline{x}_d^T[(k+1)T]W_e[(k+1)T]\underline{x}_d[(k+1)T] \\ & -2\,\underline{x}_d^T[(k+1)T]W_e[(k+1)T]\{\phi(T)\delta\underline{x}[(k-1)T] \\ & + \theta(T)\delta u[(k-1)T]\} + \{\phi(T)\delta\underline{x}[(k-1)T] \\ & + \theta(T)\delta\underline{u}[(k-1)T]\}^T W_e[(k+1)T]\{\phi(T)\delta\underline{x}[(k-1)T] \\ & + \theta(T)\delta\underline{u}[(k-1)T]\} \end{aligned} \tag{7}$$

Therefore, in order to minimize the cost functional, the control $\underline{u}_g(kT)$ is given by

$$\underline{u}_g(kT) = \underline{u}[(k-1)T] + \delta\underline{u}[(k-1)T] \tag{8}$$

where

$$\begin{aligned} \delta\underline{u}^T[(k-1)T] = {} & \{\underline{x}_d^T[(k+1)T] - (x(kT) + \phi(T)\delta\underline{x}[(k-1)T])^T\} \\ & W_e[(k+1)T]\theta(T)\{\theta^T(T)W_e[(k+1)T]\theta(T)\}^{-1} \end{aligned} \tag{9}$$

Application of the control law given by equations (8) and (9) to certain desired flight paths results in a

---

*The selection of the weighing matrix W_e is discussed in detail in Appendix A.

maximum/minimum control. Therefore in order to avoid this condition alternate cost functions can be considered.

If the computed control is not feasible then the obvious solution is to minimize an objective function which weights the control, i.e., consider

$$J = E^T[(k+1)T]W_e[(k+1)T]E[(k+1)T] + \underline{u}^T(kT)W_u(kT)\underline{u}(kT) \qquad (10)$$

The control that minimizes (10) is given by

$$\delta\underline{u}^T(kT) = \{\underline{x}_d^T[(k+1)T] - (\underline{x}^T(kT) + \delta\underline{x}^T(kT)\phi^T(T)\}W_e[(k+1)T]\theta(T) \{\theta^T(T)W_e[(k+1)T]\theta(T) + W_u(kT)\}^{-1} \qquad (11)$$

Generation of this control for certain desired flight paths resulted in a control vector $\underline{u}$ which was not feasible. Clearly this control should satisfy all control constraints provided the time varying weighting matrix W_u is chosen correctly. Therein lies the problem, i.e., how does one choose the weighting matrix W_e as a function of time?* Attempts were made to select $W_u(kT)$ to no avail.

In order to motivate the algorithm which does produce a control which satisfies all control constraints, consider again equation (11). Note the effect of the control weighting function is to add to the penalty associated with the state error, i.e., the last term in brackets of

---

*Appendix A discusses the technique used to obtain $W_u(kT)$.

equation (11) grows larger. Therefore consider the control given by equation (9). This equation can be written as

$$\delta u^T(kT) = \underline{\tilde{x}}[(k+1)T]\{\theta^T(T)W_e\ [(k+1)T]\theta(T)\}^{-1} \tag{12}$$

where

$$\underline{\tilde{x}}[(k+1)T] \stackrel{\Delta}{=} \{\underline{x}_d[(k+1)T] - (\underline{x}(kT) + \phi(T)\ \delta\underline{x}[(k-1)T])\}^T W_e[(k+1)T]\theta(T)$$

Comparing equations (11) and (12) indicates that if

$$\{\theta^T(T)W_e[(k+1)T]\theta(T) + W_u(kT)\}^{-1} = \{\theta^T(T)W_e[(k+1)T]\theta(T)\} \tag{13}$$

the two equations are identical. Equation (13) can also be written

$$\{\theta^T(T)W_{eu}[(k+1)T]\theta(T)\} = \{\theta^T(T)W_e[(k+1)T]\theta(T)\} \tag{14}$$

Now assume that the control law generated using equation (9) is not feasible. The solution for the kT time is given by

$$\delta\underline{u}_j^T(kT) = \underline{\tilde{x}}^T(kT)[\theta^T(T)W_e[(k+1)T\theta(T)]^{-1} \tag{15}$$

solving for $\underline{\tilde{x}}$ (kT) yields

$$\underline{\tilde{x}}_j(kT) = \delta\underline{u}^T(kT)[\theta^T(T)W_e[(k+1)T]\theta(T)] \tag{16}$$

Since the control given by (9) is not acceptable, i.e., it is too large or too small, consider an iteration that will guarantee feasibility.

The first jth iteration is given by (15), the j+1 iteration yields the control

$$\delta \underline{u}_{j+1}^T(kT) = \tilde{\underline{x}}^T\ [(k+1)T][\theta^T(T)W_{eu}\theta(T)]^{-1} \tag{17}$$

Therefore, it follows that

$$\delta \underline{x}^T[(k+1)T] = \delta u_{j+1}^T(kT)[\theta^T(T)W_{eu}\theta(T)] \tag{18}$$

Note in essence the objective function in the jth iteration is equation (5), whereas the j+1 iteration utilizes the cost function given in equation (10). Note however the necessity to select both a weighting matrix for state and one for the control no longer exists.

In order to demonstrate the feasibility of the control consider

$$\delta u_j^T(kT)\delta u_j(kT) = \tilde{x}^T[(k+1)T][\theta^T(T)W_e[(k+1)T]\theta(T)]^{-1}$$
$$[\theta^T(T)W_e[(k+1)T]\theta(T)]\tilde{x}[(k+1)T] \tag{19}$$

Substituting equation (18) into (19) yields

$$\delta u_j^T(kT)\delta u_j(kT) = \delta u_{j+1}^T(kT)[\theta^T(T)W_{eu}\theta(T)]$$
$$[\theta^T(T)W_e[(k+1)T]\theta(T)]^{-1}[\theta^T(T)W_e[(k+1)T]\theta(T)]^{-1}$$
$$[\theta^T(T)W_{eu}\theta(T)]^T\delta \underline{u}_j(kT) \tag{20}$$

Then subtracting $\delta \underline{u}_j{}^T\delta \underline{u}_j$ from $\delta \underline{u}_{j+1}{}^T\delta \underline{u}_{j+1}$ yields

$$\delta u_{j+1}^T \delta u_{j+1} - \delta u_j^T \delta u_j = \tag{21}$$

$$\delta u_{j+1}^T \{I - \theta^T W_{eu} \theta [(\theta^T W_e \theta)^{-1} (\theta^T W_e \theta)^{-T}] \theta^T W_{eu} \theta\} \delta u_{j+1}$$

where the time parameters have been omitted for clarity. Now in order that the j+1 iteration be less than the jth iteration, the term in brackets must be less than a preselected negative definitive matrix P, i.e.

$$I - RMR \leq P \tag{22}$$

where

$$R \triangleq \theta^T W_{eu} \theta$$

$$M \triangleq (\theta^T W_e \theta)^{-1} (\theta^T W_e \theta)^{-T}$$

Note the matrix M is a known constant, hence solving equation (22) for R will insure a feasible control. The solution of equation (22) is given in Appendix B.

RESULTS AND CONCLUSIONS

In order to demonstrate the application of modern control techniques to helicopter motion, four flight paths were considered. These four consisted of the helicopter in the configuration of a level flight, climb, dive, and a turn. In order to compare nonlinear vs linear models, inertial position and angular velocities of the helicopter were plotted as a function of time. Figures 3 through 22 illustrate the results for the different configurations.

Comparison of Figures 11, 12, 13 and 14 indicates that the predicted roll matches the desired state within ± 0.4 of a radian. Although roll was not matched as well in the climb orientation, it nevertheless matches the shape of the desired state better than that of the level flight, or dive. Note that in the turn flight path, the shape of the predicted roll closely follows the desired trajectory. Examination of the figures also reveal that the linear model attempts to follow the trend of the desired for those flight paths which give rise to maximum motion, i.e., examine the roll histograms.
The oscillatory nature of Figure 13 may be explained by noting that the system to be controlled is of the 10th order. Note that the frequency content of the desired roll is quite low, hence the control of the roll parameter is delegated a lower priority than the control responsible for controlling the forward velocity. This is illustrated by Figures 31-34 which gives the control histograms for the dive trajectory.

As might be expected, results of the climb flight path are mirrored in the dive trajectory. This is very apparent when comparing the time traces of pitch for both cases. The stability of the level flight might certainly be questioned after examination of the pitch channel for that particular configuration. However, noting that the amplitude at the end of 2 seconds is less than that obtained at 1.4 seconds, gives evidence that the trajectory is stable. Credence to this conjecture is given by examination of the pitch channel for the turn, i.e., the turn consists of a level flight for the first 2 seconds.

Having examined the characteristics of roll and pitch, expectations are that the yaw channel would exhibit the same type of performance. Examination of Figures 19 through 22 indicate that this is indeed true.

It is interesting to note that in all angular velocity channels the response in the linear model appears to lag behind that of the desired flight path. Also in every case considered the magnitude of the response is much larger than that of the nominal. This is best illustrated by Figure 12. Cause of these anomalies can be explained by the linear model chosen to represent the nonlinear helicopter. In selecting a suitable model to approximate the helicopter two linear configurations were initially considered. The models considered were:

$$\delta \underline{x}_1[(k+1)T] = \phi(T)\delta\underline{x}(kT) + \theta(T)\delta\underline{u}(kT) \tag{23}$$

and

$$\begin{aligned}\delta \underline{x}_1[(k+1)T] &= \phi(T)\delta\underline{x}(kT) + \Psi(T,T-1)\delta\underline{x}[(k-1)T] \\ &\quad + \theta(T)\delta\underline{u}(kT) + \underline{\Gamma}[T,T-1]\delta\underline{u}[(k-1)T]\end{aligned} \tag{24}$$

Equation (23) was chosen for the following reasons: 1) reference [11] indicated that it could indeed approximate the nonlinear model, 2) a model similar to (23) was used in reference [12] and 3) simplicity of (23) as compared to the complexity of (24).

The anomalies mentioned above can be explained by the omission in (23) of information contained in the coefficient matrices Ψ and Γ of (24). Clearly by neglecting Ψ, information regarding the frequency content of the system will be lost. Similarly omission of Γ may result in generation of a control law which exceeds the bounds of a feasible control.

In concluding, this paper demonstrates that modern control techniques can be applied to a helicopter which allow the vehicle to follow a predetermined flight path, i.e., feasibility of a helicopter auto pilot. Clearly performance of the algorithm selected to generate the control law yields a measure of the linear system chosen to represent the nonlinear helicopter. However, due to errors in the linear model, a technique had to be developed whereby a feasible control law could be obtained. In order to achieve this, an algorithm was developed to determine a weighting matrix as a function of time. This technique can be implemented on other systems with a similar effect.

FUTURE CONSIDERATIONS AND EXTENSIONS

In the previous section it was noted that the calculation of the control goal does not account for the pilot response. It is presumed that the goal is instantaneously predicted; however, it is evident that the pilot cannot respond with such precise behavior. To approximate the pilot's response in performing the control task the describing function developed for a tracking can be included as the action part of the pilot model. Such a pilot action model coupled with the alternate linear model discussed in the previous section are natural extensions of this dissertation. Discussion of the alternate linear representation was presented in the previous section. Therefore, only the pilot action model [5] will be discussed at this time.

Two of the most evident human characteristics are a variable gain and a delayed response. The simplest form of the transfer function would be

$$G(s) = Ke^{-\tau s} \tag{25}$$

The gain K is dependent upon the system dynamic characteristics, the nature of the control task, the physical and emotional condition of the operator, and other factors influencing the difficulty of the control task. For unpredictable signals the time delay, τ, may be as much as 0.5 seconds but decreases in magnitude with operator experience. Generally, a value of from 0.1 to 0.2 seconds could be assumed.

In addition to the pure delay a first order neuromuscular lag has been observed. Several early investigators suggested various combinations of derivative and integral control modes to better describe the adaptive nature of the human operator. These have evolved into the form

$$G(s) = \frac{Ke^{-\tau s}(1+\tau_1 s)}{(1+\tau_n s)(1+\tau_i s)} \quad . \tag{26}$$

Equation (26) is expanded in block diagram form in Figure 39. As shown, the nonlinear function of the pilot is described by a linearized transfer function and an assumed remnant term. In a complicated task such as the control of a helicopter, the remnant could be quite large. Since it is difficult to exacly specify this term, it is more easily treated as a superimposed noise. Some investigators have criticized the indiscriminate use of (26) since the data for developing the linearized equation was primarily for single input-output tasks. However, based on reference [13], equation (26) can be utilized to describe the pilot transfer function and hence is a natural extension to the work presented previously.

Acknowledgements

The authors wish to express their gratitude to Dr. D. A. Gyorog for his assistance in preparation of this work.

REFERENCES

1. Gessow, A. and Meyers, G. Jr., Aerodynamics of the Helicopter, New York: Macmillan Company, 1952.

2. Nikolsky, A., Helicopter Analysis, New York: Wiley, 1951.

3. Gyorog, D., "Helicopter Rotor Analysis," U.S. Army WECOM Report, November 1970.

4. Fermelia, A., Matson, J., and Gyorog, D., "Helicopter Flight Path Simulation, Part I. Helicopter Dynamics (ECOM) Model," U.S. Army WECOM Report, October 1971.

5. Gyorog, D., and Fermelia, A., "Helicopter Flight Path Simulation, Part II. Pilot Model Preliminary Analysis," U.S. Army WECOM Report, October 1971.

6. Benjamin, P., "A Hierarchial Model of a Helicopter Pilot," Human Factors, Vol. 12, No. 4, August 1970, 361-374.

7. Burgett, A. L., "A Study of Human Operator Performance Using Regression Analysis," NASA CR-1259, January 1969.

8. Dorf, T. C., Time-Domain Analysis and Design of Control Systems, Addison-Wesley, 1965.

9. Takahashi, Y., Rabins, M., and Auslander, D., Control, Addison-Wesley, 1965.

10. Sage, A. P., Optimum Systems Control, Prentice-Hall, Inc., 1968.

11. Fermelia, A., Flanigan, V. J., "Linearization of Equations Which Govern the Motion of a Heli-Copter," U.S. Army WECOM Report, August 1973.

12. ________, Fundamentals of Helicopter Stability and Control, Boeing Vertol Division.

13. Obermayer, R. W., and Muckler, F. A., "Modern Control System Theory and Human Control Functions," NASA CR-256, 1965.

LIST OF ILLUSTRATIONS

Figure Page

1. Helicopter Flight Path Model 94
2. Pilot Model Function 95
3. Control Problem 95
4. Inertial Position for Level Flight 96
5. Inertial Position for Climb Configuration 97
6. Inertial Position for Climb Configuration 97
7. Inertial Position for Dive Configuration 98
8. Inertial Position for Dive Configuration 98
9. Inertial Position for Turn Configuration 99
10. Turn Configuration Altitude Vs. Time 100
11. Level Flight Roll Vs. Time 101
12. Climb Configuration Roll Vs. Time 101
13. Dive Configuration Roll Vs. Time 102
14. Turn Configuration Roll Vs. Time 102
15. Level Flight Pitch Vs. Time 103
16. Climb Configuration Pitch Vs. Time 103
17. Dive Configuration Pitch Vs. Time 104
18. Turn Configuration Pitch Vs. Time 104
19. Level Flight YAW Vs. Time 105
20. Climb Configuration YAW Vs. Time 105
21. Dive Configuration YAW Vs. Time 106

Figure Page

22. Turn Configuration YAW Vs. Time 106

23. Level Flight Collective Pitch 107

24. Level Flight Lateral Cyclic 107

25. Level Flight Longitudinal Cyclic 108

26. Level Flight Tail Rotor Pitch 108

27. Climb Configuration Collective Pitch . . . 109

28. Climb Configuration Lateral Cyclic 109

29. Climb Configuration Longitudinal Cyclic 110

30. Climb Configuration Tail Rotor Pitch 110

31. Dive Configuration Collective Pitch 111

32. Dive Configuration Lateral Cyclic 111

33. Dive Configuration Longitudinal Cyclic 112

34. Dive Configuration Tail Rotor Pitch 112

35. Turn Configuration Collective Pitch 113

36. Turn Configuration Lateral Cyclic 114

37. Turn Configuration Longitudinal Cyclic 115

38. Turn Configuration Tail Rotor Pitch 116

39. Pilot Action Response 117

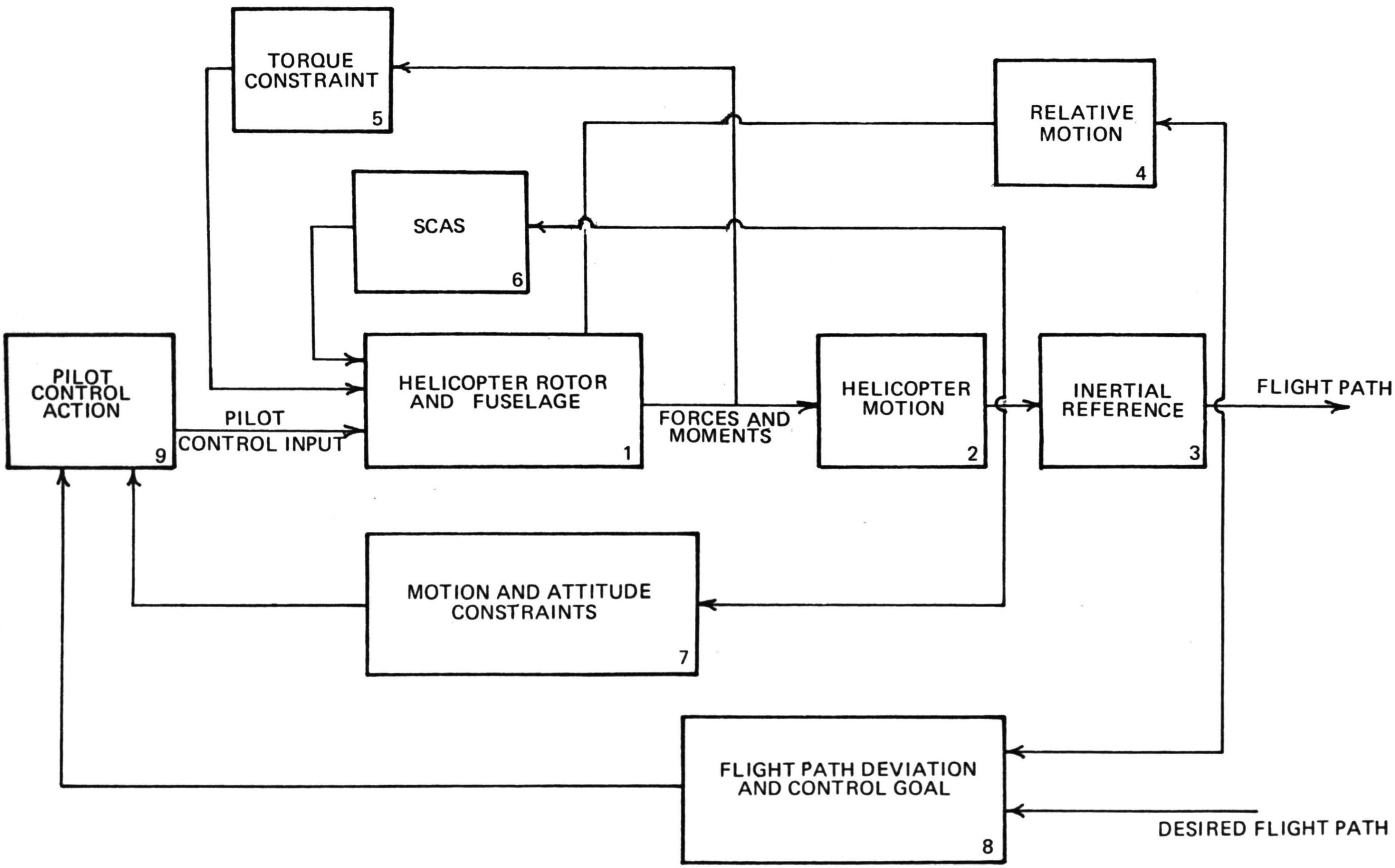
TORQUE CONSTRAINT
5
RELATIVE MOTION
4
SCAS
6
PILOT CONTROL ACTION
9
PILOT CONTROL INPUT
HELICOPTER ROTOR AND FUSELAGE
1
FORCES AND MOMENTS
HELICOPTER MOTION
2
INERTIAL REFERENCE
3
FLIGHT PATH
MOTION AND ATTITUDE CONSTRAINTS
7
FLIGHT PATH DEVIATION AND CONTROL GOAL
8
DESIRED FLIGHT PATH

Figure 1

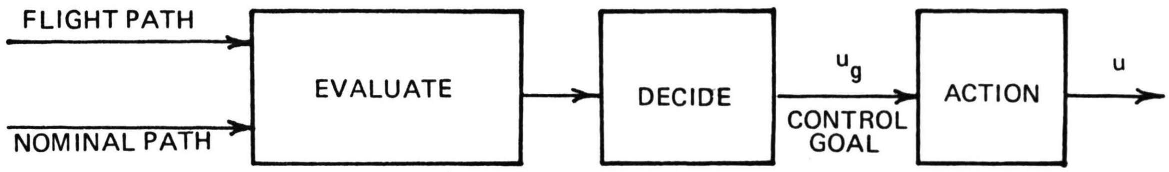

Figure 2 - Pilot Model Function

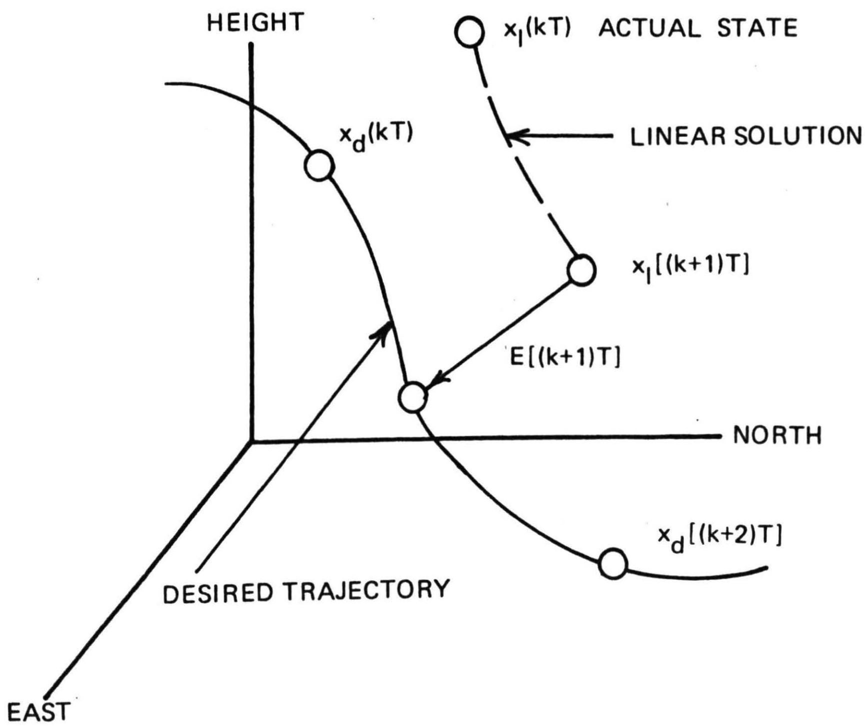

Figure 3

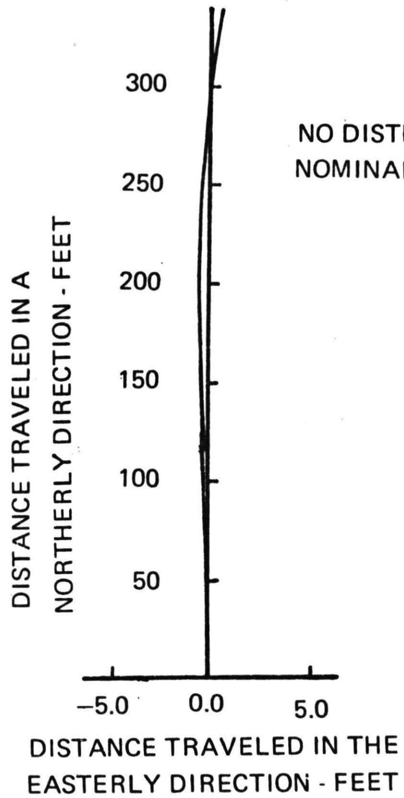
300
250
200
150
100
50
NO DISTINCTION BETWEEN NOMINAL AND PREDICTED
DISTANCE TRAVELED IN A NORTHERLY DIRECTION - FEET
−5.0
0.0
5.0
DISTANCE TRAVELED IN THE EASTERLY DIRECTION - FEET

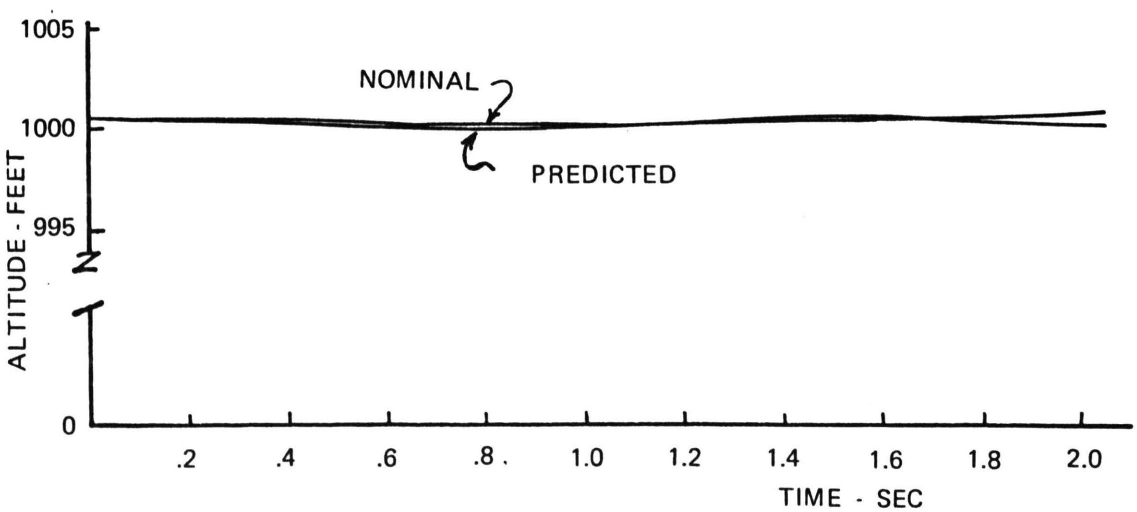
1005
1000
995
0
NOMINAL
PREDICTED
ALTITUDE - FEET
.2
.4
.6
.8
1.0
1.2
1.4
1.6
1.8
2.0
TIME - SEC

Figure 4

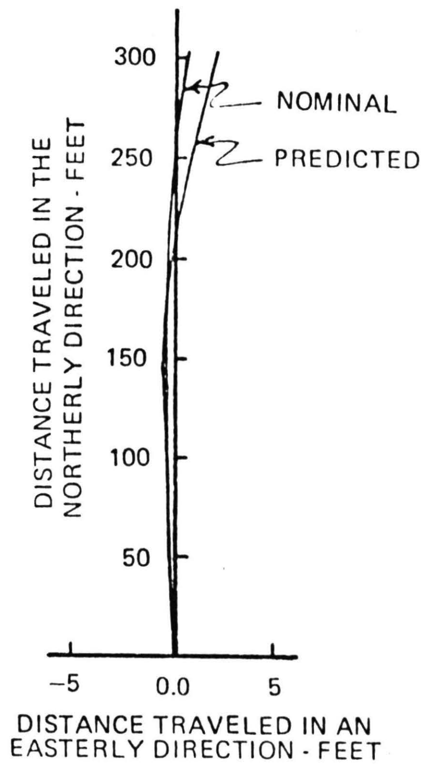

Figure 5

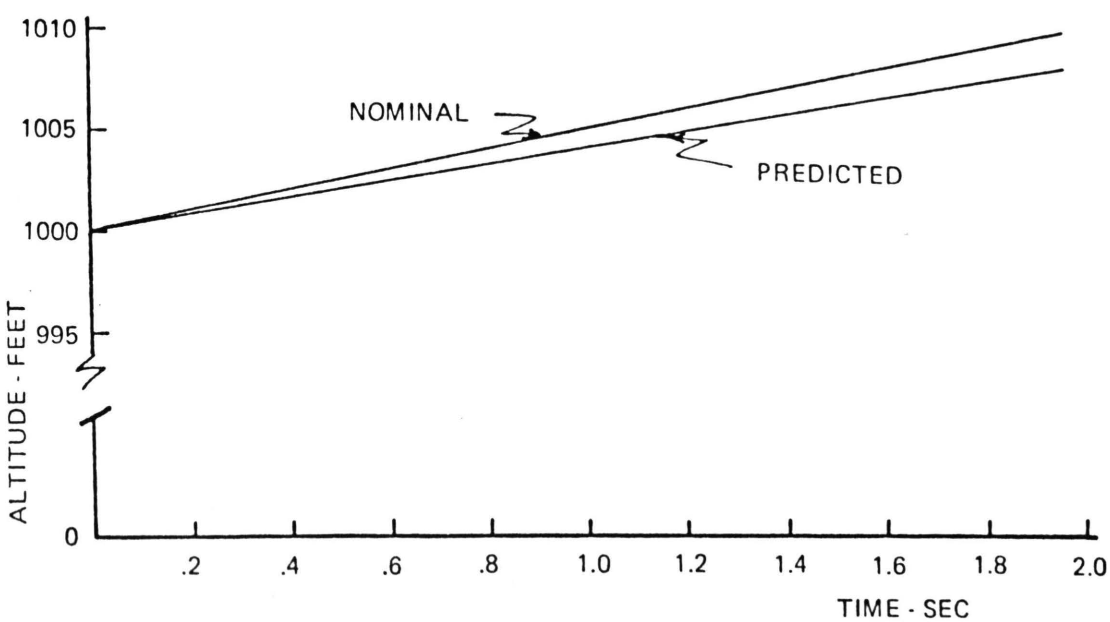

Figure 6

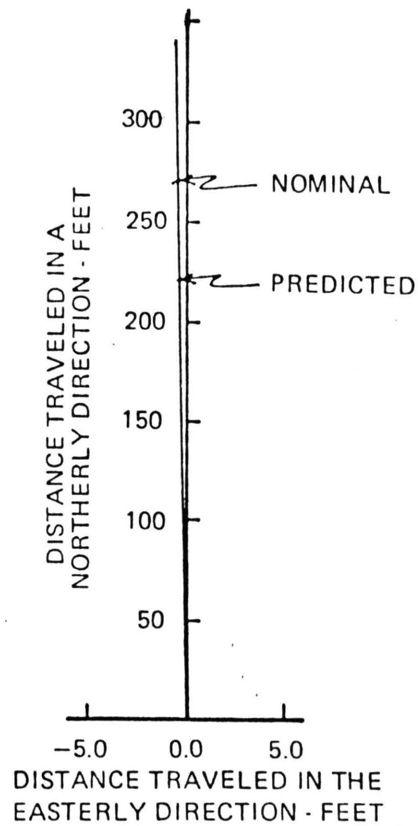

Figure 7

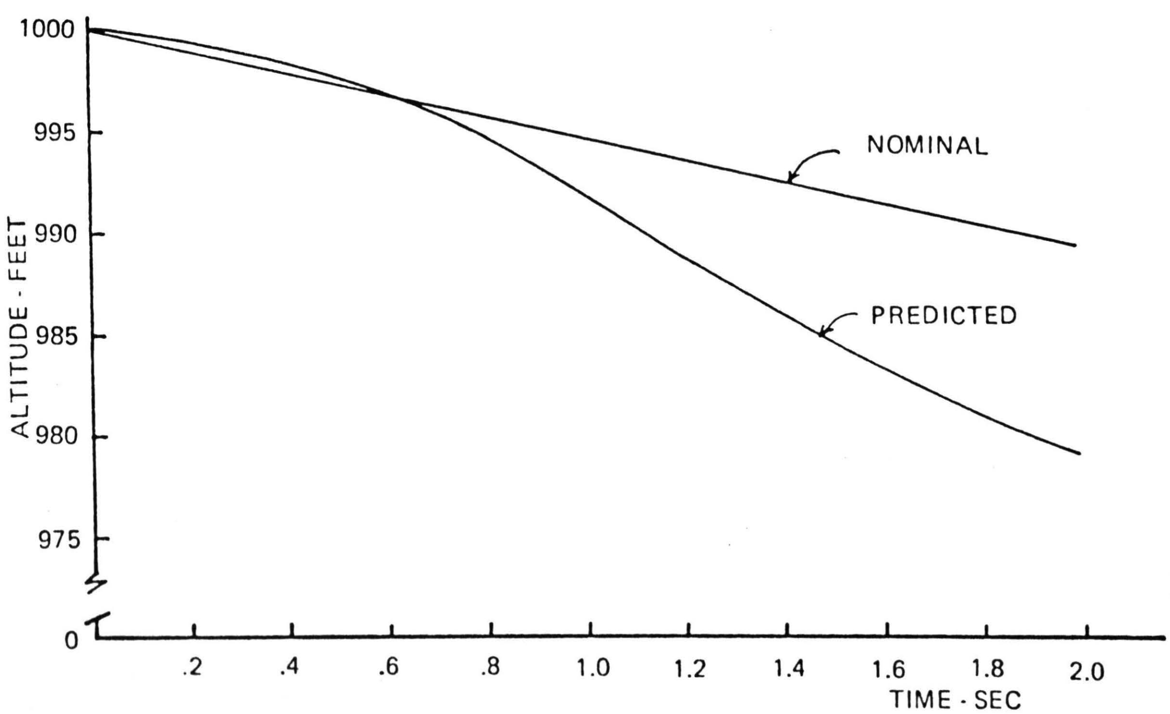

Figure 8

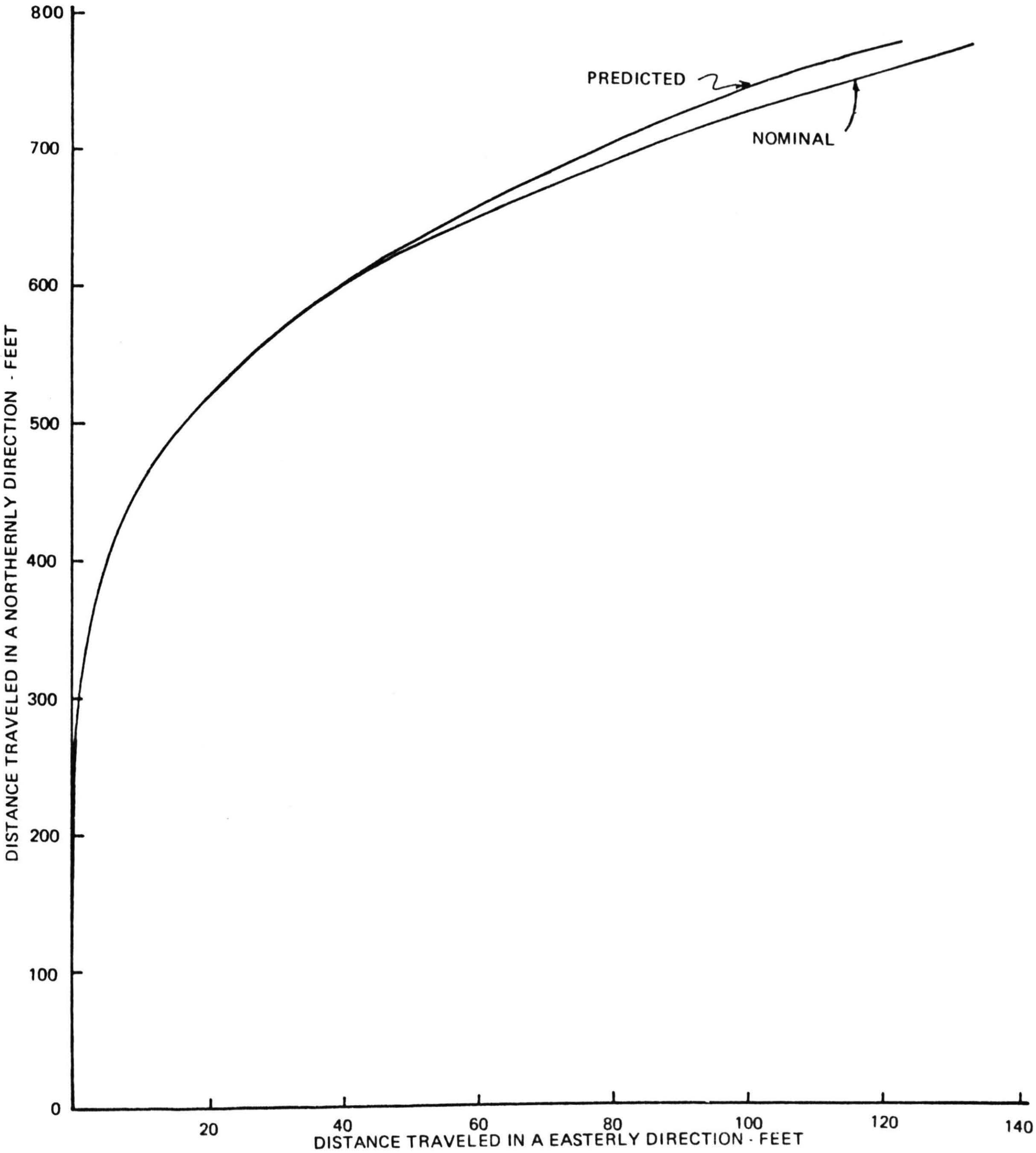

800
700
600
500
400
300
200
100
0
PREDICTED
NOMINAL
DISTANCE TRAVELED IN A NORTHERNLY DIRECTION - FEET
20
40
60
80
100
120
140
DISTANCE TRAVELED IN A EASTERLY DIRECTION - FEET

Figure 9

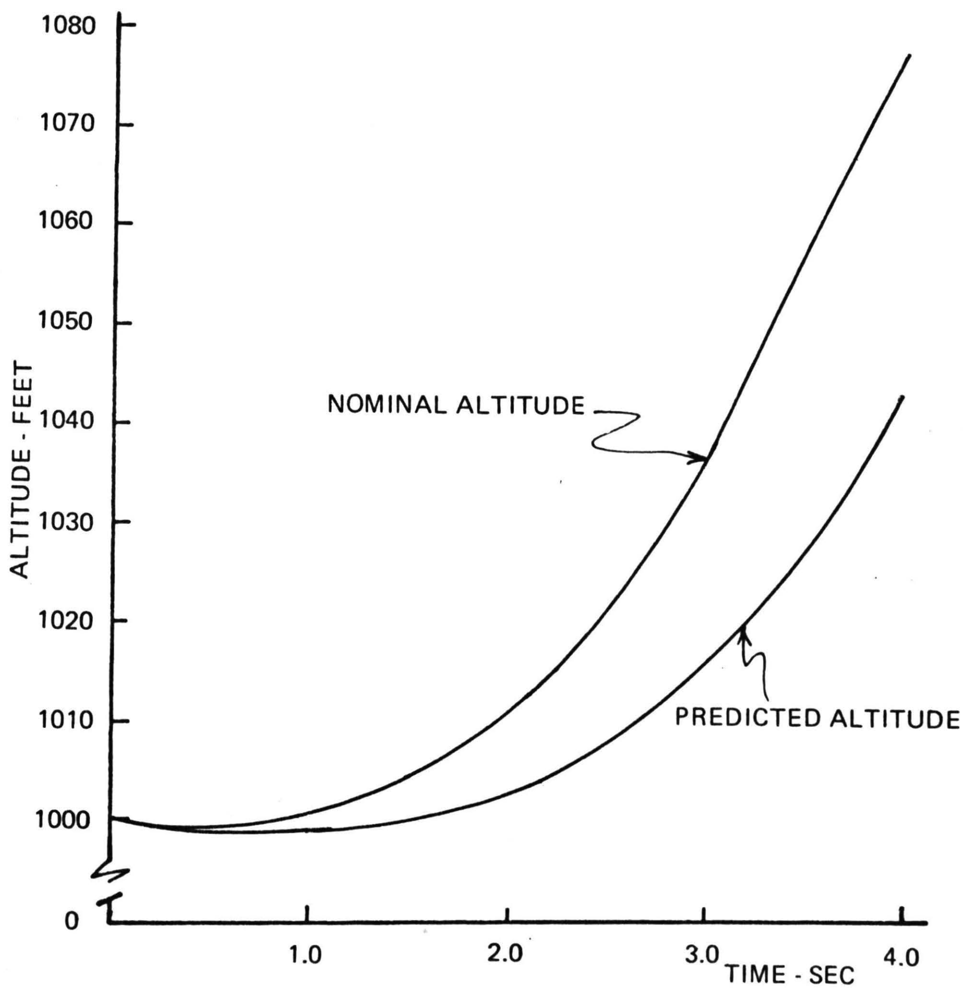
1080
1070
1060
1050
1040
1030
1020
1010
1000
0
ALTITUDE - FEET
NOMINAL ALTITUDE
PREDICTED ALTITUDE
1.0
2.0
3.0
4.0
TIME - SEC

Figure 10

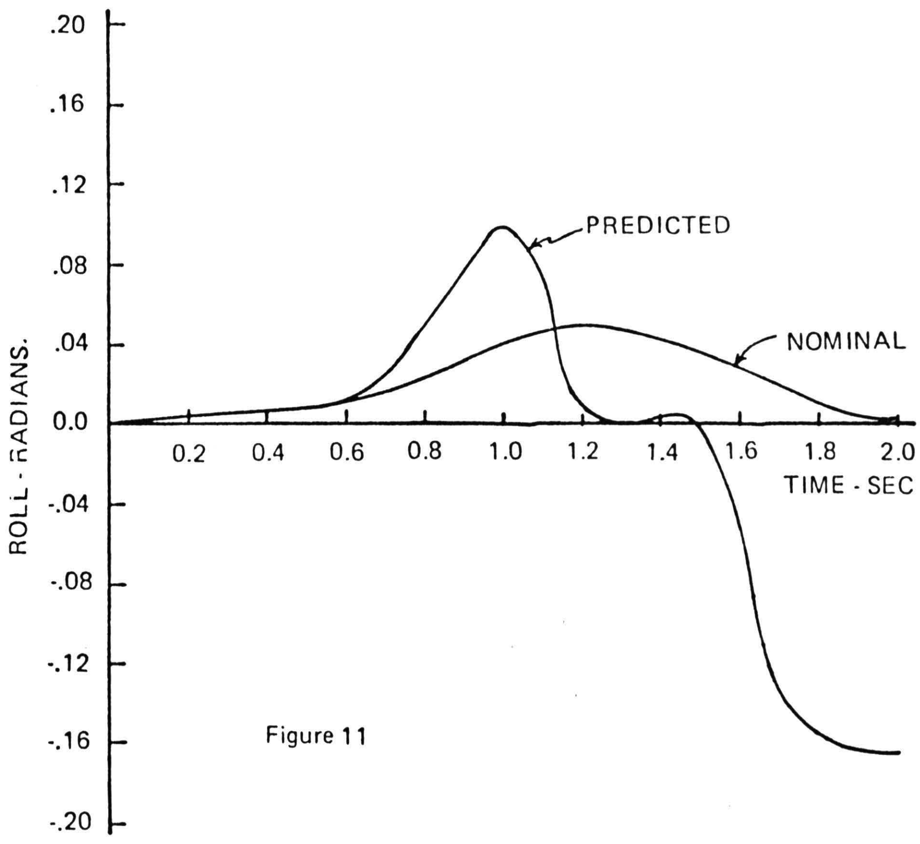

Figure 11

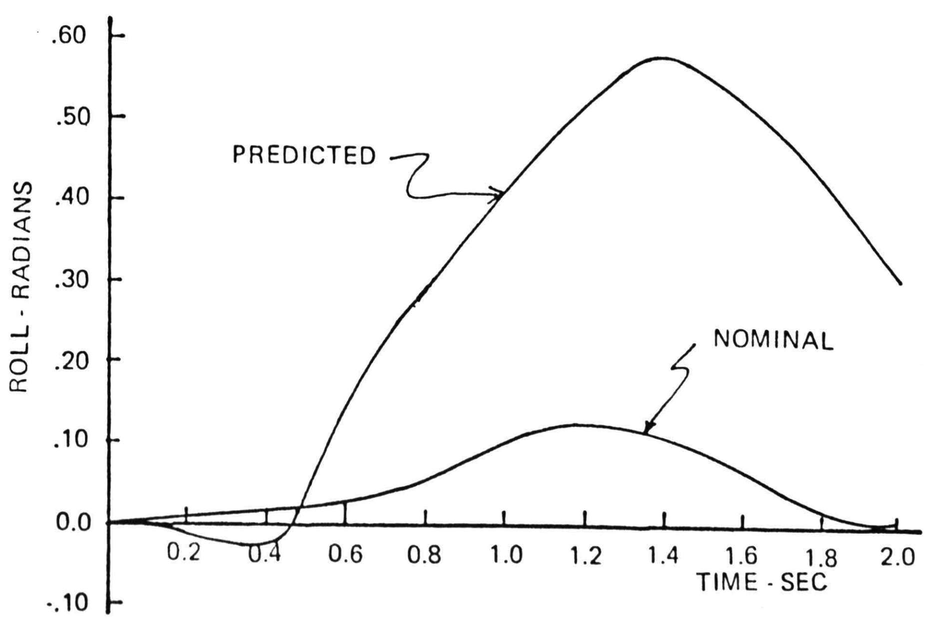

Figure 12

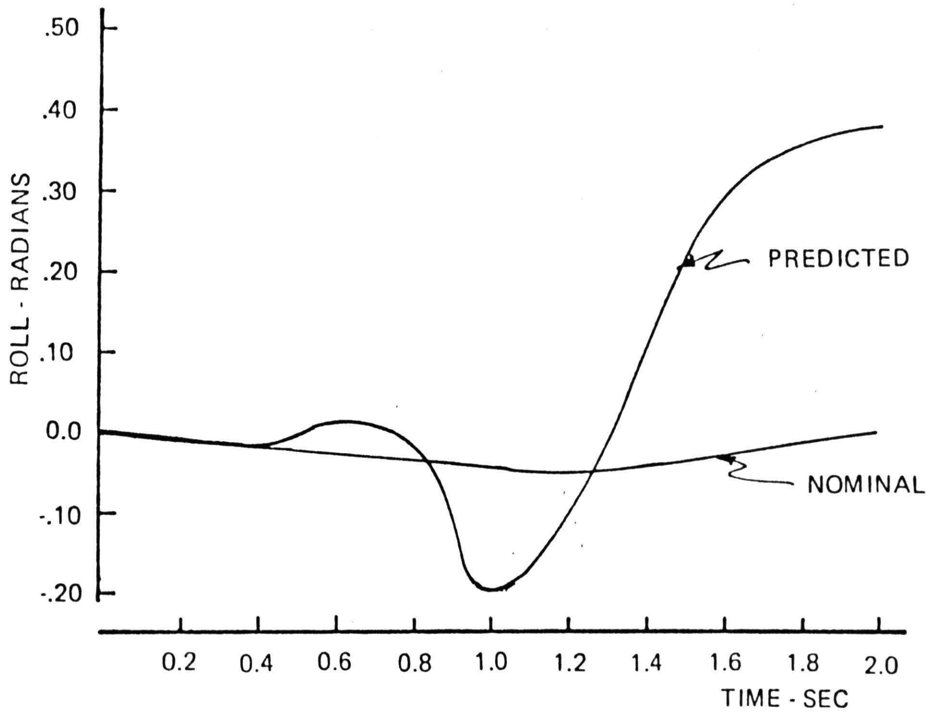

Figure 13

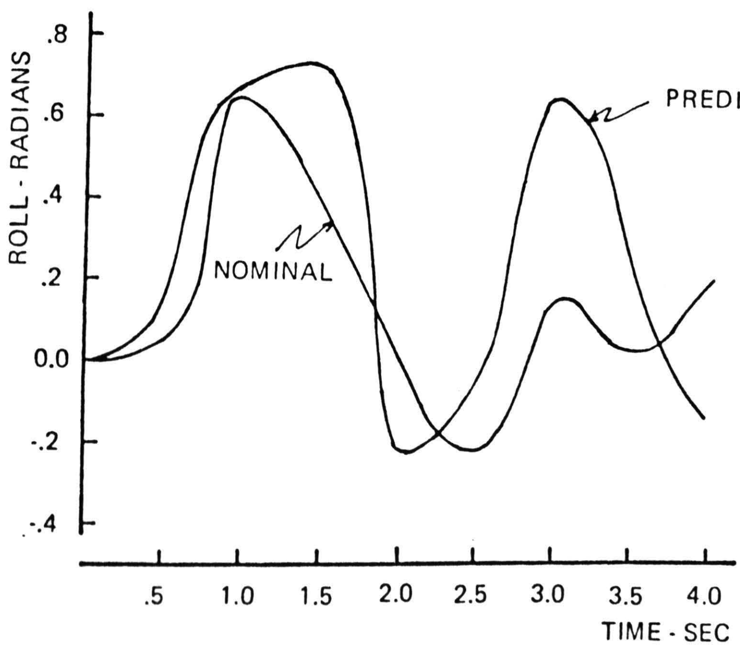

Figure 14

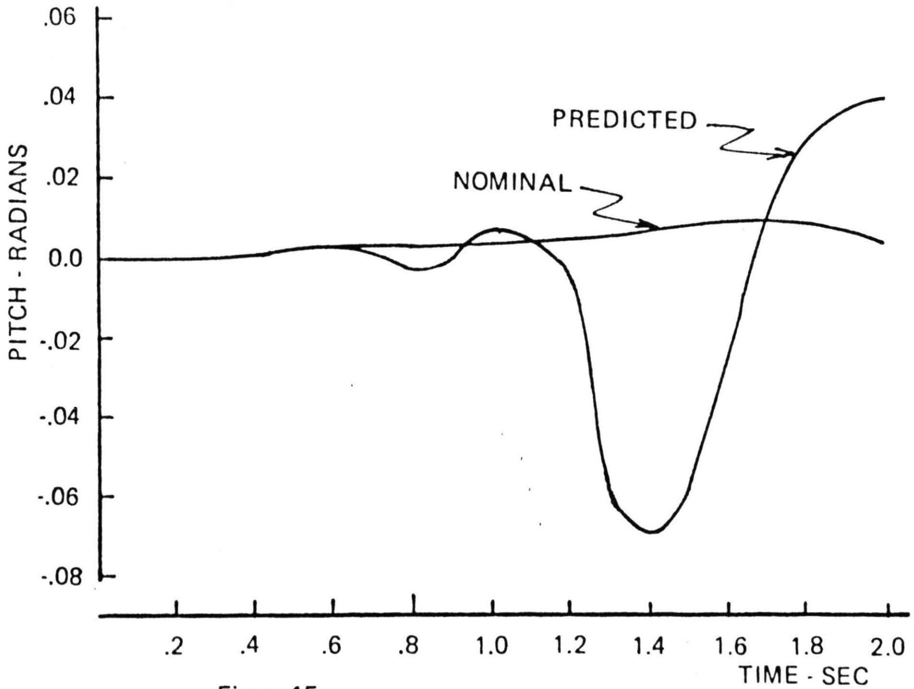

Figure 15

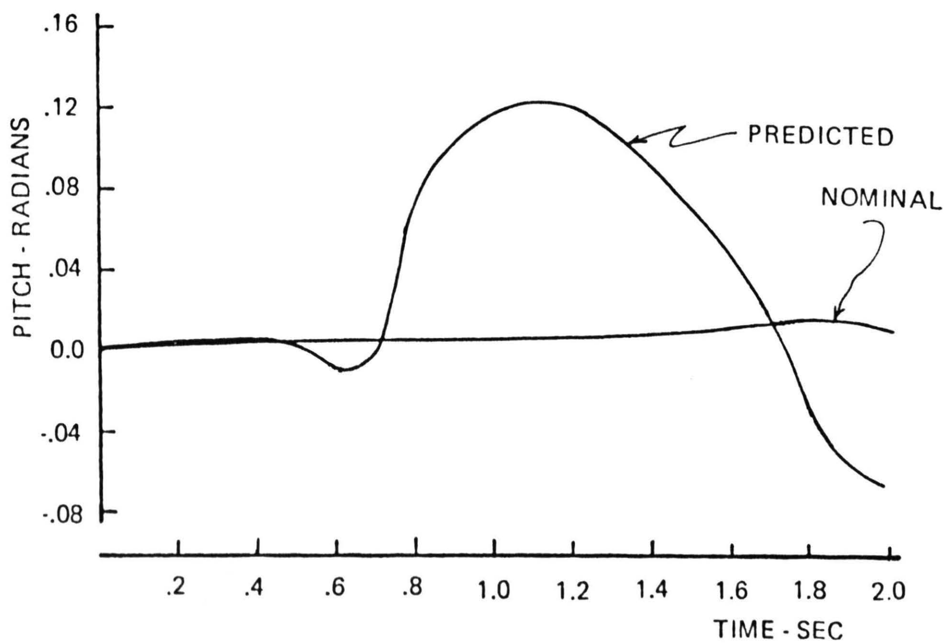

Figure 16

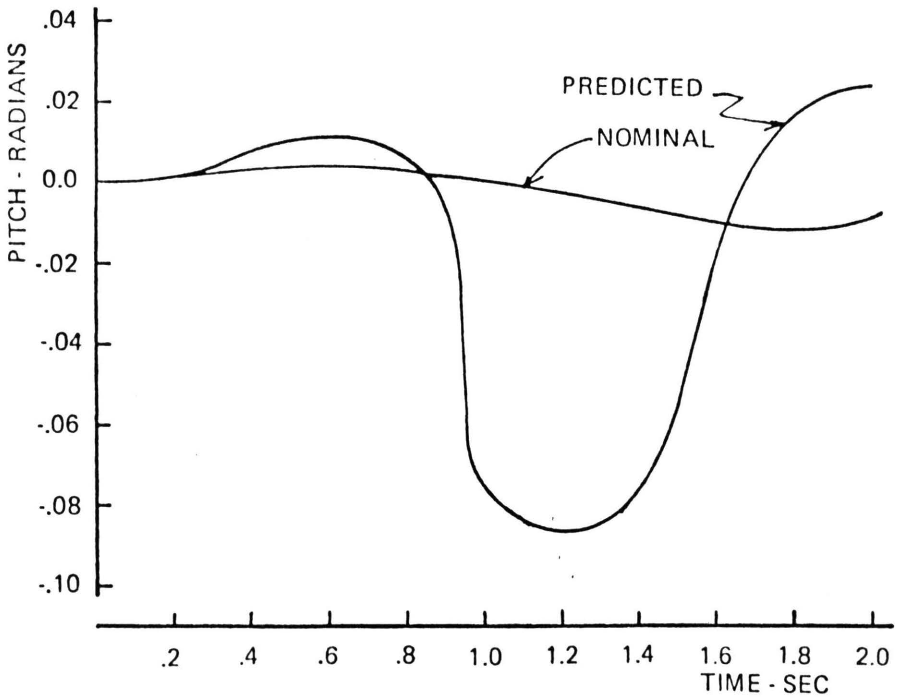

Figure 17

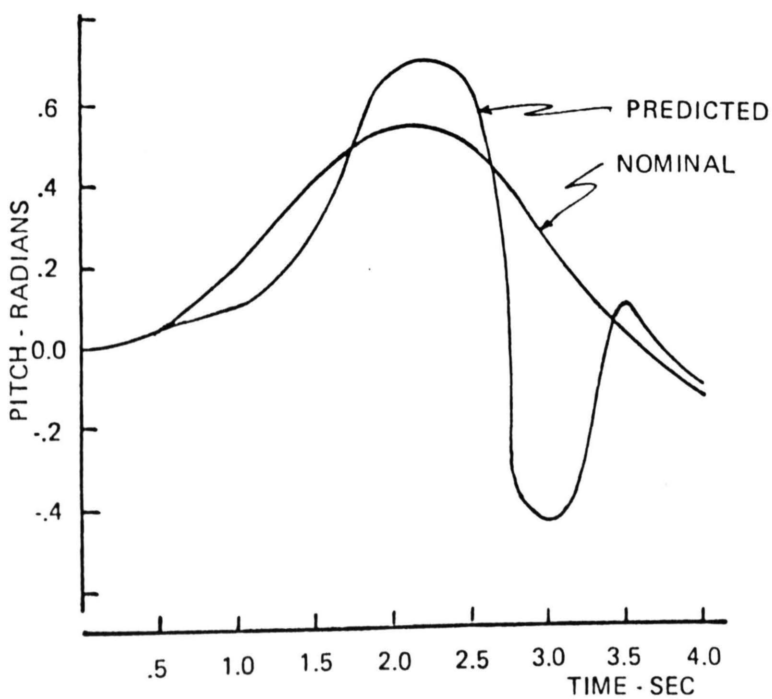

Figure 18

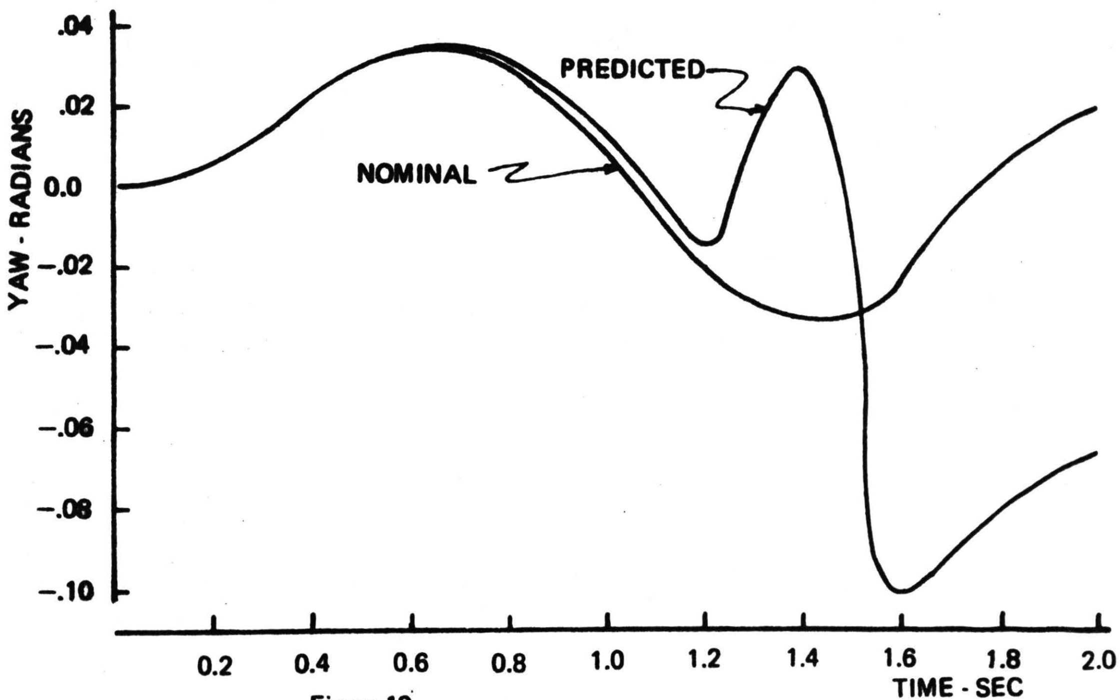

Figure 19

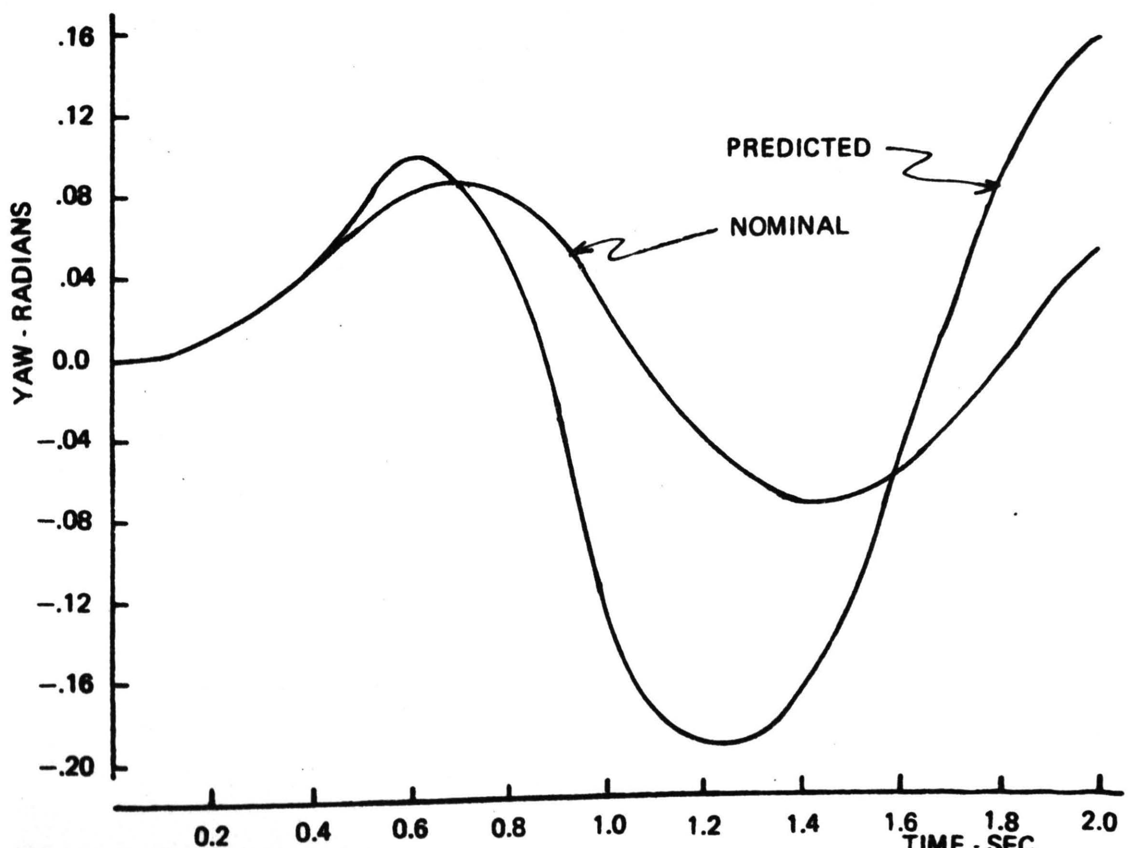

Figure 20

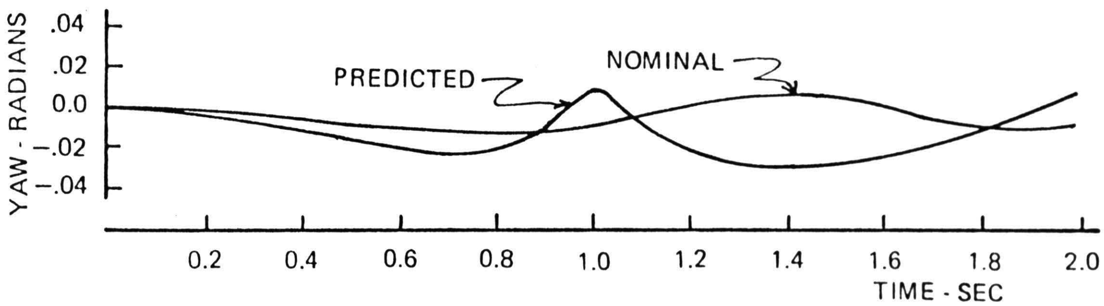

Figure 21

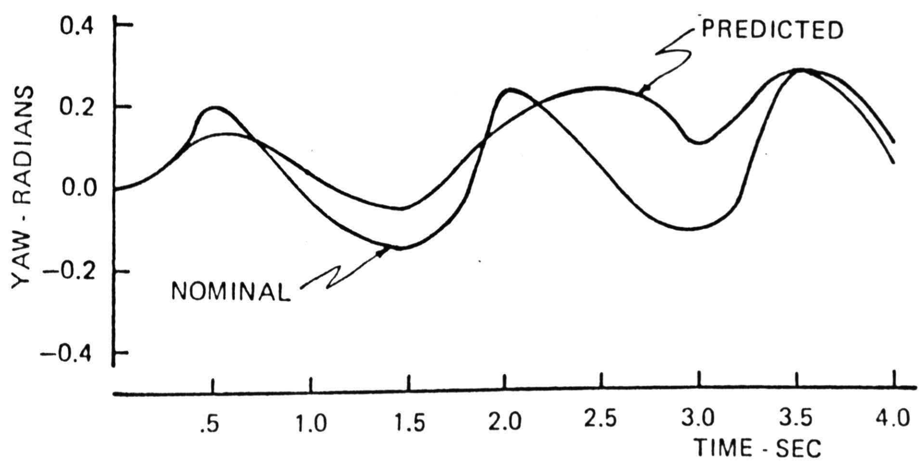

Figure 22

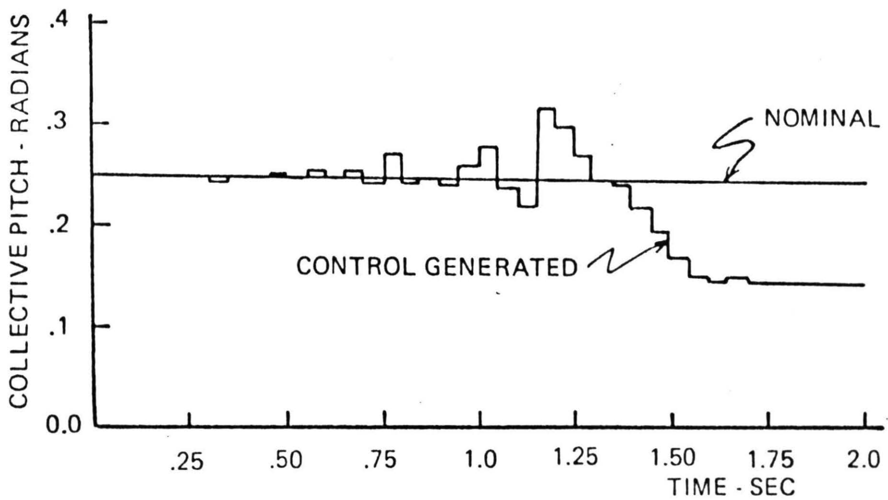

Figure 23

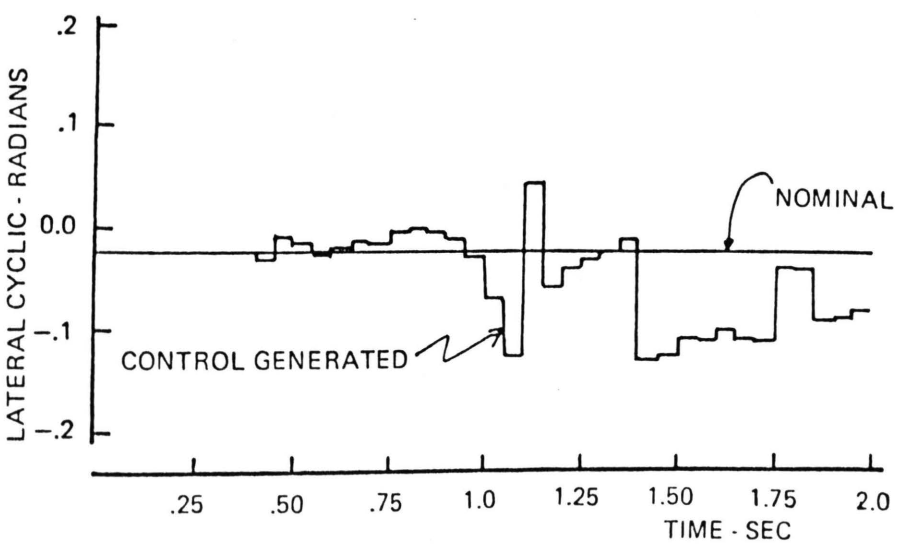

Figure 24

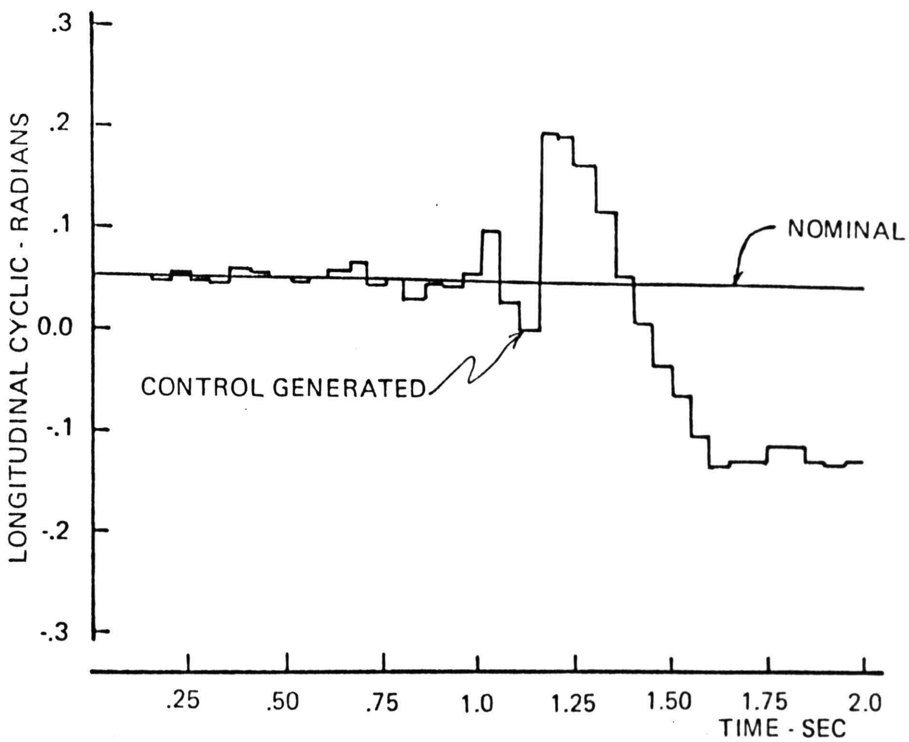

Figure 25

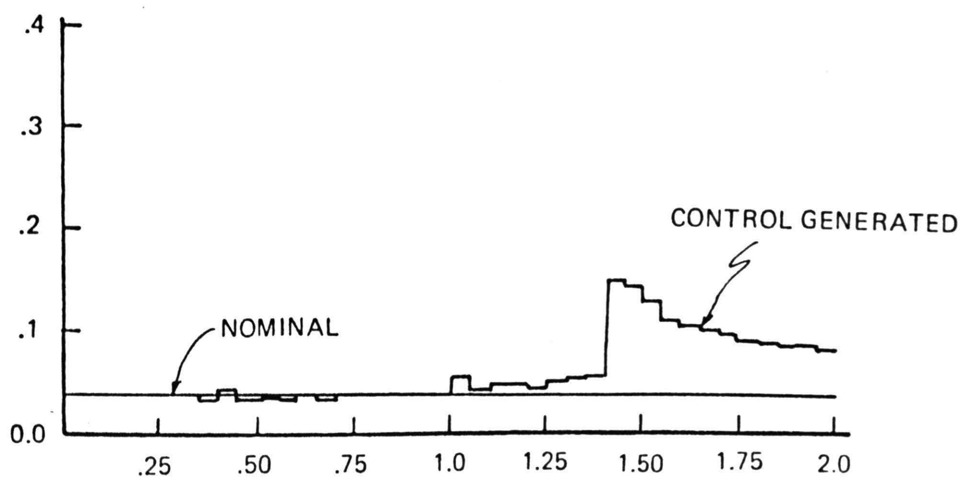

Figure 26

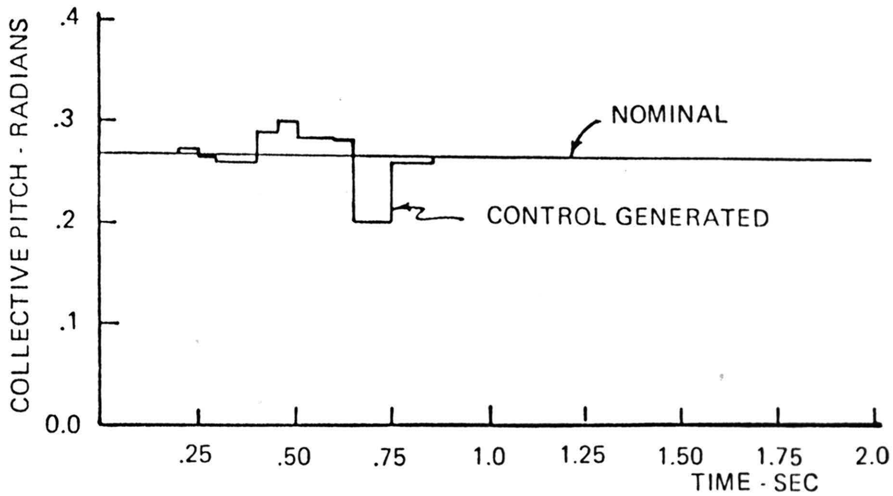

Figure 27

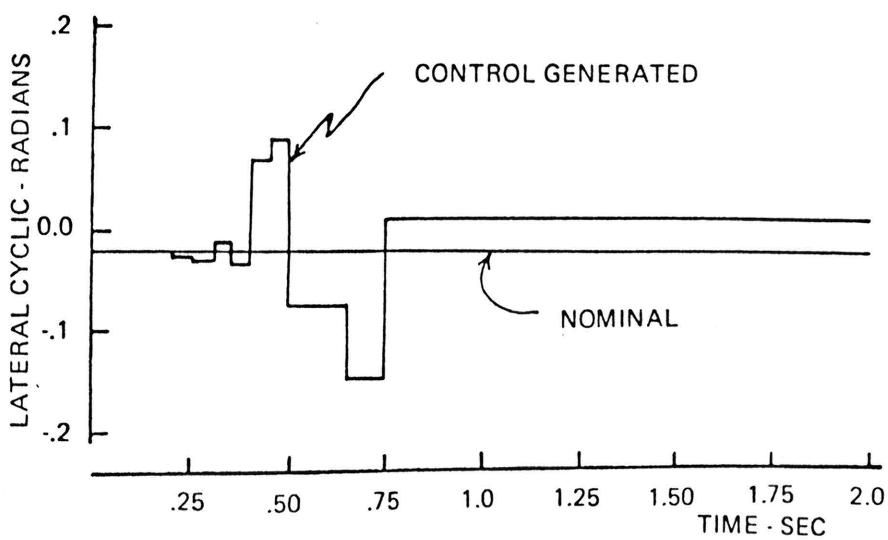

Figure 28

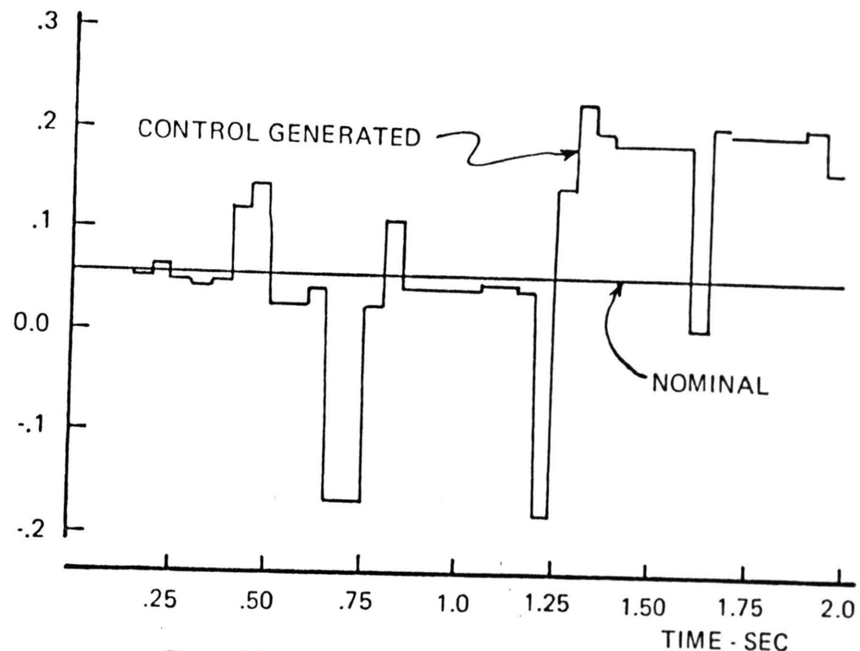

Figure 29

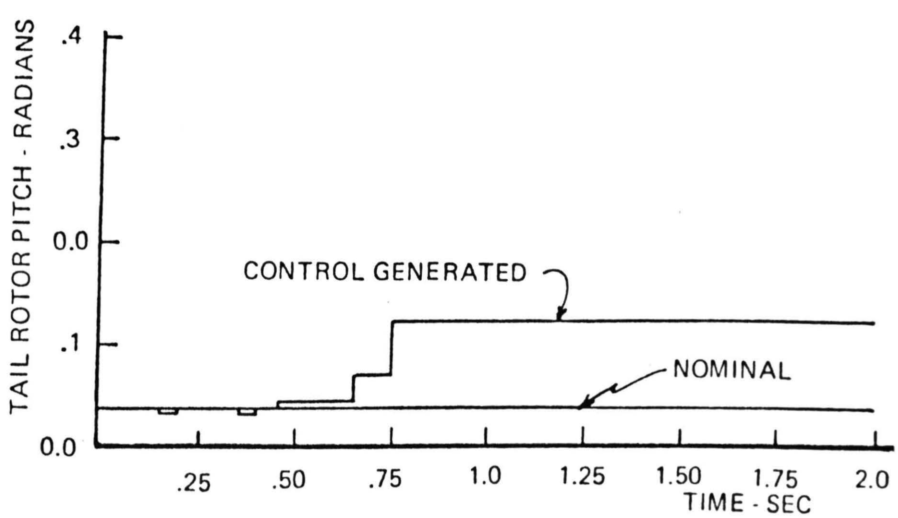

Figure 30

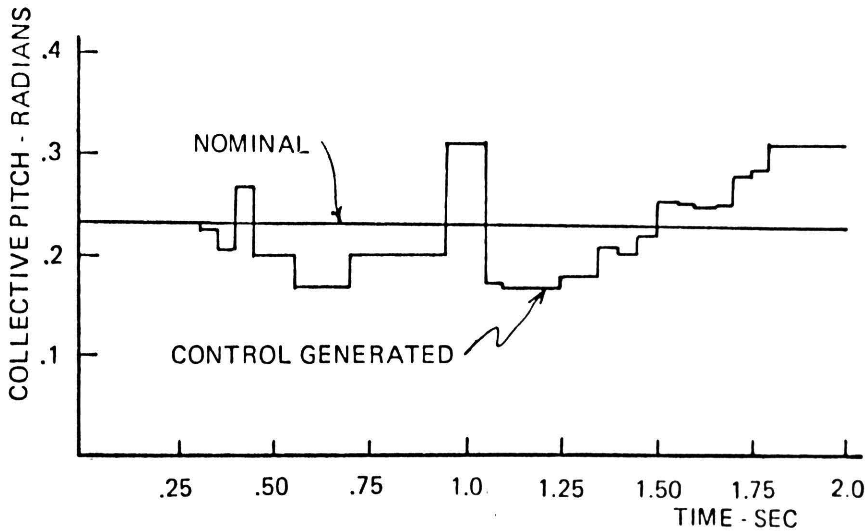

Figure 31

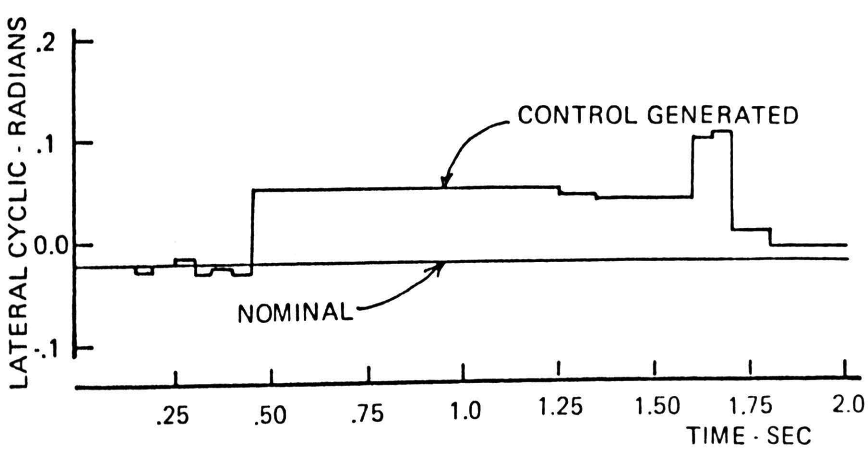

Figure 32

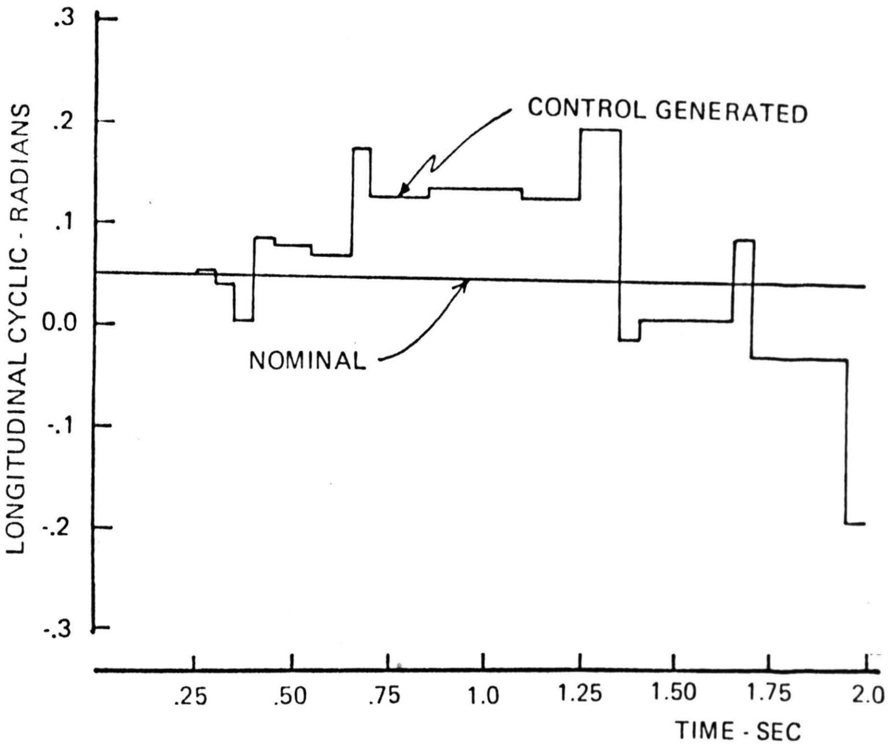

Figure 33

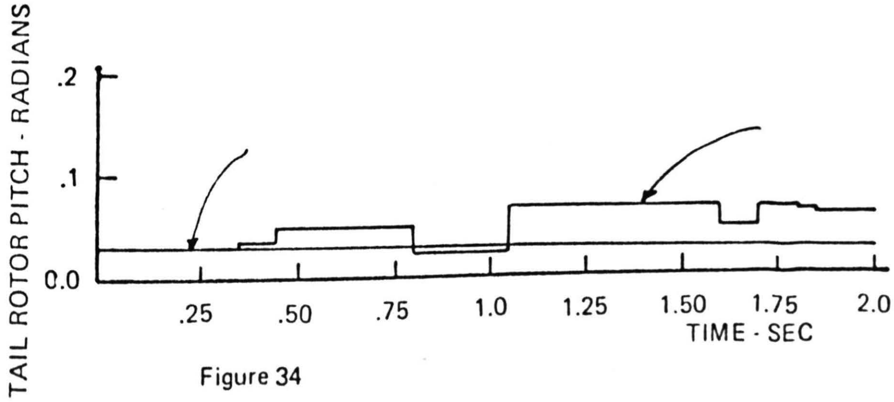

Figure 34

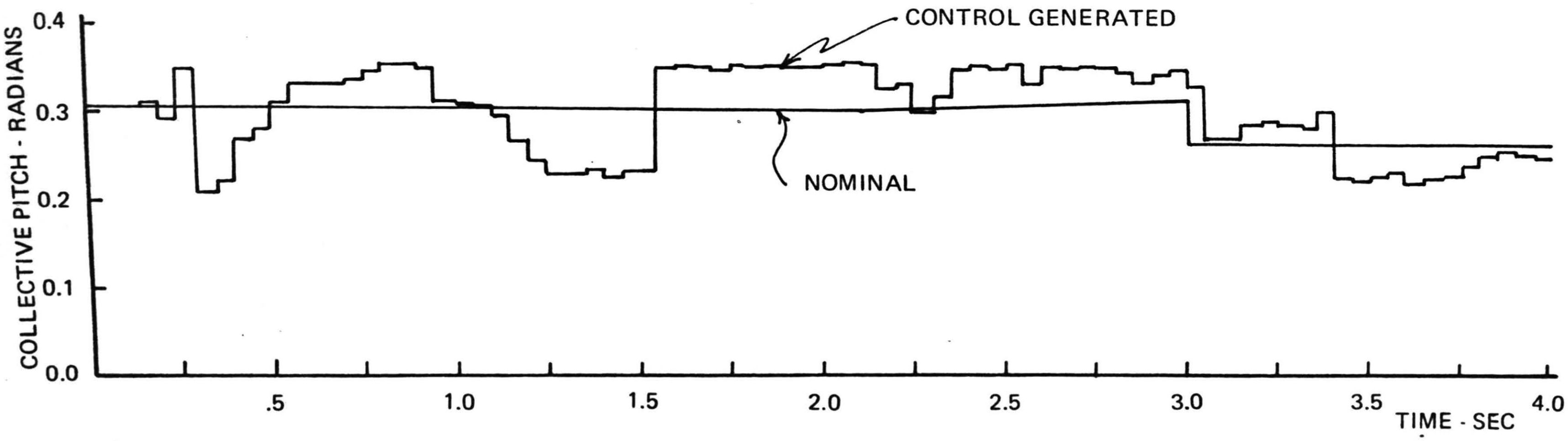
CONTROL GENERATED
NOMINAL
COLLECTIVE PITCH - RADIANS
0.4
0.3
0.2
0.1
0.0
.5
1.0
1.5
2.0
2.5
3.0
3.5
4.0
TIME - SEC

Figure 35

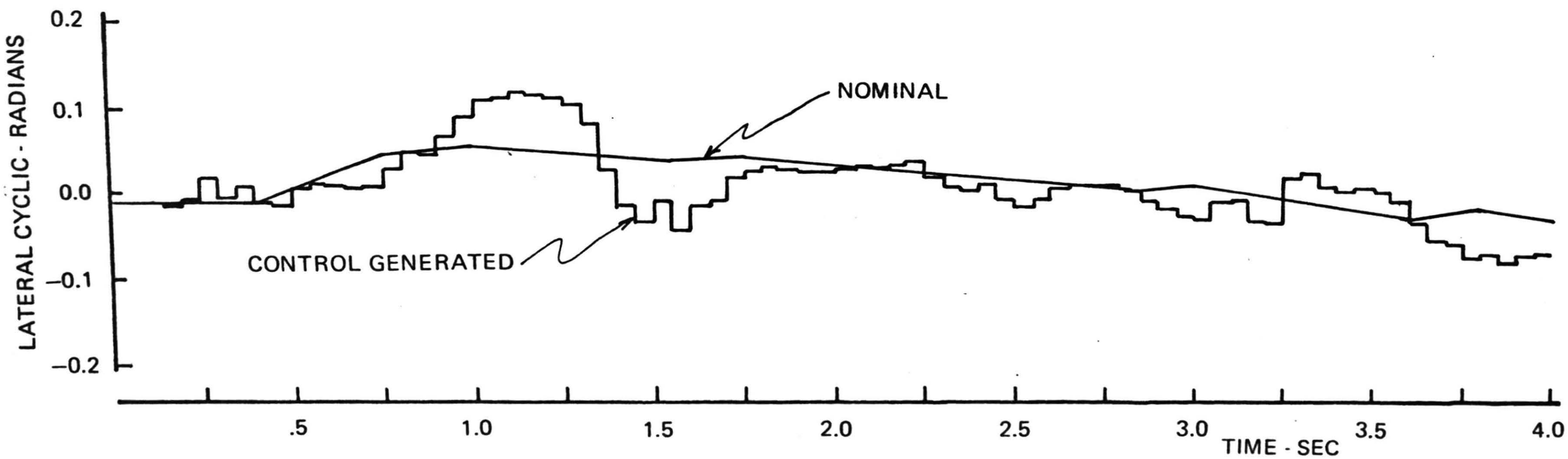
LATERAL CYCLIC - RADIANS
0.2
0.1
0.0
−0.1
−0.2
NOMINAL
CONTROL GENERATED
.5
1.0
1.5
2.0
2.5
3.0
3.5
4.0
TIME - SEC

Figure 36

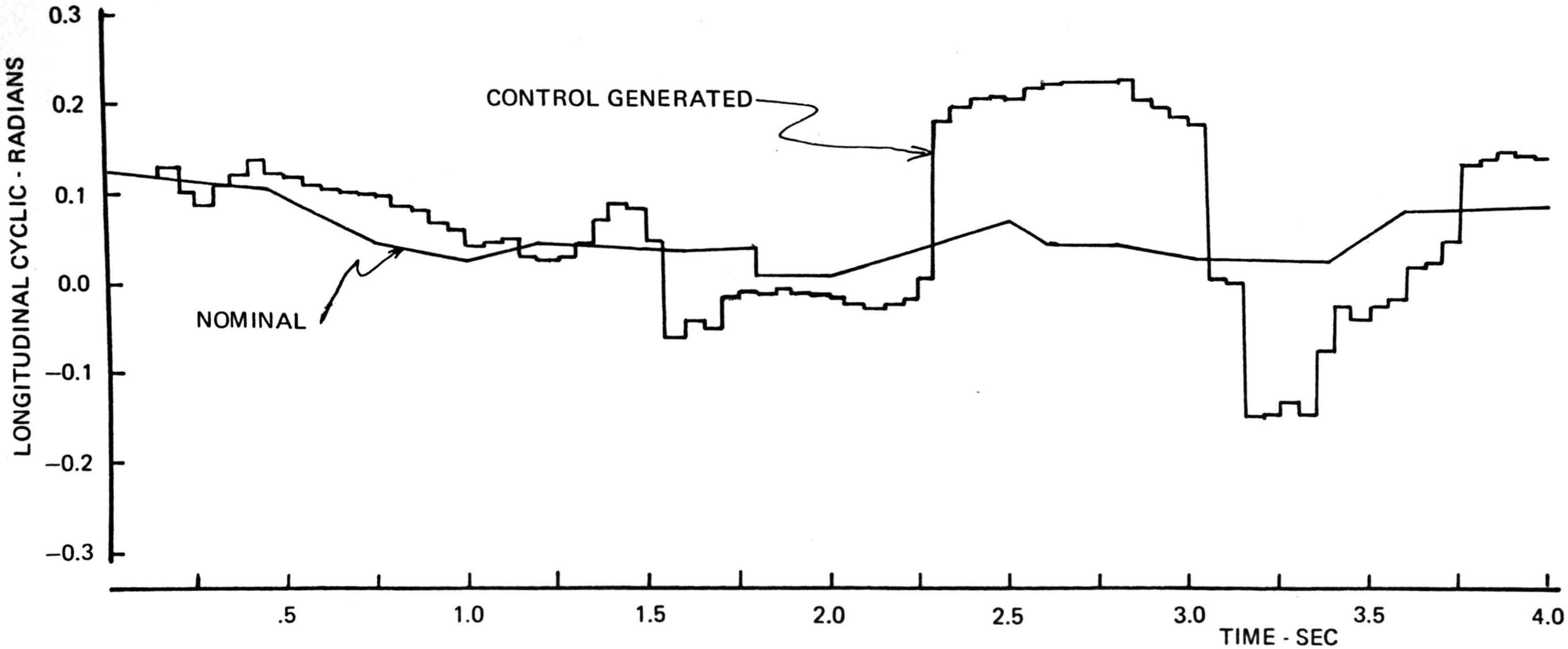
LONGITUDINAL CYCLIC - RADIANS
0.3
0.2
0.1
0.0
−0.1
−0.2
−0.3
CONTROL GENERATED
NOMINAL
.5
1.0
1.5
2.0
2.5
3.0
3.5
4.0
TIME - SEC

Figure 37

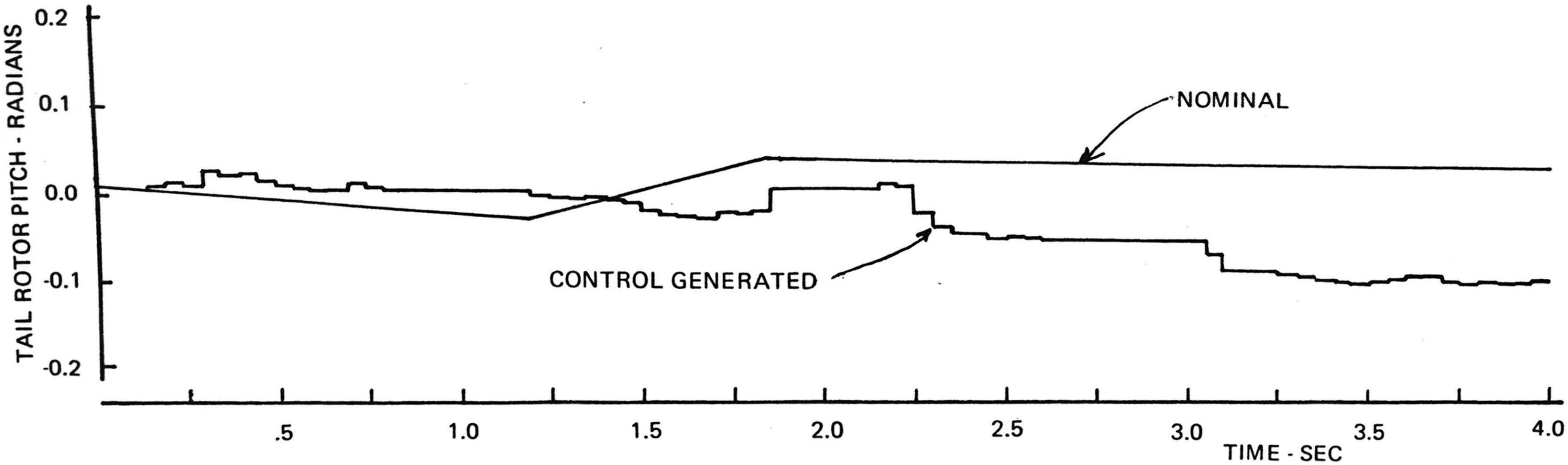

TAIL ROTOR PITCH - RADIANS
0.2
0.1
0.0
-0.1
-0.2
NOMINAL
CONTROL GENERATED
.5
1.0
1.5
2.0
2.5
3.0
3.5
4.0
TIME - SEC

Figure 38

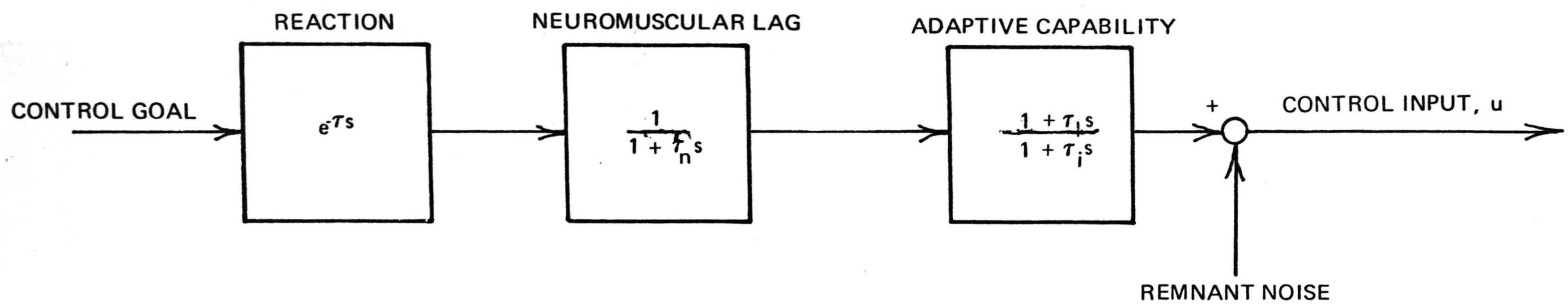

τ = REACTION DELAY TIME, 0.1 to 0.5 SEC.

τ_n = NEUROMUSCULAR LAG TIME, 0.1 SEC

τ_l = ANTICIPATION LEAD TIME, 0 to 2 SEC.

τ_i = ERROR SMOOTHING LAG TIME, 0 to 0.2 SEC.

Figure 39

APPENDIX A

WEIGHTING MATRICES

The selection of the weighting matrix W_e is obtained in the following manner. Since the desired state at time kT is known apriori, the error between desired and actual state is approximated by

$$e_i^2(kT) = \left\{ x_d^i(kT) - \{x^i[(k-1)T] + \dot{x}^i[(k-1)T]\Delta t\} \right\}^2$$

where

$$i = 1,2, \ldots 10$$

and

$$\Delta t \triangleq \text{sample time.}$$

The corresponding diagonal weighting function is given by

$$W_e(kT) = \begin{bmatrix} \frac{1}{e_1^2} & 0 & \cdots & 0 \\ 0 & \frac{1}{e_2^2} & & \\ \vdots & & \ddots & \\ 0 & & \cdots & \frac{1}{e_{10}^2} \end{bmatrix}$$

In a similar fashion the weighting function, W_u, on the control can be obtained. However, note that in selecting the weighting function on the control, the problem of singularity becomes increasingly severe. That is, the control may remain constant over two or more sample times making the inversion of W_u impossible.

APPENDIX B

SOLUTION OF THE MATRIX RICCATI EQUATION

To solve

$$XA^T + AX - X(H^TR^{-1}H)X = -P \tag{B-1}$$

where X, A, P, R are n x n matrices, H is an n x m matrix and R is an m x m matrix apply the following algorithm:

1) Find the characteristic equation of the 2n x 2n matrix

$$W = \begin{bmatrix} A^T & H^TR^{-1}H \\ P & -A \end{bmatrix} \tag{B-2}$$

It will have even powers in the unknown.

2) Find all the roots of this equation, retaining the n roots which have negative real parts.

3) Use these complex quantities to generate the coefficients of the polynominal having them as roots. Denote the result by

$$\tilde{\Delta}(s) = s^n + \alpha_{n-1}s^{n-1} + \cdots + \alpha_1 s + \alpha_o = 0 \tag{B-3}$$

4) Find the matrix

$$\tilde{\Delta}(W) = \begin{bmatrix} W_{11} & W_{12} \\ W_{21} & W_{22} \end{bmatrix} \tag{B-4}$$

5) Evaluate X from

$$X = W_{12}^{-1} W_{11} \text{ or } X = W_{22}^{-1} W_{21} \tag{B-5}$$

The equation

$$XA^T + AX - XMX + P = 0 \qquad \text{(B-6)}$$

where A, X, M, P are n x n matrices, holds if and only if

$$\tilde{W} = XWX^{-1} \qquad \text{(B-7)}$$

where

$$X \triangleq \begin{bmatrix} I & O \\ X & I \end{bmatrix} \quad X^{-1} = \begin{bmatrix} I & O \\ -X & I \end{bmatrix} \qquad \text{(B-8)}$$

$$W \triangleq \begin{bmatrix} A^T & M \\ P & -A \end{bmatrix} \quad \tilde{W} = \begin{bmatrix} \tilde{A}^T & M \\ O & -\tilde{A} \end{bmatrix}$$

with $\tilde{A} \triangleq A - MX$.

Proof: The desired result is obtained by direct expansion of (B-7) according to the definitions in (B-8).

I can also be shown that

$$\det(sI-W) = (-1)^n \tilde{\Delta}(s)\tilde{\Delta}(-s), \qquad \text{(B-9)}$$

where

$$\tilde{\Delta}(s) \triangleq \det(sI-\tilde{A}). \qquad \text{(B-10)}$$

From the above

$$\begin{aligned} \det(sI-W) &= \det\,(sI-X^{-1}\tilde{W}X) \\ &= \det\ X^{-1}\det(sI-\tilde{W})\det X. \end{aligned} \qquad \text{(B-11)}$$

By inspection, $\det X = \det X^{-1}$, so that

$$\det\,(sI-W) = \det(sI-\tilde{W}) \qquad \text{(B-12)}$$

Using this result and the definition of $\tilde{W}$,

$$\det(s\,I - W) = \det \begin{bmatrix} I & Y \\ O & I \end{bmatrix} \begin{bmatrix} sI - \tilde{A}^T & -M \\ O & s\,I + \tilde{A} \end{bmatrix} \tag{B-13}$$

$$= \det \begin{bmatrix} sI - \tilde{A}^T & -M + Y(sI + \tilde{A}) \\ O & sI + \tilde{A} \end{bmatrix}$$

for arbitrary Y. Choose $Y = M(sI + \tilde{A})^{-1}$ and obtain

$$\det(sI - W) = \det(sI - \tilde{A}^T) \det(sI + \tilde{A}). \tag{B-14}$$

Now

$$\det(sI + \tilde{A}) = \det\,[-I(-sI - \tilde{A})] = (-1)^n \det(-sI - \tilde{A}). \tag{B-15}$$

By combining this with (B-13) and B-10, the desired result (B-9) is obtained.

From (B-9) it is clear that the characteristic equation of W has even power only.

VITA

April 27, 1942 -	Born - Rock Springs, Wyoming
1964-	B.S.M.E., University of Wyoming
1964-1967	Mechanical Engineer, General Dynamics Astronautics, San Diego, California
1966-	M.S.E.S., University of California, San Diego, California
1967-1970	Aerospace Engineer, Naval Electronics Laboratory Center, San Diego, California